

Projected climate and canopy change lead to thermophilization and homogenization of forest floor vegetation in a hotspot of plant species richness

Kristin H. Braziunas¹  | Lisa Geres^{2,3}  | Tobias Richter^{1,2} | Felix Glasmann⁴ |
 Cornelius Senf¹ | Dominik Thom¹  | Sebastian Seibold^{1,2,5} | Rupert Seidl^{1,2} 

¹Ecosystem Dynamics and Forest Management Group, TUM School of Life Sciences, Technical University of Munich, Freising, Germany

²Berchtesgaden National Park, Berchtesgaden, Germany

³Faculty of Biological Sciences, Institute for Ecology, Evolution and Diversity, Conservation Biology, Goethe University Frankfurt, Frankfurt am Main, Germany

⁴Professorship of Forest and Agroforest Systems, TUM School of Life Sciences, Technical University of Munich, Freising, Germany

⁵Forest Zoology, Technische Universität Dresden, Tharandt, Germany

Correspondence

Kristin H. Braziunas, Ecosystem Dynamics and Forest Management Group, TUM School of Life Sciences, Technical University of Munich, Freising, Germany.
 Email: kristin.braziunas@tum.de

Funding information

European Research Council, Grant/Award Number: 101001905; Bayerisches Staatsministerium für Umwelt und Verbraucherschutz

Abstract

Mountain forests are plant diversity hotspots, but changing climate and increasing forest disturbances will likely lead to far-reaching plant community change. Projecting future change, however, is challenging for forest understory plants, which respond to forest structure and composition as well as climate. Here, we jointly assessed the effects of both climate and forest change, including wind and bark beetle disturbances, using the process-based simulation model iLand in a protected landscape in the northern Alps (Berchtesgaden National Park, Germany), asking: (1) *How do understory plant communities respond to 21st-century change in a topographically complex mountain landscape, representing a hotspot of plant species richness?* (2) *How important are climatic changes (i.e., direct climate effects) versus forest structure and composition changes (i.e., indirect climate effects and recovery from past land use) in driving understory responses at landscape scales?* Stacked individual species distribution models fit with climate, forest, and soil predictors (248 species currently present in the landscape, derived from 150 field plots stratified by elevation and forest development, overall area under the receiving operator characteristic curve = 0.86) were driven with projected climate (RCP4.5 and RCP8.5) and modeled forest variables to predict plant community change. Nearly all species persisted in the landscape in 2050, but on average 8% of the species pool was lost by the end of the century. By 2100, landscape mean species richness and understory cover declined (-13% and -8%, respectively), warm-adapted species increasingly dominated plant communities (i.e., thermophilization, +12%), and plot-level turnover was high (62%). Subalpine forests experienced the greatest richness declines (-16%), most thermophilization (+17%), and highest turnover (67%), resulting in plant community homogenization across elevation zones. Climate rather than forest change was the dominant driver of understory responses. The magnitude of unabated 21st-century change is likely to erode plant diversity in a species richness hotspot, calling for stronger conservation and climate mitigation efforts.

This is an open access article under the terms of the [Creative Commons Attribution](#) License, which permits use, distribution and reproduction in any medium, provided the original work is properly cited.

© 2024 The Authors. *Global Change Biology* published by John Wiley & Sons Ltd.

KEY WORDS

biodiversity, climate change, European Alps, forest understory communities, microclimate, process-based landscape models, protected areas, species distribution models

1 | INTRODUCTION

Protected areas are central to global biodiversity conservation (UNEP-WCMC & IUCN, 2016; Watson et al., 2014). Within protected areas, local habitats are buffered against temperature extremes (Xu et al., 2022), species richness and abundance are higher (Gray et al., 2016), and species sensitive to human land use find refuge. A recent United Nations Biodiversity Conference set a target of 30% terrestrial area protected by 2030 (CBD, 2021); protected land area currently stands at 16% (UNEP-WCMC & IUCN, 2023), highlighting the need for evaluating existing and planning new protected areas. Changing climate and intensifying disturbances are likely to catalyze species range shifts and local extinctions, threatening future biodiversity even in areas where human land use is restricted (Lawler et al., 2015; Parks et al., 2023). To meet biodiversity conservation goals, it is therefore critical to understand whether and how much 21st-century change will affect species distributions and communities within currently protected areas.

Mountainous regions are biodiversity hotspots because their topographic and environmental heterogeneity create a multitude of ecological niches within a relatively compact area (Körner, 2004; Stein et al., 2014). In Europe, for instance, hotspots of local forest plant species richness are located in the northern and southern front ranges of the Alps (Večeřa et al., 2019). Yet, mountains are experiencing rapid environmental change, including widespread declines in snow cover (Carrer et al., 2023) and enhanced warming relative to the global average (Gobiet et al., 2014; Pepin et al., 2022). These changes can catalyze shifts in species diversity and community composition, with some cold-adapted species experiencing range contractions while others expand as climate conditions become more favorable for them (Parmesan, 2006; Rumpf et al., 2018). In general, high-elevation or high-latitude regions with adequate precipitation such as alpine tundra, boreal forests, and temperate coniferous forests are expected to increase in plant species richness with warming (Sommer et al., 2010; Vellend et al., 2017). However, simultaneous changes in multiple and interacting drivers, such as shifts in seasonal patterns of local precipitation (Konapala et al., 2020) and increases in forest disturbances with warmer and drier climate (Seidl et al., 2017), complicate projections of future biodiversity in mountain areas.

In mountain forests, forest floor (i.e., understory) plants including shrubs, herbs, grasses, and forbs underpin diversity, ecosystem functioning, and ecosystem services (Gilliam, 2007; Körner, 2004; Landuyt et al., 2019). Herbaceous species outnumber trees by a ratio of six to one in temperate forests (Gilliam, 2007). Understory plants provide wildlife forage (e.g., Suter et al., 2004) and habitat (e.g., Baines et al., 2004), support nutrient cycling (e.g., Elliott et al., 2015), sequester carbon (e.g., Dirnböck et al., 2020), and supply a variety of benefits to people such as food, medicine, and scenic beauty.

Changes in these plant communities can therefore have cascading effects on ecosystems and human livelihoods.

Anticipating change in forest floor vegetation is challenging because understory plants respond most directly to subcanopy conditions mediated by forest structure and composition. For example, dense forest canopies decrease forest floor light availability and buffer temperature extremes (Bramer et al., 2018), creating conditions suitable for forest specialists (Heinken et al., 2022). Forests are likely to change, in part due to long-lasting, time-lagged legacies of past human land use and management on forest density, composition, and disturbance probability in many regions (Bürgi et al., 2017; Stritih et al., 2021). Climate change will also alter forest trajectories through warming- and CO₂-induced increases in tree productivity (McDowell et al., 2020), increases in abiotic and biotic forest disturbances (Seidl et al., 2017), and upward shifts in tree line (Hansson et al., 2021). Together, direct effects of climate change (e.g., climatic warming), indirect effects of climate change mediated by forest change (e.g., increasing light availability at the forest floor due to increasing disturbances), and legacies of past land use (e.g., a densification of canopies with ongoing forest recovery or restoration efforts) will interact to affect future forest floor vegetation.

To date, most projections of understory species only account for the direct effects of climate change (Lembrechts et al., 2019), resulting in considerable uncertainty regarding the future of forest floor vegetation and diversity. Some studies have begun to address this knowledge gap by using current canopy cover or microclimate (e.g., near-ground temperature or moisture) as a proxy for future conditions (Lenoir et al., 2017; Slavich et al., 2014; Stark & Fridley, 2022), predicting understory communities under simple scenarios of overstory cover change (Mod & Luoto, 2016; Naqinezhad et al., 2022), or coupling climate and simulated forest change to predict future diversity (Thom et al., 2017). A central insight from these efforts is that incorporating fine-scale microclimate or forest drivers alters projections of future species distributions and persistence in ways that cannot be predicted from climate change alone (Lembrechts et al., 2019; Lenoir et al., 2017; Stark & Fridley, 2022). Yet, a synthetic understanding of how forest structure and composition are likely to change, how climate and forest change will jointly affect understory species distributions, and how individual species responses will shape future forest floor plant communities remains unresolved.

Here, we explored how coupled 21st-century climate and forest change interact to affect future forest floor plant communities in an 8645-ha protected mountain forest landscape (Berchtesgaden National Park, Germany; Figure 1), a hotspot of plant species richness in the northern front range of the Alps. Although protected in 1978, the forests in this landscape are still shaped by past legacies, resulting from centuries of timber production and grazing, as well as ongoing management activities in limited areas including ungulate

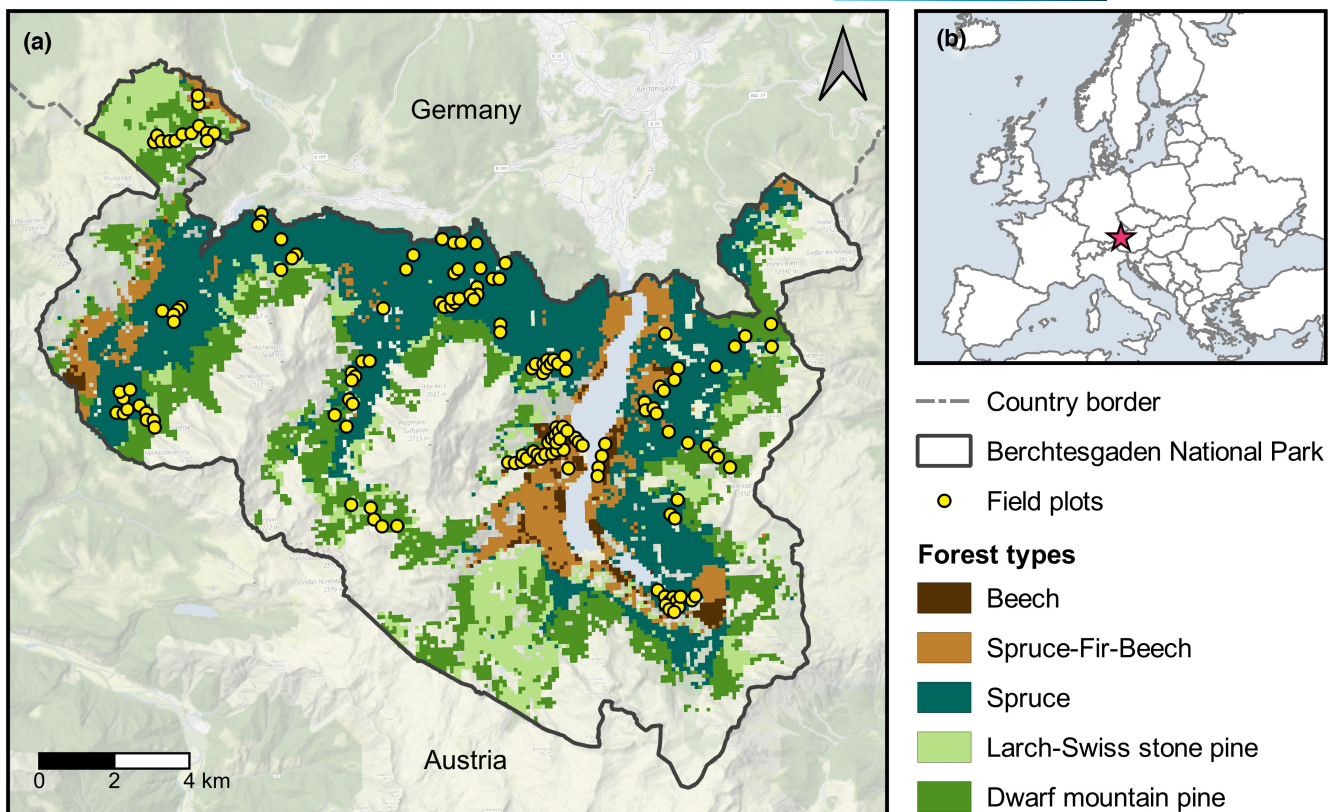


FIGURE 1 (a) Map of Berchtesgaden National Park, showing forest types and location of field plots where understory and forest inventory data was collected in 2021. (b) Location of Berchtesgaden National Park (pink star) in southeastern Germany. Map and data credits: Natural Earth, Open Street Map, QGIS, Stamen Design. Map lines delineate study areas and do not necessarily depict accepted national boundaries.

hunting, bark beetle mitigation, and forest restoration. We first fit correlative species distribution models (SDMs) for 248 understory plant species currently present in the landscape in response to historical climate, forest, and soil conditions. Future forest overstory change in the absence of management was then simulated under contrasting climate and disturbance scenarios with the individual-based forest landscape and disturbance model iLand (Seidl et al., 2012; Seidl & Rammer, 2023). Using projected climate and forest drivers as SDM inputs, we predicted emergent understory plant communities from individual species responses. We asked: (Q1) How do understory plant communities respond to 21st-century change in a topographically complex mountain landscape, representing a hotspot of plant species richness? We expected warmer temperatures to increase average understory alpha diversity because this is a cold-limited landscape (Vellend et al., 2017) and to lead to thermophilization of plant communities, indicated by increasing dominance of species that prefer warmer temperatures (Gottfried et al., 2012; Helm et al., 2017). We further expected more forest disturbances to increase average understory cover due to higher light availability at the forest floor (Halpern, 1989). However, we also expected to see fine-scale variation in community change, such as decreasing cover and diversity in areas where forest density and structural complexity increase due to recovery from past management or disturbance (Thom & Seidl, 2022). Finally, we expected to see greater changes

in community composition later in the 21st-century as climate departs further from historical baselines. We further asked: (Q2) How important are climatic changes (i.e., direct climate effects) versus forest structure and composition changes (i.e., indirect climate effects, as well as recovery from past land use) in driving understory responses at landscape scales? We expected understory community change to be driven more by changes in forests than by climate change, because forests alter light availability and moderate microclimate conditions directly experienced by forest floor vegetation (De Frenne et al., 2013).

2 | METHODS

2.1 | Study area

Berchtesgaden National Park comprises a cool temperate mountain landscape in the Northern Limestone Alps, in the southeastern tip of Germany along the border with Austria (Figure 1). The landscape is rugged and topographically complex, ranging from 603 to 2713 m in elevation (Nationalpark Berchtesgaden, 2023). Mean annual temperature decreases (7 to -2°C) and annual precipitation increases (1500–2600 mm) with elevation, and precipitation peaks during the summer. Soils are primarily derived from calcareous

limestone and dolomite, and shallow to intermediate depth Rendzic soil types and Cambisols cover much of the landscape (Nationalpark Berchtesgaden, 2023; Thom & Seidl, 2022).

The Park is 20,808ha in size, 44% of which is forested. Due to legacies of intensive timber harvest and replanting since the 1500s, much of today's forested area is dominated by structurally simple, homogeneous stands of Norway spruce [*Picea abies* (L.) Karst.]. Mixed deciduous forests dominated by European beech (*Fagus sylvatica* L.) can be found at lower elevations (submontane zone, <850m elevation). Silver fir (*Abies alba* Mill.) and European beech are locally abundant or intermixed with Norway spruce in montane forests (850–1400m elevation). Higher elevation (1400m to tree line) subalpine forests include open stands of European larch (*Larix decidua* L.), pockets of Swiss stone pine (*Pinus cembra* L.), and patches of dwarf mountain pine (*Pinus mugo* Turra) near upper tree line (~1800m; Figure 1a). Management ceased in a 13,860ha core zone following the creation of the national park in 1978, and over the past few decades forests have become more structurally complex and species rich (Thom & Seidl, 2022). Outside the core zone, management includes ungulate management (mainly hunting), bark beetle mitigation (bark or tree removal), and forest restoration (planting of tree species to restore natural assemblages). Cattle grazing is restricted to the management zone of the national park and occurs mainly in non-forested areas. Common natural disturbances include windstorms, bark beetle outbreaks, and avalanches, but disturbances tend to be small and affect a relatively low proportion of forested area (average 0.2% of area disturbed per year between 1986 and 2020, median patch size <1ha; Maroschek et al., 2023; Senf et al., 2017). Warmer climate, changes in timing and amount of precipitation, increasing disturbance impacts, and continuing recovery from past human land use are all expected to affect mountain forest development trajectories over the 21st century (Albrich et al., 2022; Dollinger et al., 2023; Thom et al., 2022).

Berchtesgaden National Park is situated in a European hotspot of plant species richness (Večeřa et al., 2019). This diversity reflects broad gradients in temperature, topography, and habitat type, coupled with high precipitation. The species pool includes many species characteristic of the northern Alps, but also relatively isolated populations of species mainly distributed in the southern and central Alps that only survived in a few northern locations following previous ice ages. A 2021 survey in Berchtesgaden National Park identified 27 forest understory species listed as threatened and 46 as extremely rare or near threatened on the German Red List.

2.2 | Simulation model overview and evaluation

We simulated forest change in Berchtesgaden National Park in the absence of future management using the individual-based forest landscape and disturbance model iLand. This process-based model simulates forest structure, functioning, and species composition as an emergent property of individual tree responses to competition, climate and environmental drivers, and disturbance

(Seidl et al., 2012; Thom et al., 2022). Competition for light is modeled at 2m horizontal resolution as a function of incoming radiation and shading by individual tree crowns. Light availability at the forest floor is further attenuated by the forest canopy and varies with height. Tree growth, mortality, and regeneration are dictated by species-specific responses to abiotic drivers such as light, temperature, and carbon dioxide concentration, as well as soil water and nutrient availability. Disturbances are spatially explicit, and effects depend on disturbance intensity, landscape context, species traits, and individual tree characteristics. For example, tree mortality due to wind disturbance varies with stand height, proximity to forest edge, and resistance to uprooting and stem breakage. In iLand, fallen spruce trees may then be colonized by the European spruce bark beetle (*Ips typographus* L.), which is the most important biotic disturbance agent in Europe (Patacca et al., 2023). Bark beetle spread and outbreak severity depend on temperature, beetle phenology, and the availability and defense of host trees above a size threshold. Full model documentation can be found online at <https://iland-model.org>.

The iLand model has been widely applied in forested landscapes across Central Europe (e.g., Petter et al., 2020; Thom et al., 2017), North America (e.g., Hansen et al., 2021; Turner et al., 2022), and Japan (Kobayashi et al., 2023). Over 30 Central European tree species have been parameterized, including all major and most minor tree species occurring in Berchtesgaden National Park. In evaluation simulations for Berchtesgaden National Park, iLand successfully reproduced expected productivity by species and stand age in comparison with independent forest inventory data, forest type in comparison with potential natural vegetation maps, and spatial patterns of wind and bark beetle disturbance in comparison with observed data (see supporting information in Thom et al., 2022 for detailed evaluations).

2.3 | Initial conditions and drivers

Spatially contiguous soil and forest conditions were previously derived for the forested area in Berchtesgaden National Park (8645ha) by Thom et al. (2022). Soil texture, depth, fertility, and carbon stocks were assigned (1-ha resolution) based on a soil type map (Konnert, 2004) and representative values from local or regional data (Seidl et al., 2009). Forest inventory data from 3559 regularly spaced plots collected between 2010 and 2012 were used in combination with a forest type map to initialize stand structure and tree species composition. Forest change was then simulated from 2011 to 2020 (Thom et al., 2022), and spatially explicit disturbances during this period were prescribed using remotely sensed data (Senf et al., 2017). The tree vegetation in the year 2020 served as the starting point for the current analysis.

Daily climate drivers (minimum and maximum temperature, precipitation, vapor pressure deficit, and solar radiation) were derived at 1-ha resolution for both historical (1980–2009) and future (2010–2100) periods (Thom et al., 2022). To estimate spatially explicit historical climate in this topographically complex landscape,



outputs from a 5-km spatial and 1-h temporal resolution dynamic regional climate model for Central Europe (Warscher et al., 2019) were bias corrected with data from 35 weather stations distributed throughout the watershed encompassing the national park and then interpolated to 100-m resolution at a daily timestep. Future regional climate change scenarios at 5-km spatial and daily temporal resolution were acquired from the Bayerisches Landesamt für Umwelt (Zier et al., 2020). Because these projections were coarse relative to the scale of the landscape, average daily climate change was computed for each scenario and used to offset 100-m resolution historical climate data, thus conserving the underlying topographic and temporal variation (see supporting information in Thom et al., 2022). For computational efficiency, climate data were further aggregated into 800 clusters characterized by consistent monthly climate values (Thom et al., 2022).

2.4 | Understory plant community and forest inventory data

Understory plant community data were collected during the 2021 growing season in a balanced sample of 150 forested plots stratified by elevation (50 each from submontane, montane, and subalpine zones) and development stage (10 per elevation zone from gap/regeneration, establishment, optimum, plenter/uneven-aged, and terminal/decay stages; Zenner et al., 2016) to represent the range of forest conditions present across Berchtesgaden National Park (Figure 1a). Understory plants were identified at the species level, and overlapping percent cover was recorded visually by species in square 200 m² plots using the Londo decimal scale (Londo, 1976). Additional information on individual species, including life form (fern, graminoid, herb, or shrub), Ellenberg indicator values (EIVs; Ellenberg et al., 2001; Ellenberg & Leuschner, 2010), and German Red List status, was compiled from the TRY Plant Trait Database (Kattge et al., 2011, 2020), Botanical Information Node Bavaria (Arbeitsgemeinschaft Flora von Bayern, 2023), and E.C.O. Institute for Ecology (personal communication, Tobias Köstl). Species were grouped into six plant functional types (PFTs) based on their EIVs for temperature and light (light: light-preferring or shade-tolerant; temperature: warm-preferring, cold-preferring, or indifferent; Table S2).

Forest inventory data and light measurements were collected in the 2021 growing season at the plot locations of the vegetation survey. Individual tree species and diameter at breast height (DBH) were recorded in variable radius subplots based on tree size (within a 500 m² circular plot all trees ≥ 20 cm DBH were recorded, within 150 m² trees ≥ 12 cm DBH, within 50 m² trees ≥ 6 cm DBH, and within 25 m² trees ≥ 0.2 m height). Light availability (total site factor [TSF]) was measured at plot center and 10 m from plot center in the four cardinal directions with a hemispheric photo taken with a Solariscope SOL 300 (Ing. Behling) two meters above ground. The best threshold separating canopy from sky was independently selected by three interpreters based on visual interpretation and

cross-checked for consistency. The most commonly selected threshold was used for each plot, or if there was high deviation ($\Delta\text{TSF} \geq 0.03$), a re-evaluation was performed before choosing the final threshold. Light measurements were averaged across the five measurements to represent the average light conditions per plot.

2.5 | Statistical modeling of understory plant communities

We fit random forest models to predict individual species presence and total understory percent cover as a function of climate, forest, and soil conditions (see [Supporting Information](#) for additional details). Understory species included only vascular plants and excluded trees (i.e., only ferns, graminoids, herbs, and shrubs were included), and models did not explicitly consider dispersal limitations. Species names were first reviewed to identify synonymous species, and individual SDMs were only fit for observations identified to the species level and for species that were present in at least five plots. This resulted in SDMs for 248 individual species (Table S2) out of a total of 445 unique understory species recorded in the field. Most species for which we did not fit an SDM (113 of 197 species not included in our models) were present in only one or two plots. Total understory cover was summed across all vascular understory plants, including those that were not modeled with individual SDMs. Percent cover could be greater than 100% because the cover of individual species can overlap.

We selected a set of potential climate, forest, and soil predictors based on drivers of biodiversity and species composition in the European Alps identified in recent studies (Chauvier et al., 2021; Helm et al., 2017; Thom et al., 2017), expectations for ecologically meaningful drivers of plant communities (Gardner et al., 2019; Landuyt et al., 2018), and available data at a comparable spatial resolution (Table S1; see also best practices outlined in Araújo et al., 2019). Climate and soil predictors were derived from the same datasets used to drive iLand simulations based on the location of plot centroids, with climate variables calculated as decadal averages from the most recent historical climate data (2000–2009). Forest predictors were derived from field data and included light availability. We identified a balanced set of three climate, three forest, and three soil variables to include as final model predictors based on a variable selection process. First, we identified highly correlated predictors (Pearson's $|r| > .7$); this included most climate predictors. Second, for forest predictors only, we fit initial random forest SDMs and identified the most important structure and composition predictors based on percent increase in mean-squared-error (%IncMSE; Figure S1). Final predictors (all pairwise $|r| < .7$) were selected based on a priori expectations about causal relationships and to provide contrasting predictive information within each category. Selected predictors were mean annual temperature (°C), summer precipitation sum (mm), and mean annual global radiation (MJ m² day⁻¹; climate); relative light availability at the forest floor (0–1), basal area (m² ha⁻¹),

and proportion beech (0–1; forest); and percent sand (%), water holding capacity (mm), and soil fertility (kg available N ha⁻¹; soil). All predictors were z-score standardized to have a mean of 0 and standard deviation of 1; if no trees were present, proportion beech was set to 0 (i.e., the mean value) after standardization.

To simultaneously evaluate individual species SDMs and plot-level predictions, we performed repeated subsampling into 70% training and 30% test data ($n=20$ subsamples, which ensured that test datasets included predictions for each individual species in each plot). Random forest models were fit using the randomForest package (Liaw & Wiener, 2002) in R 4.1.3 (R Core Team, 2022) with 1000 trees, node size of five, three predictors per split (number of predictors/3; Breiman, 2001), and weighted sampling of presences and absences to account for species prevalence (i.e., summed weight of presences = summed weight of absences). Individual SDMs were evaluated based on area under the receiving operator characteristic curve (AUC). We then stacked individual SDMs to derive community-level predictors of species richness and temperature EIV. Final species richness predictions were bias corrected to account for overestimation of richness due to weighted sampling, as well as overestimation of richness at low values and underestimation at high values. Specifically, we modeled differences between observed and predicted richness in the training data set and used parameters estimated from these models to adjust predicted richness (for detailed methods, see Calabrese et al., 2014; Zurell et al., 2020). To estimate community-level temperature EIV, we used probability ranking to determine the most likely species present in the community up to total richness (D'Amen et al., 2015) and calculated average temperature EIV across these species. Separate random forest models were fit to predict total understory percent cover. Richness, temperature EIV, and percent cover were evaluated based on goodness-of-fit (R^2) for test dataset predictions. Partial plots for each predictor were also evaluated to ensure they aligned with ecological expectations. Variable importance was assessed with %IncMSE.

Final models were fit to the full dataset. Models for species presence, bias corrected richness, temperature EIV, and percent cover were used to predict contemporary understory plant species communities at 10 m resolution across all forested areas in Berchtesgaden National Park ($n=864,466$ grid cells). Climate, soil, and forest predictors were consistent with the ones used as input for iLand. Field plots were generally representative of environmental and forest conditions across the full landscape (Figure S3). All predictors except light availability were rescaled to match standardized field data predictor values. Light availability derived from iLand is similar but not identical to field-measured TSF, so light availability was z-score standardized assuming field plots covered the range of light conditions present in the landscape.

Individual SDM fits varied among species (Table S2). We evaluated whether the inclusion of species with poorer model fits affected our overall results by generating a second set of predictions including only species with $AUC>0.7$ ($n=174$ species). All analyses were also re-run with species richness and temperature EIV derived from this subset of better-performing models.

2.6 | Simulation scenarios

We simulated a full factorial combination of two representative concentration pathways (RCPs), two general circulation models (GCMs), and two future disturbance scenarios ($n=8$ total scenarios, $2 \text{ RCP} \times 2 \text{ GCM} \times 2 \text{ disturbance}$) based on contrasts and key uncertainties in future change for this region (Zier et al., 2020). RCPs included RCP4.5 (warmer climate) and RCP8.5 (hotter climate, which most closely tracks current carbon emissions trajectories; Schwalm et al., 2020), with the respective changes in atmospheric CO₂ concentrations considered in the forest simulations with iLand. General circulation models were selected to include wetter (ICHEC-EC-EARTH) and drier (MPI-M-MPI-ESM-LR) scenarios (Zier et al., 2020). Mean annual temperature change between historical and late 21st-century (2091–2100) periods averaged +2.2°C (RCP4.5) and +5.1°C (RCP8.5), and summer precipitation either increased by 56 mm (ICHEC-EC-EARTH) or decreased by 109 mm (MPI-M-MPI-ESM-LR). Two wind disturbance scenarios were simulated, including baseline wind ("baseline disturbance"), in which historical wind frequency, timing, speed, and direction from 14 local weather stations were used to project future scenarios (Thom et al., 2022), and a uniform 15% increase in wind speed ("high disturbance"; Albrich et al., 2022), which is at the upper range of projected changes in wind speed in this region (Fink et al., 2009). Future forest change was simulated from initial conditions in 2020 until 2100 ($n=10$ replicates per scenario), and simulations also included dynamic bark beetle disturbances. We did not include future forest management or browsing in our simulations because we expect future management to be limited in this landscape.

2.7 | 21st-Century change in understory plant communities (Q1)

For each future simulation scenario, understory plant communities were predicted at 10 m resolution in Year 2050 (near-term change) and Year 2100 (long-term change). Future climate predictors were the averages of the preceding decade (e.g., 2041–2050 for 2050), and forest predictors were derived from simulated forest structure, composition, and light availability in the given year (e.g., 2050 for 2050). Richness, temperature EIV as an indicator of thermophilization, and total understory cover were averaged for each replicate ($n=80$; $2 \times \text{RCPs} \times 2 \text{ GCMs} \times 2 \text{ disturbance scenarios} \times 10 \text{ replicates}$) to analyze overall landscape trends.

To assess patterns and drivers of fine-scale change, we used Spearman's rank correlations and pairwise plots to evaluate relationships among response variables (richness, thermophilization, and cover), drivers, and elevation. We explored whether changes were consistent among responses, whether fine-scale changes in forest structure resulted in expected changes in cover and alpha diversity, and whether changes varied across the elevational gradient.



To evaluate shifts in plant community composition, temporal species turnover was calculated for each cell (Cleland et al., 2013):

$$\frac{\text{Number of new species} + \text{number of lost species in future climate year relative to 2020}}{\text{Total number of species in either 2020 or future climate year}} \times 100\%$$

We quantified gamma diversity for all species and by Red List category based on the number of species present anywhere in the full landscape. Species were further grouped by PFT or life form to examine temporal changes in group dominance across the elevational gradient and identify potential winners and losers under future change.

2.8 | Importance of climate versus forest change for future understory community change (Q2)

A random sample of 1000 10-m cells (minimum distance between samples = 100 m) was used to analyze the importance of climate versus forest change in driving understory change, while also considering the effect of local context. This sample represented the range of conditions in drivers and responses across the landscape (Figure S4). We predicted understory species richness, temperature EIV, and percent cover in each sampled cell under two climate levels (contemporary, future) and three forest levels (contemporary, baseline disturbance, high disturbance), using all four combinations of RCPs × GCMs. Because contemporary climate and contemporary forest conditions do not vary by RCP or GCM, this resulted in 21 total combinations (Table S3). For each future replicate, separate linear mixed effects models were fit explaining understory communities in 2050 and 2100 from forest change, climate change, and their interactions as fixed effects and sample cell number as a random effect (to account for variability due to local context). To address unequal variance among groups, a separate variance parameter was estimated for each fixed effect group using the nlme package in R (Pinheiro et al., 2022). Species richness was 1/square-root transformed and percent cover was square-root transformed to improve residual distributions. Some model residuals exhibited longer tails relative to normal distributions, but we concluded that model results were robust based on quantile-quantile plots and relative changes in group means (Pinheiro & Bates, 2000). Overall model fit and the relative contribution of fixed versus random effects were assessed with marginal and conditional R^2 (Nakagawa & Schielzeth, 2013). We quantified the relative and shared importance of drivers by fitting separate models for each fixed effect and calculating their contribution to marginal R^2 . Data and code that support the findings of this study are openly available at the Environmental Data Initiative (Braziunas et al., 2023).

3 | RESULTS

3.1 | Understory plant community statistical model evaluation

Individual SDMs fit test data well (overall $AUC=0.86$), although model fit varied among individual species (median $AUC=0.76$, range 0.36–0.99; Table S2). Community-level predictions were weak for species

richness ($R^2=.17$), moderate for total understory cover ($R^2=.51$), and strong for temperature EIV ($R^2=.75$; Figure 2). Model predictions

aligned well with the range of field observations (e.g., observed richness ranged from 18 to 83 species [mean 50] and predicted richness ranged from 29 to 77 species [mean 48]). Species responses to predictors were consistent with expectations based on PFTs (e.g., presence probability of light- and cold-preferring species increased with higher light availability and cooler temperatures; Figures S5–S10). Mean annual temperature was the most important overall predictor across individual SDMs, and light availability was the most important predictor for understory cover (Figure S11). Using only species with $AUC>0.7$ improved richness predictions ($R^2=.27$) but produced similar maps of contemporary species communities (Figure S12).

3.2 | Simulated future forests and disturbances

Forest basal area increased and Norway spruce dominance decreased over the 21st century, although the magnitude of change varied among scenarios (Figures S13 and S14). On average, 57% more basal area was killed by wind or bark beetles under high versus baseline disturbance scenarios. Basal area initially declined under high disturbance scenarios but subsequently increased later in the century. Norway spruce dominance declined more under high versus baseline disturbance and under hotter versus warmer climate, and basal area share of other dominant species such as European beech, European larch, and silver fir increased slightly under most scenarios. Median light availability at the forest floor increased slightly in 2050 due to increasing disturbances, but subsequently declined and was less variable across the landscape by 2100 due to the emerging young forests (Figure S4).

3.3 | 21st-Century change in understory plant communities (Q1)

Landscape mean species richness and understory cover declined over the 21st century, and plant communities were increasingly dominated by warm-adapted species (Figure 3). Changes were more pronounced in 2100 than 2050, and by 2100 all scenarios agreed on the direction of change except for warmer-wetter climate with high disturbances, in which richness slightly increased (Figure S15). The magnitude of relative change was similar for species richness (median 13% decline in richness across scenarios in 2100 relative to 2020) and thermophilization (12% increase), but lower for understory cover (8% decline). High disturbance scenarios dampened declines in understory cover in 2050 (median 2% vs. 5% decline in high versus baseline disturbance scenarios, respectively), but scenarios were more similar in 2100 (Figure 3).

Changes in understory plant communities were spatially and temporally variable (Figure 3). Declines in richness were weakly to

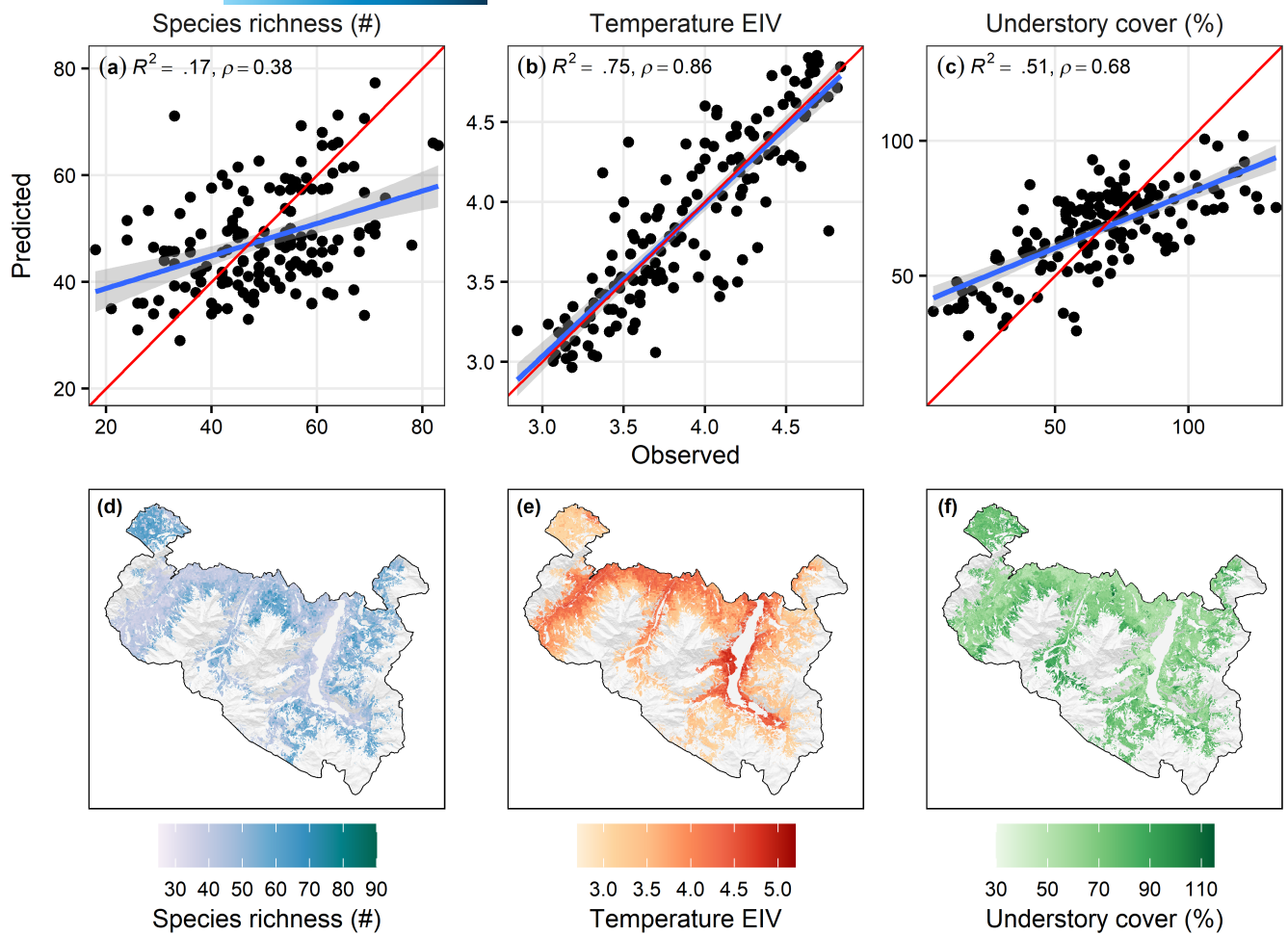


FIGURE 2 (a–c) Evaluation of model fit against holdout test data for (a) species richness and (b) mean temperature Ellenberg indicator value (EIV) derived from stacked individual species distribution models and for (c) total understorey cover from random forest regression models. Points are predicted versus observed values, red lines are 1:1 lines, and blue lines are linear regression fits with shaded confidence intervals; model goodness-of-fit (R^2) and Spearman's rank correction are shown. (d–f) Contemporary understorey plant community predictions in Berchtesgaden National Park for (d) species richness, (e) mean temperature EIV, and (f) total understorey cover.

moderately correlated with increasing thermophilization ($\rho = -0.36$ in 2050 and -0.51 in 2100) and declining cover ($\rho = 0.42$ in 2050 and 0.49 in 2100), but changes in thermophilization and cover were only very weakly correlated ($|\rho| < 0.20$; Figure S16). Changes in forest structure were strongly associated with changes in understorey cover (all $|\rho| > 0.64$) and weakly associated with richness ($|\rho| = 0.22\text{--}0.36$; Figure S17). Higher elevation areas tended to experience greater declines in richness ($\rho = -0.35$) and more thermophilization ($\rho = 0.42$) by 2100 (Figure S18). This resulted in an average 16% decline in richness and 17% increase in EIV temperature in subalpine forests between 2020 and 2100. Changes in forest structure and composition also tended to be more pronounced at high (e.g., basal area, light availability) and low (e.g., basal area, proportion beech) elevations. In most cases, pairwise correlations among responses and along the elevational gradient strengthened in 2100 relative to 2050.

Understorey plant communities experienced high rates of turnover (mean plot-level turnover was 51% in 2050 and 62% in 2100), and species composition shifted over the 21st century (Figures 4 and 5). Subalpine areas in 2100 had the highest turnover relative

to contemporary plant communities. Across the entire landscape, gamma diversity declined by an average of 2 species between 2020 and 2050 and by 19 species between 2020 and 2100, representing 1% and 8% of the current species pool, respectively. Hotter climate exacerbated species losses in 2100 (~15% of the current species pool), especially under hotter-drier scenarios (~25%). Proportional species losses were similar regardless of German Red List status (Figure S19). Light- and cold-preferring species decreased in relative dominance (mean proportion declined by 48% [0.176 to 0.091] from 2020 to 2100), while shade-tolerant, warm-preferring or temperature-indifferent species comprised a larger proportion of future plant communities. Species communities became more similar across elevation zones over the 21st century based on the relative dominance of PFT groups, and the greatest shifts in PFT composition occurred in subalpine areas (Figure 4). The relative dominance of life forms changed little between contemporary and future plant communities (Figure S20).

Results were qualitatively consistent when understorey community change was projected using only species with individual SDM

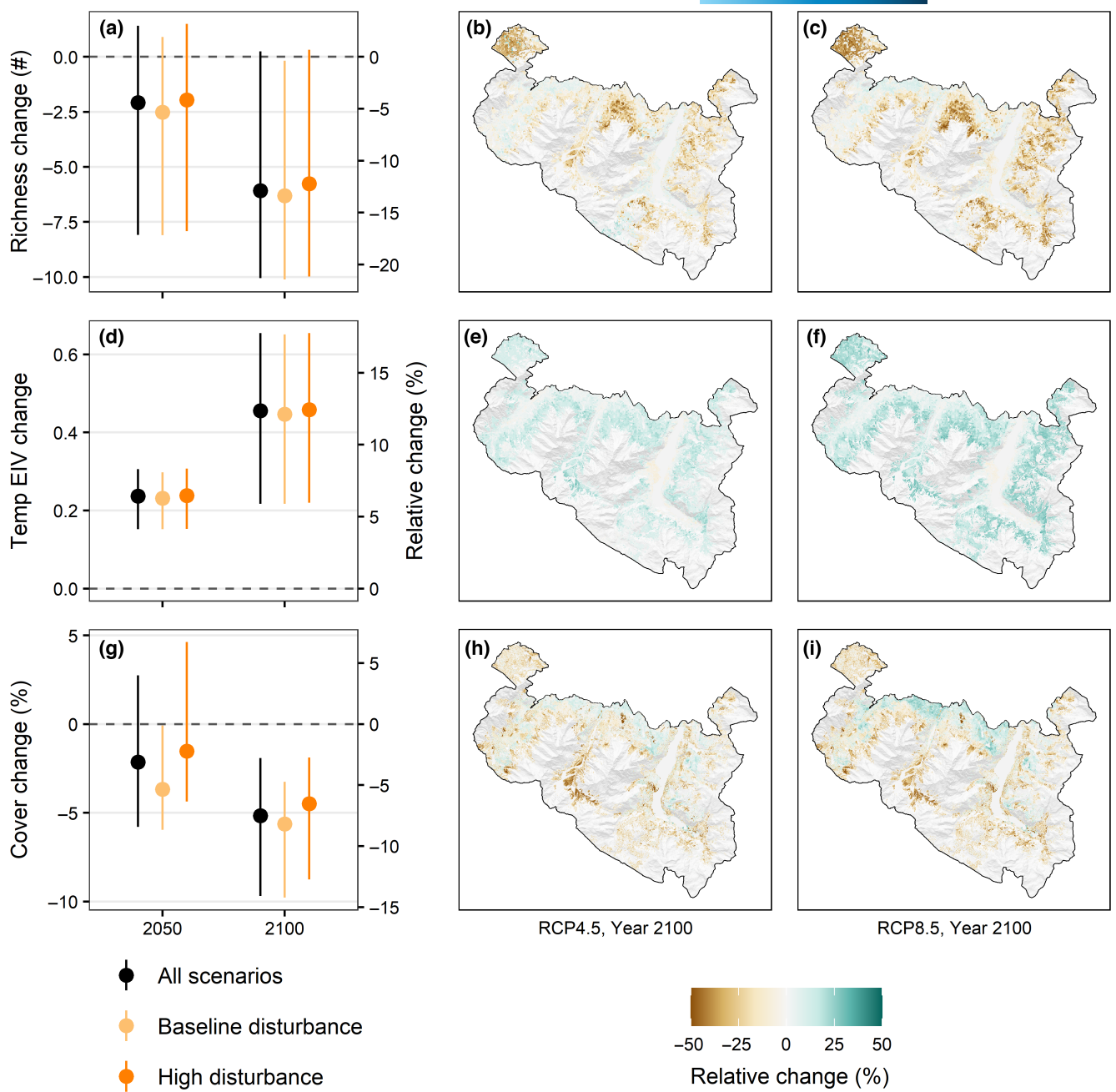


FIGURE 3 Change in (a–c) species richness, (d–f) mean temperature Ellenberg indicator value (EIV), and (g–i) total understory cover relative to contemporary plant communities in 2020. Left column (a, d, g) shows near-term (2050) and long-term (2100) change in landscape mean values for all scenarios (pooled across both GCMs, both RCPs, and both disturbance scenarios) and for different disturbance scenarios. Dashed lines at 0 show relative position of 2020 values, points are median change, and point ranges are 5th to 95th percentile change across scenarios. See Figure S15 for changes in each climate × disturbance scenario. Right two columns (b, c, e, f, h, i) show change at 10 m spatial resolution in 2100 relative to the 2020 landscape mean value under warmer (RCP4.5) or hotter (RCP8.5) climate scenarios (pooled across GCMs and disturbance levels). Values <-50% and >50% are truncated to this minimum and maximum. GCM, general circulation model; RCP, representative concentration pathways.

AUC > 0.7 (Figures S21–S23). Based on this species subset, relative changes in richness (-18% in 2100), thermophilization (+17%), and turnover (66%) were all projected to be slightly more extreme than the full SDM ensemble, and all scenarios agreed on the direction of change by 2100.

3.4 | Importance of climate versus forest change for future understory community change (Q2)

Climate change was the more dominant driver of changes in species richness and thermophilization in 2050 and 2100 (climate relative

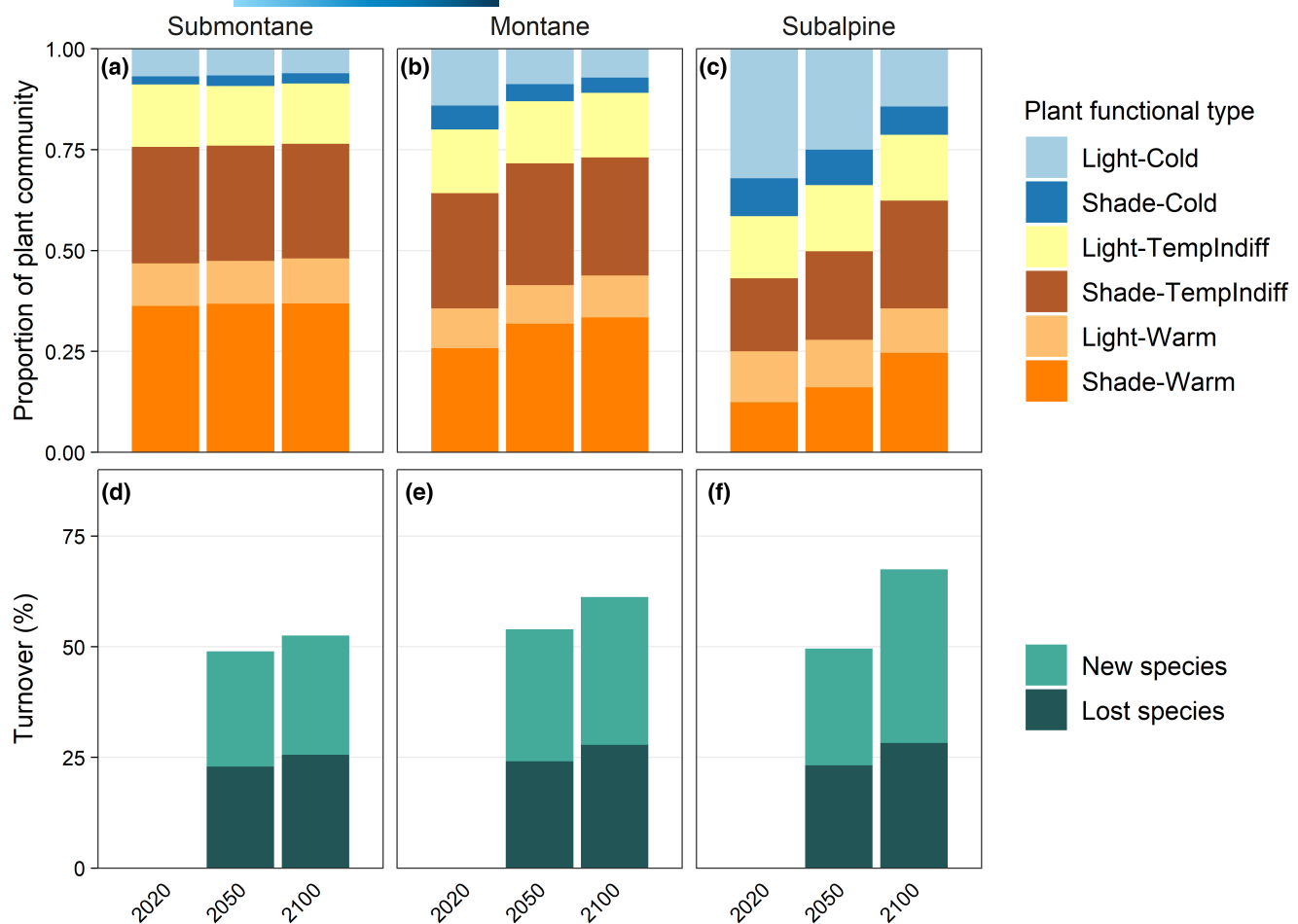


FIGURE 4 (a–c) Change in relative dominance of plant functional types in (a) submontane, (b) montane, and (c) subalpine elevation zones between contemporary and future time periods, pooled across all climate and disturbance scenarios. Dominance is calculated from species presence at 10 m resolution. (d–f) Turnover in species communities at 10 m resolution relative to contemporary 2020 understory plant communities, grouped by elevation zone [(d) submontane; (e) montane; (f) subalpine]. Turnover is the sum of new plus lost species divided by the total species pool $\times 100\%$. TemplIndiff, indifferent to temperature.

importance=0.89–0.96), and of changes in understory cover in 2100 (climate relative importance=0.50, **Table 1**; **Figure S24**). Forest and climate change were similarly important for percent cover change in 2050, and relative importance of climate versus forest change varied among simulation replicates (**Table S4**). The magnitude of change in understory plant communities was always greater under drier versus wetter future climate regardless of disturbance scenario, although the effects of hotter versus warmer climate were more variable (**Figure S15**). Fixed effects of climate and forest change explained slightly more variation in late-compared to mid-century models (average marginal $R^2_{\text{fixed}} = 0.03$ in 2050 and 0.06 in 2100), whereas the random effect of sample cell (i.e., local context) showed the opposite trend (average conditional $R^2_{\text{total}} = 0.64$ in 2050 and 0.50 in 2100; **Table 1**; **Table S4**). Results were similar for analyses using only species with individual SDM AUC>0.7 (**Table S5**).

4 | DISCUSSION

Our results suggest that protected mountain forests in a hotspot of plant diversity may be unable to maintain historical biodiversity

given unabated 21st-century climate and forest change. By 2100, alpha diversity and understory cover declined and forest floor communities thermophilized and homogenized across most scenarios, which bracketed potential changes in temperature, precipitation, and disturbance. High-elevation areas were most vulnerable to change, with the highest rates of turnover, most thermophilization, and greatest shifts in PFT composition. Under the combination of increasing temperatures and densifying forests, shade-tolerant, warm-preferring species successively replaced light- and cold-preferring species. Near-term (i.e., 2050) changes in understory plant communities were more subtle, and available ecological niches enabled almost all species to persist at least somewhere in the landscape. However, declines in gamma diversity of the existing species pool were over nine times higher in 2100 and more than doubled under hotter versus warmer climate, suggesting that the pace of species loss could accelerate nonlinearly if climate change continues unabated. Climate rather than forest change was the dominant driver of understory change and the importance of local context in determining forest floor vegetation variability declined over time. As climate warming intensifies, forest ecosystems in the

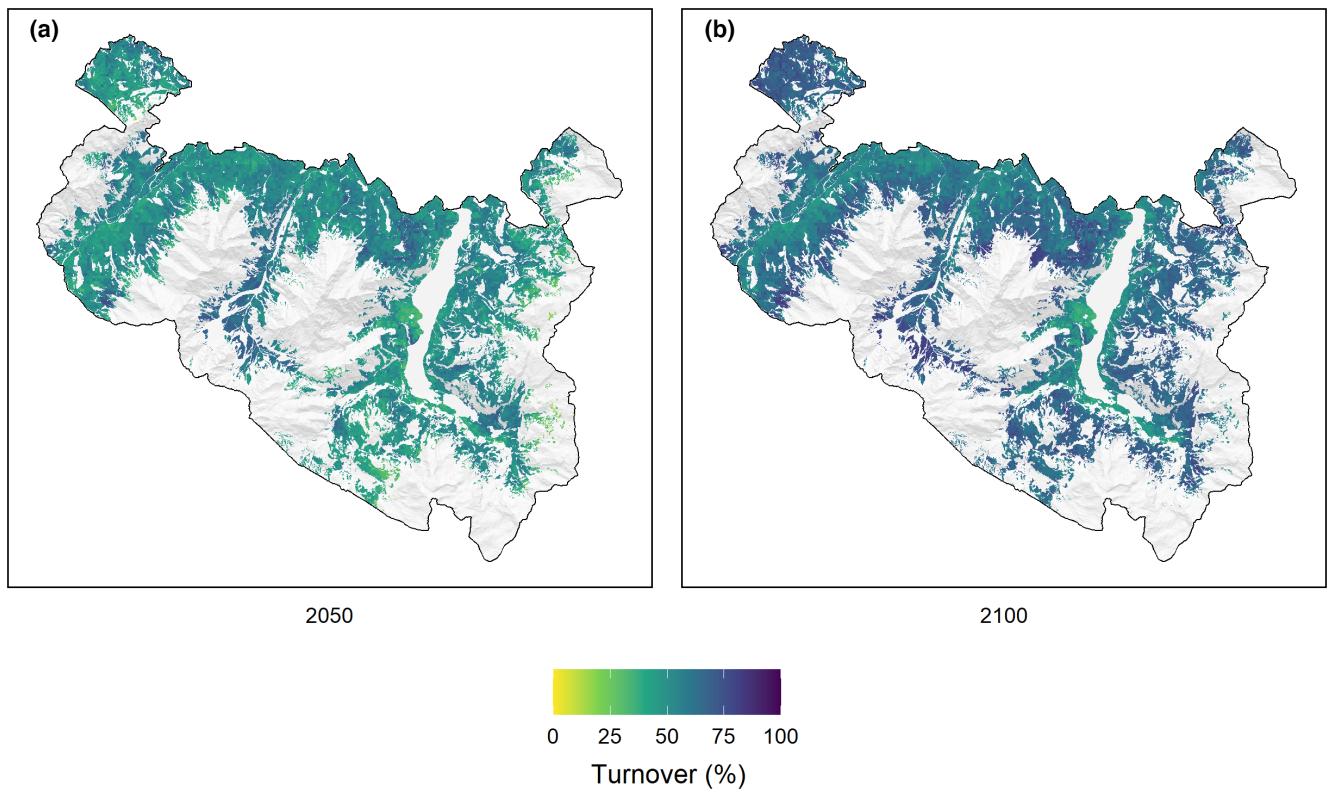


FIGURE 5 Turnover in species communities at 10 m resolution under (a) near-term change (2050) and (b) long-term change (2100) relative to contemporary 2020 understory plant communities, pooled across all climate and disturbance scenarios. Turnover is the sum of new plus lost species divided by the total species pool × 100%.

TABLE 1 Average linear mixed effects model fits ($n=10$ models for each response \times year) and relative importance of forest versus climate drivers of understory community change.

Understory community response	Year	R^2_{fixed} mean (SE)	R^2_{total} mean (SE)	Forest relative importance mean (SE)	Climate relative importance mean (SE)
Species richness	2050	0.02 (0.00)	0.56 (0.00)	0.11 (0.02)	0.89 (0.02)
Temperature EIV	2050	0.05 (0.00)	0.81 (0.00)	0.06 (0.00)	0.94 (0.00)
Understory cover	2050	0.01 (0.00)	0.54 (0.01)	0.51 (0.04)	0.49 (0.04)
Species richness	2100	0.04 (0.00)	0.45 (0.00)	0.03 (0.00)	0.96 (0.00)
Temperature EIV	2100	0.12 (0.00)	0.67 (0.00)	0.05 (0.00)	0.95 (0.00)
Understory cover	2100	0.02 (0.00)	0.38 (0.01)	0.29 (0.04)	0.50 (0.05)

Abbreviations: EIV, Ellenberg indicator value; R^2_{fixed} , marginal R^2 , variance explained by fixed effects; R^2_{total} , conditional R^2 , variance explained by full model, including random effect of sample cell number; SE, standard error among $n=10$ models fit to each replicate.

northern front range of the Alps may be locked into unavoidable patterns of diversity decline, which could also result in substantial functional change at the ecosystem level.

4.1 | Future forest floor vegetation trajectories were robust across scenarios

Future climate and disturbance scenarios generally agreed on the overall direction of understory plant community change, reflecting underlying changes in the dominant drivers of species presence

and understory cover. Counter to our expectations, alpha diversity decreased with climate warming, except when precipitation increased in concert with lower carbon emissions (ICHEC-EC-EARTH under RCP4.5). Although species diversity and richness are positively associated with higher temperatures at the global scale, the strength and direction of this relationship varies across scales, and is modulated by local context and other drivers (Field et al., 2009; Vellend et al., 2017). We only considered diversity in forested areas, and richness was highest in higher elevation forests and decreased with warming temperatures in our contemporary landscape. These patterns are consistent with hump-shaped

relationships between richness and elevation often found in mountains (Körner, 2004; Liang et al., 2020). They furthermore align with increasing plant diversity near mountain forest edges (Pöpperl & Seidl, 2021) and prevalent cold-adapted and endemic species refugia in the European Alps (Tribsch & Schönswetter, 2003). Our findings challenge assumptions that warming will increase plot-level richness in a cold-limited, temperate forested landscape with historically high precipitation (Sommer et al., 2010; Vellend et al., 2017). However, it is important to note that we only included species currently present in the landscape and did not simulate tree line shifts (for further discussion, see Section 4.4). Mapping patterns and evaluating drivers of contemporary species diversity at high spatial resolution (e.g., Figure 2; Figure S11) can improve inferences about whether a protected landscape is likely to maintain, decrease, or increase in its future species diversity.

As expected, understory communities were increasingly dominated by warm-adapted species in our simulations. Thermophilization of plant communities has been observed in recent decades in mountains and other ecoregions (Gottfried et al., 2012; Helm et al., 2017), and disturbances and higher light availability accelerate forest understory thermophilization rates (Govaert et al., 2021; Stevens et al., 2015). Differences between wetter and drier climate scenarios suggest that reduced moisture availability could interact with warming to enhance compositional shifts toward thermophilic species dominance. Patterns of species turnover indicate that contemporary plant communities were not completely replaced but rather reshuffled, with future communities including both new and retained species. These potentially novel species assemblages could interact in surprising ways that complicate projections of future change, challenge conservation planning efforts, and alter ecosystem functioning and services (Radeloff et al., 2015; Williams & Jackson, 2007).

Changes in understory cover were more sensitive to disturbance scenario in 2050 than in 2100, likely reflecting interactions between disturbances and land use legacies. Initial declines in tree basal area and dampened declines in understory percent cover under high disturbance scenarios suggest that the contemporary forested landscape is more susceptible to disturbance than the late-century landscape. Long land use legacies in the area of Berchtesgaden National Park and across Europe have promoted structurally and compositionally homogenous, contiguous, dense forests (Bebi et al., 2017; Nationalpark Berchtesgaden, 2023), which are especially vulnerable to wind and insect disturbance when trees are large (Seidl et al., 2011; Stritih et al., 2021). Overall declines in average understory cover can be explained by low area disturbed relative to total landscape area, rapid tree recovery and canopy closure in previously disturbed areas, and increasing forest extent and density (e.g., due to recovery from historical land use; Thom & Seidl, 2022). We note that forest simulations did not include competition between understory plants and regenerating trees, which could alter landscape trajectories. For example, high understory biomass can inhibit post-disturbance forest recovery, leading to sustained dominance of understory communities (Thriplleton et al., 2018). Future

studies should explicitly consider understory-tree interactions in projections of forest plant community change (Landuyt et al., 2018).

4.2 | High-elevation areas were most vulnerable to change

Understory change was particularly pronounced at high elevations, with increasing homogenization of plant communities across the elevational gradient over time. Changes in climate and forest drivers will not occur evenly across mountain landscapes, varying with elevation, topography, and current vegetation conditions (Gobiet et al., 2014; Thom & Seidl, 2022). For example, contemporary subalpine forests in our landscape are semi-open areas with high light availability, high plant diversity, and more opportunities for tree infilling than comparatively denser montane forests. Substantial changes in forest structure with elevation can therefore drive high magnitudes of change in biodiversity and community composition. Light- and cold-preferring species were especially vulnerable to loss (consistent with Gottfried et al., 2012; Rumpf et al., 2018; Verheyen et al., 2012), suggesting that enhanced microclimate temperature buffering under densifying forest canopies is unlikely to benefit shade-intolerant species. Over time, subalpine community composition may more closely resemble montane areas (Savage & Vellend, 2015). How these increasingly functionally homogeneous plant communities will affect future ecosystem functioning, services, and resilience is uncertain and warrants further research (Clavel et al., 2011).

4.3 | Climate change was the most important driver of average understory responses

In contrast to our expectations, direct effects of climate change were more important than forest change in explaining average understory change, except for near-term (2050) change in percent cover. This likely reflects the magnitude of climate versus forest change represented by our scenarios, in which mean annual temperature departed more from historical distributions than basal area (Figure S4). Furthermore, changes in future precipitation are highly uncertain in the Alps (Gobiet et al., 2014), yet have important ecological consequences (e.g., resulting in over 300% higher losses of alpha and gamma diversity in drier versus wetter scenarios by 2100 in our simulations). The effects of forest change would likely be more prominent in landscapes vulnerable to extensive forest to non-forest conversion (e.g., due to increases in wildfire activity; Turner et al., 2022). At fine spatial scales, forest drivers were important predictors of species presence and understory cover and were closely associated with understory change. Variability in forest conditions in our landscape also likely contributed to lagged responses in gamma diversity change under near-term change or warmer versus hotter climate by maintaining refugia for climate-sensitive species (Richard et al., 2021; Stark & Fridley, 2022).

4.4 | Limitations

We did not consider the potential influx of new species, which could affect expectations about richness and higher rates of change at high elevations. However, our landscape represents most of the elevational gradient, forest types, and forest understory species pool present in this region. Higher rates of compositional change at high versus low elevations have also been documented in observational studies (Bertrand et al., 2011; Savage & Vellend, 2015), and average turnover is similar to late-century projections for this biogeographical region (Thuiller et al., 2005), suggesting that our findings are robust. Other factors not considered here, such as long-distance or human-mediated dispersal of new, invasive species, could nevertheless catalyze rapid and widespread plant community change (Simberloff, 2010; Vellend et al., 2017). Furthermore, dispersal limitations of the existing species pool were not explicitly considered in our predictive models. Projected diversity declines for the current species pool are therefore conservative, as accounting for dispersal could limit the ability of species movement to favorable sites (Franklin et al., 2016).

We made some simplifying assumptions for this study, such as omitting species that occurred in fewer than five plots. We prioritized using recently collected, high quality and high resolution data (i.e., individual species, presence-absence, stratified sampling design, forest inventory data recorded on the same plot), and the 248 included species captured 96% of average plot-level species richness. SDMs were fit with random forests, which do not enable extrapolation beyond the set of conditions for which they are trained. Projections are therefore less reliable at lower elevations where future mean annual temperature exceeded historical values, and species losses could be higher than estimated (Thuiller et al., 2004). We did not simulate upward shifts in tree line and restricted our projections to forested areas. This may partly account for low variance explained for species richness predictions, compared to models including different land cover types. Other studies that predicted understory plant diversity only within forests had similar, low R^2 values (Thom et al., 2017; Zellweger et al., 2015). We evaluated the uncertainty associated with poorer model fits by re-running all analyses with only species with SDM AUC > 0.7, which improved species richness R^2 but produced consistent results and did not change the main findings. Finally, we did not consider other drivers of change that are important for understory composition, such as nitrogen deposition (Rumpf et al., 2018; Verheyen et al., 2012) or herbivory (Suzuki et al., 2013).

4.5 | Implications for conserving plant diversity under global change

To conserve biodiversity, targets need to consider more than amount of area protected (Maxwell et al., 2020), because today's biodiversity hotspots are vulnerable to future change (Lawler et al., 2015). Our results suggest that protected mountain forest landscapes may

buffer understory communities (sensu Richard et al., 2021) against near-term climate change (i.e., until 2050) or moderate warming scenarios if precipitation also increases, and that Red List species were not consistently more vulnerable to loss in our highly heterogeneous landscape. However, over longer timescales and more extreme changes in climate, conservation efforts must consider and plan for potential changes in species communities. This could entail prioritizing greater connectivity along migration corridors for species tracking climate change (Littlefield et al., 2019; Parks et al., 2023), supporting processes that enable ecosystems to self-organize and adapt to change (e.g., allowing natural disturbances and regeneration to create fine-scale heterogeneity; Filotas et al., 2014; Sallou & Strith, 2023), and monitoring multiple metrics of biodiversity (Maxwell et al., 2020). Priority should be given to protecting areas likely to harbor high levels of biodiversity as climate warms, such as environmentally complex landscapes with abundant microrefugia (Dobrowski, 2011; Thom et al., 2017). Nonetheless, without proactive climate change mitigation, protected areas may be unable to sustain historical biodiversity. In a biodiversity hotspot, we found the forest understory species communities declined in alpha and gamma diversity, were increasingly dominated by warm-adapted species, and homogenized across elevation. Subalpine forests were at particular risk for understory plant community change, highlighting a priority ecosystem for future conservation efforts. Mountain landscapes may buffer plant biodiversity against moderate, but not strong, changes in climate, and accelerating species losses are likely under 21st-century change.

AUTHOR CONTRIBUTIONS

Kristin H. Braziunas: Conceptualization; data curation; formal analysis; methodology; visualization; writing – original draft. **Lisa Geres:** Data curation; investigation; writing – review and editing. **Tobias Richter:** Data curation; investigation; writing – review and editing. **Felix Glasmann:** Data curation; writing – review and editing. **Cornelius Senf:** Data curation; investigation; methodology; writing – review and editing. **Dominik Thom:** Data curation; software; writing – review and editing. **Sebastian Seibold:** Investigation; project administration; writing – review and editing. **Rupert Seidl:** Conceptualization; funding acquisition; methodology; project administration; software; supervision; writing – original draft.

ACKNOWLEDGMENTS

We are grateful to the TRY Plant Trait Database for understory species trait data and to Lawinenwarndienst Bayern (www.lawinenwarndienst-bayern.de) for providing weather station data for Berchtesgaden National Park. Understory field data was collected by the E.C.O. Institute for Ecology. We thank all students, Anna-Maria Bachleitner (project manager), and Robin Reiter (field technician) for supporting and conducting the forest inventory and light measurements in 2021. We thank Marc Grüning for statistical advice in developing species distribution models and three anonymous reviewers for comments that improved this manuscript. Funding support for this project was provided by the European Research

Council under the European Union's Horizon 2020 research and innovation program (Grant Agreement 101001905). Support for data collection, LG, and TR was provided by the "Climate Change Research Initiative of the Bavarian National Parks" funded by the Bavarian State Ministry of the Environment and Consumer Protection. Open Access funding enabled and organized by Projekt DEAL.

CONFLICT OF INTEREST STATEMENT

The authors declare no conflict of interest.

DATA AVAILABILITY STATEMENT

Data and code that support the findings of this study are openly available at the Environmental Data Initiative at <https://doi.org/10.6073/pasta/06954751c87ea7695dd043844e2745f9>.

ORCID

Kristin H. Braziunas  <https://orcid.org/0000-0001-5350-8463>

Lisa Geres  <https://orcid.org/0009-0009-8251-135X>

Dominik Thom  <https://orcid.org/0000-0001-8091-6075>

Rupert Seidl  <https://orcid.org/0000-0002-3338-3402>

REFERENCES

- Albrich, K., Seidl, R., Rammer, W., & Thom, D. (2022). From sink to source: Changing climate and disturbance regimes could tip the 21st century carbon balance of an unmanaged mountain forest landscape. *Forestry: An International Journal of Forest Research*, 95(5), 742. <https://doi.org/10.1093/forestry/cpac033>
- Araújo, M. B., Anderson, R. P., Barbosa, A. M., Beale, C. M., Dormann, C. F., Early, R., Garcia, R. A., Guisan, A., Maiorano, L., Naimi, B., O'Hara, R. B., Zimmermann, N. E., & Rahbek, C. (2019). Standards for distribution models in biodiversity assessments. *Science Advances*, 5(1), aat4858. <https://doi.org/10.1126/sciadv.aat4858>
- Arbeitsgemeinschaft Flora von Bayern. (2023). Botanischer Informationsknoten Bayern. Staatliche Naturwissenschaftliche Sammlungen Bayerns. <http://daten.bayernflora.de>
- Baines, D., Moss, R., & Dugan, D. (2004). Capercaille breeding success in relation to forest habitat and predator abundance. *Journal of Applied Ecology*, 41(1), 59–71. <https://doi.org/10.1111/j.1365-2664.2004.00875.x>
- Bebi, P., Seidl, R., Motta, R., Fuhr, M., Firm, D., Krumm, F., Conedera, M., Ginzler, C., Wohlgemuth, T., & Kulakowski, D. (2017). Changes of forest cover and disturbance regimes in the mountain forests of the Alps. *Forest Ecology and Management*, 388, 43–56. <https://doi.org/10.1016/j.foreco.2016.10.028>
- Bertrand, R., Lenoir, J., Piedallu, C., Dillon, G. R., Ruffray, P. D., Vidal, C., Pierrat, J. C., & Gégout, J. C. (2011). Changes in plant community composition lag behind climate warming in lowland forests. *Nature*, 479(7374), 517–520. <https://doi.org/10.1038/nature10548>
- Bramer, I., Anderson, B. J., Bennie, J., Bladon, A. J., De Frenne, P., Hemming, D., Hill, R. A., Kearney, M. R., Körner, C., Korstjens, A. H., Lenoir, J., Maclean, I. M. D., Marsh, C. D., Morecroft, M. D., Ohlemüller, R., Slater, H. D., Suggitt, A. J., Zellweger, F., & Gillingham, P. K. (2018). Chapter three—Advances in monitoring and modelling climate at ecologically relevant scales. In D. A. Bohan, A. J. Dumbrell, G. Woodward, & M. Jackson (Eds.), *Next generation biomonitoring: Part 1* (Vol. 58, pp. 101–161). Academic Press. <https://doi.org/10.1016/bs.aecr.2017.12.005>
- Braziunas, K. H., Geres, L., Richter, T., Glasemann, F., Senf, C., Thom, D., Seibold, S., & Seidl, R. (2023). Projected climate and canopy change lead to thermophilization and homogenization of forest floor vegetation in a hotspot of plant species richness. Berchtesgaden National Park, Bavaria, Germany ver 1 [Data set]. Environmental Data Initiative. <https://doi.org/10.6073/pasta/06954751c87ea7695dd043844e2745f9>
- Breiman, L. (2001). Random forests. *Machine Learning*, 45, 5–32. <https://doi.org/10.1023/A:1010933404324>
- Bürgi, M., Östlund, L., & Mladenoff, D. J. (2017). Legacy effects of human land use: Ecosystems as time-lagged systems. *Ecosystems*, 20(1), 94–103. <https://doi.org/10.1007/s10021-016-0051-6>
- Calabrese, J. M., Certain, G., Kraan, C., & Dormann, C. F. (2014). Stacking species distribution models and adjusting bias by linking them to macroecological models. *Global Ecology and Biogeography*, 23(1), 99–112. <https://doi.org/10.1111/geb.12102>
- Carrer, M., Dibona, R., Prendin, A. L., & Brunetti, M. (2023). Recent waning snowpack in the Alps is unprecedented in the last six centuries. *Nature Climate Change*, 13(2), 155–160. <https://doi.org/10.1038/s41558-022-01575-3>
- CBD. (2021). *First draft of the post-2020 global biodiversity framework*. CBD/WG2020/3/3. Convention on Biological Diversity.
- Chauvier, Y., Thuiller, W., Brun, P., Lavergne, S., Descombes, P., Karger, D. N., Renaud, J., & Zimmermann, N. E. (2021). Influence of climate, soil, and land cover on plant species distribution in the European Alps. *Ecological Monographs*, 91(2), e01433. <https://doi.org/10.1002/ecm.1433>
- Clavel, J., Julliard, R., & Devictor, V. (2011). Worldwide decline of specialist species: Toward a global functional homogenization? *Frontiers in Ecology and the Environment*, 9(4), 222–228. <https://doi.org/10.1890/080216>
- Cleland, E. E., Collins, S. L., Dickson, T. L., Farrer, E. C., Gross, K. L., Gherardi, L. A., Hallett, L. M., Hobbs, R. J., Hsu, J. S., Turnbull, L., & Suding, K. N. (2013). Sensitivity of grassland plant community composition to spatial vs. temporal variation in precipitation. *Ecology*, 94(8), 1687–1696. <https://doi.org/10.1890/12-1006.1>
- D'Amen, M., Dubuis, A., Fernandes, R. F., Pottier, J., Pellissier, L., & Guisan, A. (2015). Using species richness and functional traits predictions to constrain assemblage predictions from stacked species distribution models. *Journal of Biogeography*, 42(7), 1255–1266. <https://doi.org/10.1111/jbi.12485>
- De Frenne, P., Rodríguez-Sánchez, F., Coomes, D. A., Baeten, L., Verstraeten, G., Vellen, M., Bernhardt-Römermann, M., Brown, C. D., Brunet, J., Cornelis, J., Decocq, G. M., Dierschke, H., Eriksson, O., Gilliam, F. S., Hédl, R., Heinken, T., Hermy, M., Hommel, P., Jenkins, M. A., ... Verheyen, K. (2013). Microclimate moderates plant responses to macroclimate warming. *Proceedings of the National Academy of Sciences of the United States of America*, 110(46), 18561–18565. <https://doi.org/10.1073/pnas.1311190110>
- Dirnböck, T., Kraus, D., Grote, R., Klatt, S., Kobler, J., Schindlbacher, A., Seidl, R., Thom, D., & Kiese, R. (2020). Substantial understory contribution to the C sink of a European temperate mountain forest landscape. *Landscape Ecology*, 35(2), 483–499. <https://doi.org/10.1007/s10980-019-00960-2>
- Dobrowski, S. Z. (2011). A climatic basis for microrefugia: The influence of terrain on climate. *Global Change Biology*, 17(2), 1022–1035. <https://doi.org/10.1111/j.1365-2486.2010.02263.x>
- Dollinger, C., Rammer, W., & Seidl, R. (2023). Climate change accelerates ecosystem restoration in the mountain forests of Central Europe. *Journal of Applied Ecology*, 60(12), 2665–2675. <https://doi.org/10.1111/1365-2664.14520>
- Ellenberg, H., Düll, R., Wirth, V., Werner, W., & Paulissen, D. (2001). *Zeigerwerte von Pflanzen in Mitteleuropa* (3rd ed.). Scripta Geobotanica XVIII. Verlag Erich Goltze GmbH & Co. KG.

- Ellenberg, H., & Leuschner, C. (2010). *Vegetation Mitteleuropas mit den Alpen in ökologischer, dynamischer und historischer Sicht* (6th ed.). UTB.
- Elliott, K. J., Vose, J. M., Knoepp, J. D., Clinton, B. D., & Kloeppe, B. D. (2015). Functional role of the herbaceous layer in eastern deciduous forest ecosystems. *Ecosystems*, 18(2), 221–236. <https://doi.org/10.1007/s10021-014-9825-x>
- Field, R., Hawkins, B. A., Cornell, H. V., Currie, D. J., Diniz-Filho, J. A. F., Guégan, J. F., Kaufman, D. M., Kerr, J. T., Mittelbach, G. G., Oberdorff, T., O'Brien, E. M., & Turner, J. R. G. (2009). Spatial species-richness gradients across scales: A meta-analysis. *Journal of Biogeography*, 36(1), 132–147. <https://doi.org/10.1111/j.1365-2699.2008.01963.x>
- Filotas, E., Parrott, L., Burton, P. J., Chazdon, R. L., Coates, K. D., Coll, L., Haeussler, S., Martin, K., Nocentini, S., Puettmann, K. J., Putz, F. E., Simard, S. W., & Messier, C. (2014). Viewing forests through the lens of complex systems science. *Ecosphere*, 5(1), 1–23. <https://doi.org/10.1890/ES13-00182.1>
- Fink, A. H., Brücher, T., Ermert, V., Krüger, A., & Pinto, J. G. (2009). The European storm Kyrill in January 2007: Synoptic evolution, meteorological impacts and some considerations with respect to climate change. *Natural Hazards and Earth System Sciences*, 9(2), 405–423. <https://doi.org/10.5194/nhess-9-405-2009>
- Franklin, J., Serra-Diaz, J. M., Syphard, A. D., & Regan, H. M. (2016). Global change and terrestrial plant community dynamics. *Proceedings of the National Academy of Sciences of the United States of America*, 113(14), 3725–3734. <https://doi.org/10.1073/pnas.1519911113>
- Gardner, A. S., Maclean, I. M. D., & Gaston, K. J. (2019). Climatic predictors of species distributions neglect biophysically meaningful variables. *Diversity and Distributions*, 25(8), 1318–1333. <https://doi.org/10.1111/ddi.12939>
- Gilliam, F. S. (2007). The ecological significance of the herbaceous layer in temperate forest ecosystems. *Bioscience*, 57(10), 845–858. <https://doi.org/10.1641/B571007>
- Gobiet, A., Kotlarski, S., Beniston, M., Heinrich, G., Rajczak, J., & Stoffel, M. (2014). 21st century climate change in the European Alps—A review. *Science of the Total Environment*, 493, 1138–1151. <https://doi.org/10.1016/j.scitotenv.2013.07.050>
- Gottfried, M., Pauli, H., Futschik, A., Akhalkatsi, M., Barančok, P., Alonso, J. L. B., Coldea, G., Dick, J., Erschbamer, B., Calzado, M. R. F., Kazakis, G., Krajčí, J., Larsson, P., Mallaun, M., Michelsen, O., Moiseev, D., Moiseev, P., Molau, U., Merzouki, A., ... Grabbherr, G. (2012). Continent-wide response of mountain vegetation to climate change. *Nature Climate Change*, 2(2), 111–115. <https://doi.org/10.1038/nclimate1329>
- Govaert, S., Vangansbeke, P., Blondeel, H., Steppe, K., Verheyen, K., & De Frenne, P. (2021). Rapid thermophilization of understorey plant communities in a 9 year-long temperate forest experiment. *Journal of Ecology*, 109(6), 2434–2447. <https://doi.org/10.1111/1365-2745.13653>
- Gray, C. L., Hill, S. L. L., Newbold, T., Hudson, L. N., Boirger, L., Contu, S., Hoskins, A. J., Ferrier, S., Purvis, A., & Scharlemann, J. P. W. (2016). Local biodiversity is higher inside than outside terrestrial protected areas worldwide. *Nature Communications*, 7, 12306. <https://doi.org/10.1038/ncomms12306>
- Halpern, C. B. (1989). Early successional patterns of forest species: Interactions of life history traits and disturbance. *Ecology*, 70(3), 704–720. <https://doi.org/10.2307/1940221>
- Hansen, W. D., Fitzsimmons, R., Olnes, J., & Williams, A. P. (2021). An alternate vegetation type proves resilient and persists for decades following forest conversion in the North American boreal biome. *Journal of Ecology*, 109(1), 85–98. <https://doi.org/10.1111/1365-2745.13446>
- Hansson, A., Dargusch, P., & Shulmeister, J. (2021). A review of modern treeline migration, the factors controlling it and the implications for carbon storage. *Journal of Mountain Science*, 18(2), 291–306. <https://doi.org/10.1007/s11629-020-6221-1>
- Heinenk, T., Diekmann, M., Liira, J., Orczevska, A., Schmidt, M., Brunet, J., Chytrý, M., Chabré, O., Decocq, G., De Frenne, P., Dřevojan, P., Dzwonko, Z., Ewald, J., Feilberg, J., Graae, B. J., Grytnes, J. A., Hermy, M., Kriebitzsch, W. U., Laivinš, M., ... Vanneste, T. (2022). The European forest plant species list (EuForPlant): Concept and applications. *Journal of Vegetation Science*, 33(3), e13132. <https://doi.org/10.1111/jvs.13132>
- Helm, N., Essl, F., Mirtl, M., & Dirnböck, T. (2017). Multiple environmental changes drive forest floor vegetation in a temperate mountain forest. *Ecology and Evolution*, 7(7), 2155–2168. <https://doi.org/10.1002/ece3.2801>
- Kattge, J., Bönisch, G., Díaz, S., Lavorel, S., Prentice, I. C., Leadley, P., Tautenhahn, S., Werner, G. D. A., Aakala, T., Abedi, M., Acosta, A. T. R., Adamidis, G. C., Adamson, K., Aiba, M., Albert, C. H., Alcántara, J. M., Carolina Alcázar, C., Aleixo, I., Ali, H., ... Wirth, C. (2020). TRY plant trait database – Enhanced coverage and open access. *Global Change Biology*, 26(1), 119–188. <https://doi.org/10.1111/gcb.14904>
- Kattge, J., Díaz, S., Lavorel, S., Prentice, I. C., Leadley, P., Bönisch, G., Garnier, E., Westoby, M., Reich, P. B., Wright, I. J., Cornelissen, J. H. C., Violle, C., Harrison, S. P., Bodegom, P. M. V., Reichstein, M., Enquist, B. J., Soudzilovskaia, N. A., Ackerly, D. D., Anand, M., ... Wirth, C. (2011). TRY – A global database of plant traits. *Global Change Biology*, 17(9), 2905–2935. <https://doi.org/10.1111/j.1365-2486.2011.02451.x>
- Kobayashi, Y., Seidl, R., Rammer, W., Suzuki, K. F., & Mori, A. S. (2023). Identifying effective tree planting schemes to restore forest carbon and biodiversity in Shiretoko National Park, Japan. *Restoration Ecology*, 31(1), e13681.
- Konapala, G., Mishra, A. K., Wada, Y., & Mann, M. E. (2020). Climate change will affect global water availability through compounding changes in seasonal precipitation and evaporation. *Nature Communications*, 11(1), 3044. <https://doi.org/10.1038/s41467-020-16757-w>
- Konnert, V. (2004). Standortkarte Nationalpark Berchtesgaden. *Forschungsbericht 49*. Nationalpark Berchtesgaden.
- Körner, C. (2004). Mountain biodiversity, its causes and function. *Ambio*, 33(Spec. No. 13), 11–17. <https://doi.org/10.1007/0044-7447-33-SP13.11>
- Landuyt, D., De Lombaerde, E., Perring, M. P., Hertzog, L. R., Ampoorter, E., Maes, S. L., De Frenne, P., Ma, S., Proesmans, W., Blondeel, H., Sercu, B. K., Wang, B., Wasof, S., & Verheyen, K. (2019). The functional role of temperate forest understorey vegetation in a changing world. *Global Change Biology*, 25(11), 3625–3641. <https://doi.org/10.1111/gcb.14756>
- Landuyt, D., Perring, M. P., Seidl, R., Taubert, F., Verbeeck, H., & Verheyen, K. (2018). Modelling understorey dynamics in temperate forests under global change – Challenges and perspectives. *Perspectives in Plant Ecology, Evolution and Systematics*, 31, 44–54. <https://doi.org/10.1016/j.ppees.2018.01.002>
- Lawler, J. J., Ackerly, D. D., Albano, C. M., Anderson, M. G., Dobrowski, S. Z., Gill, J. L., Heller, N. E., Pressey, R. L., Sanderson, E. W., & Weiss, S. B. (2015). The theory behind, and the challenges of, conserving nature's stage in a time of rapid change. *Conservation Biology*, 29(3), 618–629. <https://doi.org/10.1111/cobi.12505>
- Lembrechts, J. J., Nijs, I., & Lenoir, J. (2019). Incorporating microclimate into species distribution models. *Ecography*, 42(7), 1267–1279. <https://doi.org/10.1111/ecog.03947>
- Lenoir, J., Hattab, T., & Pierre, G. (2017). Climatic microrefugia under anthropogenic climate change: Implications for species redistribution. *Ecography*, 40(2), 253–266. <https://doi.org/10.1111/ecog.02788>
- Liang, J., Ding, Z., Lie, G., Zhou, Z., Singh, P. B., Zhang, Z., & Hu, H. (2020). Species richness patterns of vascular plants and their drivers along an elevational gradient in the central Himalayas. *Global Ecology and*

- Conservation, 24, e01279. <https://doi.org/10.1016/j.gecco.2020.e01279>
- Liaw, A., & Wiener, M. (2002). Classification and regression by randomForest. *R News*, 2(3), 18–22.
- Littlefield, C. E., Krosby, M., Michalak, J. L., & Lawler, J. J. (2019). Connectivity for species on the move: Supporting climate-driven range shifts. *Frontiers in Ecology and the Environment*, 17(5), 270–278. <https://doi.org/10.1002/fee.2043>
- Londo, G. (1976). The decimal scale for relevés of permanent quadrats. *Vegetatio*, 33(1), 61–64. <https://doi.org/10.1007/BF00055300>
- Maroscheck, M., Seidl, R., Poschlod, B., & Senf, C. (2023). Quantifying patch size distributions of forest disturbances in protected areas across the European Alps. *Journal of Biogeography*. <https://doi.org/10.1111/jbi.14760>
- Maxwell, S. L., Cañal, V., Dudley, N., Hoffmann, M., Rodrigues, A. S. L., Stoltz, S., Visconti, P., Woodley, S., Kingston, N., Lewis, E., Maron, M., Strassburg, B. B. N., Wenger, A., Jonas, H. D., Venter, O., & Watson, J. E. M. (2020). Area-based conservation in the twenty-first century. *Nature*, 586(7828), 217–227. <https://doi.org/10.1038/s41586-020-2773-z>
- McDowell, N. G., Allen, C. D., Anderson-Teixeira, K., Aukema, B. H., Bond-Lamberty, B., Chini, L., Clark, J. S., Dietze, M., Grossiord, C., Hanbury-Brown, A., Hurt, G. C., Jackson, R. B., Johnson, D. J., Kueppers, L., Lichstein, J. W., Ogle, K., Poulter, B., Pugh, T. A. M., Seidl, R., ... Xu, C. (2020). Pervasive shifts in forest dynamics in a changing world. *Science*, 368(6494), aaz9463. <https://doi.org/10.1126/science.aaz9463>
- Mod, H. K., & Luoto, M. (2016). Arctic shrubification mediates the impacts of warming climate on changes to tundra vegetation. *Environmental Research Letters*, 11(12), 124028. <https://doi.org/10.1088/1748-9326/11/12/124028>
- Nakagawa, S., & Schielzeth, H. (2013). A general and simple method for obtaining R^2 from generalized linear mixed-effects models. *Methods in Ecology and Evolution*, 4(2), 133–142. <https://doi.org/10.1111/j.2041-210x.2012.00261.x>
- Naqinezhad, A., De Lombaerde, E., Gholizadeh, H., Wasof, S., Perring, M. P., Meeussen, C., De Frenne, P., & Verheyen, K. (2022). The combined effects of climate and canopy cover changes on understorey plants of the Hyrcanian forest biodiversity hotspot in northern Iran. *Global Change Biology*, 28(3), 1103–1118. <https://doi.org/10.1111/gcb.15946>
- Nationalpark Berchtesgaden. (2023). *Nationalparkplan 2023–2033: Bestandesplan–Grundlagen und Analysen*. Bayerisches Staatsministerium für Landesentwicklung Und Umweltfragen.
- Parks, S. A., Holsinger, L. M., Abatzoglou, J. T., Littlefield, C. E., & Zeller, K. A. (2023). Protected areas not likely to serve as steppingstones for species undergoing climate-induced range shifts. *Global Change Biology*, 29(10), 2681–2696. <https://doi.org/10.1111/gcb.16629>
- Parmesan, C. (2006). Ecological and evolutionary responses to recent climate change. *Annual Review of Ecology, Evolution, and Systematics*, 37, 637–669. <https://doi.org/10.1146/annurev.ecolsys.37.091305.110100>
- Patacca, M., Lindner, M., Lucas-Borja, M. E., Cordonnier, T., Fidej, G., Gardiner, B., Hauf, Y., Jasinevičius, G., Labonne, S., Linkevičius, E., Mahnken, M., Milanovic, S., Nabuurs, G.-J., Nagel, T. A., Nikinmaa, L., Panyatov, M., Bercak, R., Seidl, R., Ostrogović Sever, M. Z., ... Schelhaas, M.-J. (2023). Significant increase in natural disturbance impacts on European forests since 1950. *Global Change Biology*, 29(5), 1359–1376. <https://doi.org/10.1111/gcb.16531>
- Pépin, N. C., Arnone, E., Gobiet, A., Haslinger, K., Kotlarski, S., Notarnicola, C., Palazzi, E., Seibert, P., Serafin, S., Schöner, W., Terzaghi, S., Thornton, J. M., Vuille, M., & Adler, C. (2022). Climate changes and their elevational patterns in the mountains of the world. *Reviews of Geophysics*, 60(1), e2020RG000730. <https://doi.org/10.1029/2020RG000730>
- Petter, G., Mairotta, P., Albrich, K., Bebi, P., Brúna, J., Bugmann, H., Haffenden, A., Scheller, R. M., Schmitz, D. R., Seidl, R., Speich, M., Vacchiano, G., & Lischke, H. (2020). How robust are future projections of forest landscape dynamics? Insights from a systematic comparison of four forest landscape models. *Environmental Modelling and Software*, 134, 104844. <https://doi.org/10.1016/j.envsoft.2020.104844>
- Pinheiro, J. C., & Bates, D. M. (2000). *Mixed-effects models in S and S-plus: Statistics and computing*. Springer-Verlag.
- Pinheiro, J. C., Bates, D. M., DebRoy, S., Sarkar, D., & R Core Team. (2022). *nlme: Linear and nonlinear mixed effects models* [computer software]. R package version 3.1-155. <https://CRAN.R-project.org/package=nlme>
- Pöpperl, F., & Seidl, R. (2021). Effects of stand edges on the structure, functioning, and diversity of a temperate mountain forest landscape. *Ecosphere*, 12(8), e03692. <https://doi.org/10.1002/ecs2.3692>
- R Core Team. (2022). *R: A language and environment for statistical computing*. R Foundation for Statistical Computing.
- Radeloff, V. C., Williams, J. W., Bateman, B. L., Burke, K. D., Carter, S. K., Childress, E. S., Cromwell, K. J., Gratton, C., Hasley, A. O., Kraemer, B. M., Latzka, A. W., Marin-Spiotta, E., Meine, C. D., Munoz, S. E., Neeson, T. M., Pidgeon, A. M., Rissman, A. R., Rivera, R. J., Szymanski, L. M., & Usinowicz, J. (2015). The rise of novelty in ecosystems. *Ecological Applications*, 25(8), 2051–2068. <https://doi.org/10.1890/14-1781.1>
- Richard, B., Dupouey, J. L., Corcket, E., Alard, D., Archaux, F., Aubert, M., Boulanger, V., Gillet, F., Langlois, E., Macé, S., Montpied, P., Beaufils, T., Begeot, C., Behr, P., Boissier, J. M., Camaret, S., Chevalier, R., Decocq, G., Dumas, Y., ... Lenoir, J. (2021). The climatic debt is growing in the understorey of temperate forests: Stand characteristics matter. *Global Ecology and Biogeography*, 30(7), 1474–1487. <https://doi.org/10.1111/geb.13312>
- Rumpf, S. B., Hülber, K., Klonner, G., Moser, D., Schütz, M., Wessely, J., Willner, W., Zimmermann, N. E., & Dullinger, S. (2018). Range dynamics of mountain plants decrease with elevation. *Proceedings of the National Academy of Sciences of the United States of America*, 115(8), 1848–1853. <https://doi.org/10.1073/pnas.1713936115>
- Sallou, N., & Stritih, A. (2023). In complexity we trust: Learning from the socialist calculation debate for ecosystem management. *Environmental Research Letters*, 18(5), 051001. <https://doi.org/10.1088/1748-9326/accc45>
- Savage, J., & Vellend, M. (2015). Elevational shifts, biotic homogenization and time lags in vegetation change during 40 years of climate warming. *Ecography*, 38(6), 546–555. <https://doi.org/10.1111/ecog.01131>
- Schwalm, C. R., Glendon, S., & Duffy, P. B. (2020). RCP8.5 tracks cumulative CO_2 emissions. *Proceedings of the National Academy of Sciences of the United States of America*, 117(33), 19656–19657. <https://doi.org/10.1073/PNAS.2007117117>
- Seidl, R., & Rammer, W. (2023). *iLand online model documentation*. <https://iland-model.org/>
- Seidl, R., Rammer, W., & Lexer, M. J. (2009). Schätzung von Bodenmerkmalen und Modellparametern für die Waldökosystemsimulation auf Basis einer Großrauminventur. *Allgemeine Forst- Und Jagdzeitung*, 180 (1–2), 35–44.
- Seidl, R., Rammer, W., Scheller, R. M., & Spies, T. A. (2012). An individual-based process model to simulate landscape-scale forest ecosystem dynamics. *Ecological Modelling*, 231, 87–100. <https://doi.org/10.1016/j.ecolmodel.2012.02.015>
- Seidl, R., Schelhaas, M. J., & Lexer, M. J. (2011). Unraveling the drivers of intensifying forest disturbance regimes in Europe. *Global Change Biology*, 17(9), 2842–2852. <https://doi.org/10.1111/j.1365-2486.2011.02452.x>
- Seidl, R., Thom, D., Kautz, M., Martin-Benito, D., Peltoniemi, M., Vacchiano, G., Wild, J., Ascoli, D., Petr, M., Honkaniemi, J., Lexer, M. J., Trotsiuk, V.,

- Mairotta, P., Svoboda, M., Fabrika, M., Nagel, T. A., & Reyer, C. P. O. (2017). Forest disturbances under climate change. *Nature Climate Change*, 7(6), 395–402. <https://doi.org/10.1038/nclimate3303>
- Senf, C., Pflugmacher, D., Hostert, P., & Seidl, R. (2017). Using Landsat time series for characterizing forest disturbance dynamics in the coupled human and natural systems of Central Europe. *ISPRS Journal of Photogrammetry and Remote Sensing*, 130, 453–463. <https://doi.org/10.1016/j.isprsjprs.2017.07.004>
- Simberloff, D. (2010). Invasions of plant communities more or the same, something very different, or both? *American Midland Naturalist*, 163(1), 220–233. <https://doi.org/10.1674/0003-0031-163.1.220>
- Slavich, E., Warton, D. I., Ashcroft, M. B., Gollan, J. R., & Ramp, D. (2014). Topoclimate versus macroclimate: How does climate mapping methodology affect species distribution models and climate change projections? *Diversity and Distributions*, 20(8), 952–963. <https://doi.org/10.1111/ddi.12216>
- Sommer, J. H., Kreft, H., Kier, G., Jetz, W., Mutke, J., & Barthlott, W. (2010). Projected impacts of climate change on regional capacities for global plant species richness. *Proceedings of the Royal Society B: Biological Sciences*, 277(1692), 2271–2280. <https://doi.org/10.1098/rspb.2010.0120>
- Stark, J. R., & Fridley, J. D. (2022). Microclimate-based species distribution models in complex forested terrain indicate widespread cryptic refugia under climate change. *Global Ecology and Biogeography*, 31(3), 562–575. <https://doi.org/10.1111/geb.13447>
- Stein, A., Gerstner, K., & Kreft, H. (2014). Environmental heterogeneity as a universal driver of species richness across taxa, biomes and spatial scales. *Ecology Letters*, 17(7), 866–880. <https://doi.org/10.1111/ele.12277>
- Stevens, J. T., Safford, H. D., Harrison, S., & Latimer, A. M. (2015). Forest disturbance accelerates thermophilization of understory plant communities. *Journal of Ecology*, 103(5), 1253–1263. <https://doi.org/10.1111/1365-2745.12426>
- Stritih, A., Senf, C., Seidl, R., Grêt-Regamey, A., & Bebi, P. (2021). The impact of land-use legacies and recent management on natural disturbance susceptibility in mountain forests. *Forest Ecology and Management*, 484, 118950. <https://doi.org/10.1016/j.foreco.2021.118950>
- Suter, W., Suter, U., Krüsi, B., & Schütz, M. (2004). Spatial variation of summer diet of red deer *Cervus elaphus* in the eastern Swiss Alps. *Wildlife Biology*, 10(1), 43–50. <https://doi.org/10.2981/wlb.2004.008>
- Suzuki, M., Miyashita, T., Kabaya, H., Ochiai, K., Asada, M., & Kikvidze, Z. (2013). Deer herbivory as an important driver of divergence of ground vegetation communities in temperate forests. *Oikos*, 122(1), 104–110. <https://doi.org/10.1111/j.1600-0706.2012.20431.x>
- Thom, D., Rammer, W., Dirnböck, T., Müller, J., Kobler, J., Katzensteiner, K., Helm, N., & Seidl, R. (2017). The impacts of climate change and disturbance on spatio-temporal trajectories of biodiversity in a temperate forest landscape. *Journal of Applied Ecology*, 54(1), 28–38. <https://doi.org/10.1111/1365-2664.12644>
- Thom, D., Rammer, W., Laux, P., Smiatek, G., Kunstmüller, H., Seibold, S., & Seidl, R. (2022). Will forest dynamics continue to accelerate throughout the 21st century in the Northern Alps? *Global Change Biology*, 28(10), 3260–3274. <https://doi.org/10.1111/gcb.16133>
- Thom, D., & Seidl, R. (2022). Accelerating mountain forest dynamics in the Alps. *Ecosystems*, 25(3), 603–617. <https://doi.org/10.1007/s10021-021-00674-0>
- Thriplleton, T., Bugmann, H., & Snell, R. S. (2018). Herbaceous competition and browsing may induce arrested succession in central European forests. *Journal of Ecology*, 106(3), 1120–1132. <https://doi.org/10.1111/1365-2745.12889>
- Thuiller, W., Brotons, L., Araújo, M. B., & Lavorel, S. (2004). Effects of restricting environmental range of data to project current and future species distributions. *Ecography*, 27(2), 165–172. <https://doi.org/10.1111/j.0906-7590.2004.03673.x>
- Thuiller, W., Lavorel, S., Araújo, M. B., Sykes, M. T., & Prentice, I. C. (2005). Climate change threats to plant diversity in Europe. *Proceedings of the National Academy of Sciences of the United States of America*, 102(23), 8245–8250. <https://doi.org/10.1073/pnas.0409902102>
- Tribsch, A., & Schönswetter, P. (2003). Patterns of endemism and comparative phylogeography confirm palaeoenvironmental evidence for Pleistocene refugia in the Eastern Alps. *Taxon*, 52(3), 477–497. <https://doi.org/10.2307/3647447>
- Turner, M. G., Braziunas, K. H., Hansen, W. D., Hoecker, T. J., Rammer, W., Ratajczak, Z., Westerling, A. L., & Seidl, R. (2022). The magnitude, direction, and tempo of forest change in Greater Yellowstone in a warmer world with more fire. *Ecological Monographs*, 92, e01485. <https://doi.org/10.1002/ecm.1485>
- UNEP-WCMC, & IUCN. (2016). *Protected Planet Report 2016: How protected areas contribute to achieving global targets for biodiversity*. UNEP.
- UNEP-WCMC, & IUCN. (2023). *Protected planet: The world database on protected areas (WDPA)*. www.protectedplanet.net
- Večeřa, M., Divišek, J., Lenoir, J., Jiménez-Alfaro, B., Biurrun, I., Knollová, I., Agrillo, E., Campos, J. A., Čarní, A., Jiménez, G. C., Čuk, M., Dimopoulos, P., Ewald, J., Fernández-González, F., Gégout, J. C., Indreica, A., Jandt, U., Jansen, F., Kącki, Z., ... Chytrý, M. (2019). Alpha diversity of vascular plants in European forests. *Journal of Biogeography*, 46(9), 1919–1935. <https://doi.org/10.1111/jbi.13624>
- Vellend, M., Baeten, L., Becker-Scarpitta, A., Boucher-Lalonde, V., McCune, J. L., Messier, J., Myers-Smith, I. H., & Sax, D. F. (2017). Plant biodiversity change across scales during the Anthropocene. *Annual Review of Plant Biology*, 68, 563–586. <https://doi.org/10.1146/annurev-arplant-042916-040949>
- Verheyen, K., Baeten, L., De Frenne, P. D., Bernhardt-Römermann, M., Brunet, J., Cornelis, J., Decocq, G., Dierschke, H., Eriksson, O., Hédil, R., Heinken, T., Hermy, M., Hommel, P., Kirby, K., Naaf, T., Peterken, G., Petřík, P., Pfadenhauer, J., Calster, H. V., ... Verstraeten, G. (2012). Driving factors behind the eutrophication signal in understory plant communities of deciduous temperate forests. *Journal of Ecology*, 100(2), 352–365. <https://doi.org/10.1111/j.1365-2745.2011.01928.x>
- Warscher, M., Wagner, S., Marke, T., Laux, P., Smiatek, G., Strasser, U., & Kunstmüller, H. (2019). A 5 km resolution regional climate simulation for Central Europe: Performance in high mountain areas and seasonal, regional and elevation-dependent variations. *Atmosphere*, 10(11), 682. <https://doi.org/10.3390/atmos10110682>
- Watson, J. E. M., Dudley, N., Segar, D. B., & Hockings, M. (2014). The performance and potential of protected areas. *Nature*, 515(7525), 67–73. <https://doi.org/10.1038/nature13947>
- Williams, J. W., & Jackson, S. T. (2007). Novel climates, no-analog communities, and ecological surprises. *Frontiers in Ecology and the Environment*, 5(9), 475–482. <https://doi.org/10.1890/070037>
- Xu, X., Huang, A., Belle, E., De Frenne, P., & Jia, G. (2022). Protected areas provide thermal buffer against climate change. *Science Advances*, 8(44), abo0119. <https://doi.org/10.1126/sciadv.abo0119>
- Zellweger, F., Braunisch, V., Morsdorf, F., Baltensweiler, A., Abegg, M., Roth, T., Bugmann, H., & Bollmann, K. (2015). Disentangling the effects of climate, topography, soil and vegetation on stand-scale species richness in temperate forests. *Forest Ecology and Management*, 349, 36–44. <https://doi.org/10.1016/j.foreco.2015.04.008>
- Zenner, E. K., Peck, J. L. E., Hobi, M. L., & Commarmot, B. (2016). Validation of a classification protocol: Meeting the prospect requirement and ensuring distinctiveness when assigning forest development phases. *Applied Vegetation Science*, 19(3), 541–552. <https://doi.org/10.1111/avsc.12231>
- Zier, C., Müller, C., Komischke, H., Steinbauer, A., & Bäse, F. (2020). *Das Bayerische Klimaprojektionsensembles-Audit und Ensemblebildung*. Bayerisches Landesamt für Umwelt (LfU).

Zurell, D., Zimmermann, N. E., Gross, H., Baltensweiler, A., Sattler, T., & Wüest, R. O. (2020). Testing species assemblage predictions from stacked and joint species distribution models. *Journal of Biogeography*, 47(1), 101–113. <https://doi.org/10.1111/jbi.13608>

SUPPORTING INFORMATION

Additional supporting information can be found online in the Supporting Information section at the end of this article.

How to cite this article: Braziunas, K. H., Geres, L., Richter, T., Glasmann, F., Senf, C., Thom, D., Seibold, S., & Seidl, R. (2024). Projected climate and canopy change lead to thermophilization and homogenization of forest floor vegetation in a hotspot of plant species richness. *Global Change Biology*, 30, e17121. <https://doi.org/10.1111/gcb.17121>

Projected climate and canopy change lead to thermophilization and homogenization of forest floor vegetation in a hotspot of plant species richness

Kristin H. Braziunas, Lisa Geres, Tobias Richter, Felix Glasmann, Cornelius Senf, Dominik Thom, Sebastian Seibold, and Rupert Seidl

Supporting information

1. Supplementary methods

Statistical modeling of understory plant communities

We compiled an initial list of 27 climate, 15 forest, and 5 soil predictors (Table S1) prior to variable selection. For forest predictors only, we used initial species distribution model (SDM) fits to evaluate variable importance after excluding highly correlated predictors (Pearson's $|r| < 0.7$). Variable importance for each forest predictor was averaged across individual SDMs, and negative importance values (percent increase in mean-squared-error) were set to 0 prior to averaging. The three final forest predictors included light availability, the most important structure predictor (basal area), and the most important composition predictor (proportion beech; Figure S1). The same predictor set was used for each individual SDM and for a separate random forest model fit to total percent cover.

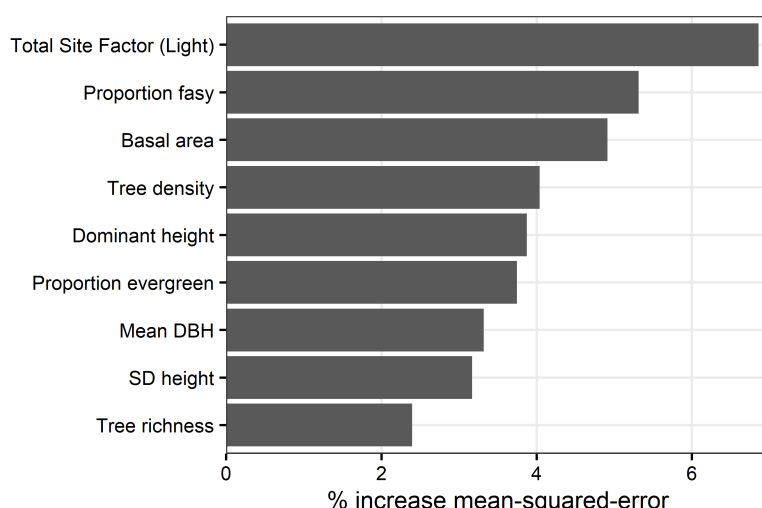


Figure S1. Forest predictor variable importance ranking used for variable selection, based on average percent increase mean-squared error. DBH: diameter at breast height; SD: standard deviation.

Table S1. Initial climate, forest, and soil predictors considered during variable selection process. Where applicable, WorldClim codes (e.g., BIO1) are noted for climate predictors.

Climate predictors	Forest predictors	Soil predictors
Mean annual temperature (BIO1)	Total site factor	Percent sand
Mean diurnal temperature range (BIO2)	Stand density	Percent clay
Isothermality (BIO3 = BIO2/BIO7)	Basal area	Effective soil depth
Temperature seasonality (BIO4)	Mean diameter at breast height (DBH)	Soil fertility
Maximum temperature of warmest month (BIO5)	Standard deviation of DBH	Water holding capacity
Minimum temperature of coldest month (BIO6)	Mean height	
Annual temperature range (BIO7 = BIO5-BIO6)	Standard deviation of height	
Mean summer temperature (June-Aug, BIO10)	Dominant height	
Mean winter temperature (Dec-Feb, BIO11)	Tree species richness	
Annual precipitation (BIO12)	Proportion needleleaved	
Precipitation in the wettest month (BIO13)	Proportion broadleaved	
Precipitation in the driest month (BIO14)	Proportion deciduous	
Precipitation seasonality (BIO15)	Proportion evergreen	
Summer precipitation (BIO18)	Proportion Norway spruce	
Winter precipitation (BIO19)	Proportion beech	
Difference between summer and winter temperature (BIO10-BIO11)		
Annual precipitation range (BIO13-BIO14)		
Difference between summer and winter precipitation (BIO18-BIO19)		
Mean daily solar radiation		
Mean annual vapor pressure deficit		
Number of frost days (minimum temperature < 0 °C)		
Frost change frequency (minimum temperature < 0 °C and maximum temperature > 0 °C)		
Growing degree days (based on mean temperature > 5 °C)		
Growing season length (growing season starts when at least 6 days with mean temperature > 5 °C and ends when at least 6 days with mean temperature < 5 °C)		
Growing season mean temperature		
Growing season maximum temperature		
Growing season precipitation		

A separate random forest macroecological model (MEM) was fit to species richness to determine whether accounting for macroecological constraints on total richness would improve model fit (Calabrese et al., 2014; Guisan & Rahbek, 2011). As in Zurell et al. (2020), we performed a full evaluation of whether bias correction with observations versus MEM predictors and probability ranking (D'Amen et al., 2015) with or without bias correction would affect model fit. Model goodness-of-fit was similar across all methods, and bias correcting with observed values plus probability ranking resulted in predictions that aligned well with the range of observed richness, better accounted for bias at low or high richness values (i.e., steeper slope of predicted versus observed data), and enabled community-level analyses of binarized species presence-absence data (Figure S2). Rather than introduce additional assumptions about macroecological constraints on species richness, stacking SDMs allows individual species responses to environmental drivers to shape emergent plant community change (Biber et al., 2020).

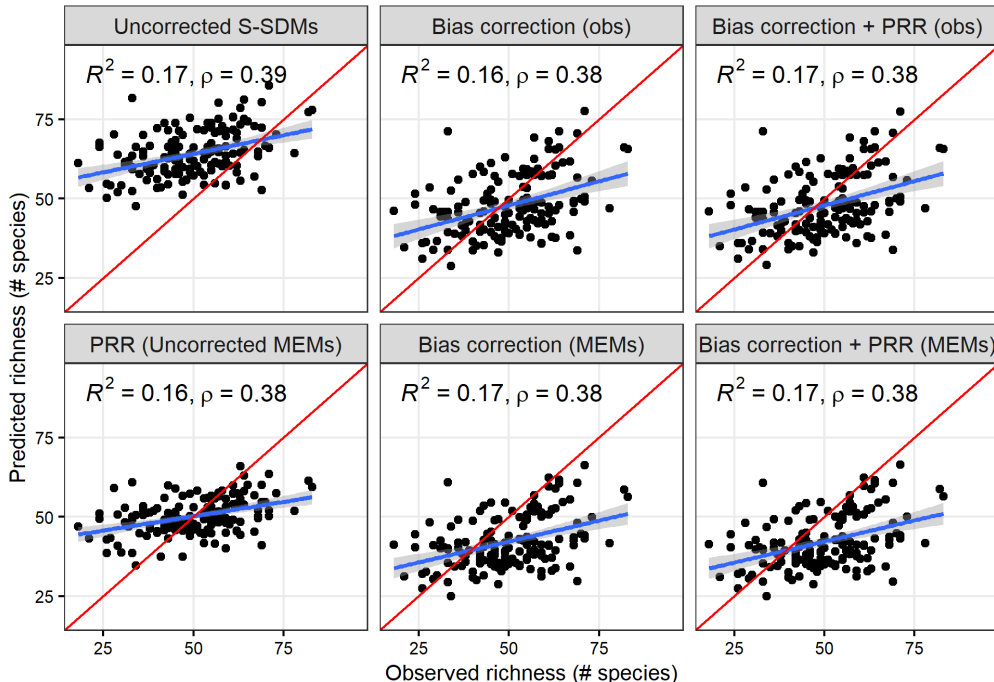


Figure S2. Predicted versus observed species richness using different methods for bias correction (uncorrected, corrected with training observations [obs], or corrected with macroecological model [MEM] predictions) and with or without applying the probability ranking rule (PRR). Red lines are 1:1 lines, blue lines are linear regression fits with shaded confidence intervals, and model goodness-of-fit (R^2) and Spearman's rank correction are shown. S-SDMs: Stacked species distribution models.

Prior to predicting understory plant community composition and cover across the entire forested landscape of Berchtesgaden National Park, field plot and landscape predictor values were compared to ensure that field plots adequately represented the full range of variation. The values and distribution of field plot predictors aligned well with the distribution of landscape predictors (Figure S3). Field plot predictors were standardized for model fitting, so landscape predictors also had to be rescaled. The mean ($mean_{field}$) and standard deviation (sd_{field}) of each field data predictor was calculated prior to standardization and used to rescale landscape predictors in 2020 and future years:

$$scaled\ predictor\ value = \frac{(original\ predictor\ value - mean_{field})}{sd_{field}}$$

For light availability, the mean and standard deviation from simulated values for 2020 was used to rescale predictors for future years. Soil variables did not change over time, so 2020 landscape predictors were used for all years.

Literature cited

- Biber, M. F., Voskamp, A., Niamir, A., Hickler, T., & Hof, C. (2020). A comparison of macroecological and stacked species distribution models to predict future global terrestrial vertebrate richness. *Journal of Biogeography*, 47(1), 114–129.
<https://doi.org/10.1111/jbi.13696>
- Calabrese, J. M., Certain, G., Kraan, C., & Dormann, C. F. (2014). Stacking species distribution models and adjusting bias by linking them to macroecological models. *Global Ecology and Biogeography*, 23(1), 99–112. <https://doi.org/10.1111/geb.12102>
- D'Amen, M., Dubuis, A., Fernandes, R. F., Pottier, J., Pellissier, L., & Guisan, A. (2015). Using species richness and functional traits predictions to constrain assemblage predictions from stacked species distribution models. *Journal of Biogeography*, 42(7), 1255–1266. <https://doi.org/10.1111/jbi.12485>
- Guisan, A., & Rahbek, C. (2011). SESAM - a new framework integrating macroecological and species distribution models for predicting spatio-temporal patterns of species assemblages. *Journal of Biogeography*, 38(8), 1433–1444.
<https://doi.org/10.1111/j.1365-2699.2011.02550.x>
- Zurell, D., Zimmermann, N. E., Gross, H., Baltensweiler, A., Sattler, T., & Wüest, R. O. (2020). Testing species assemblage predictions from stacked and joint species distribution models. *Journal of Biogeography*, 47(1), 101–113.
<https://doi.org/10.1111/jbi.13608>

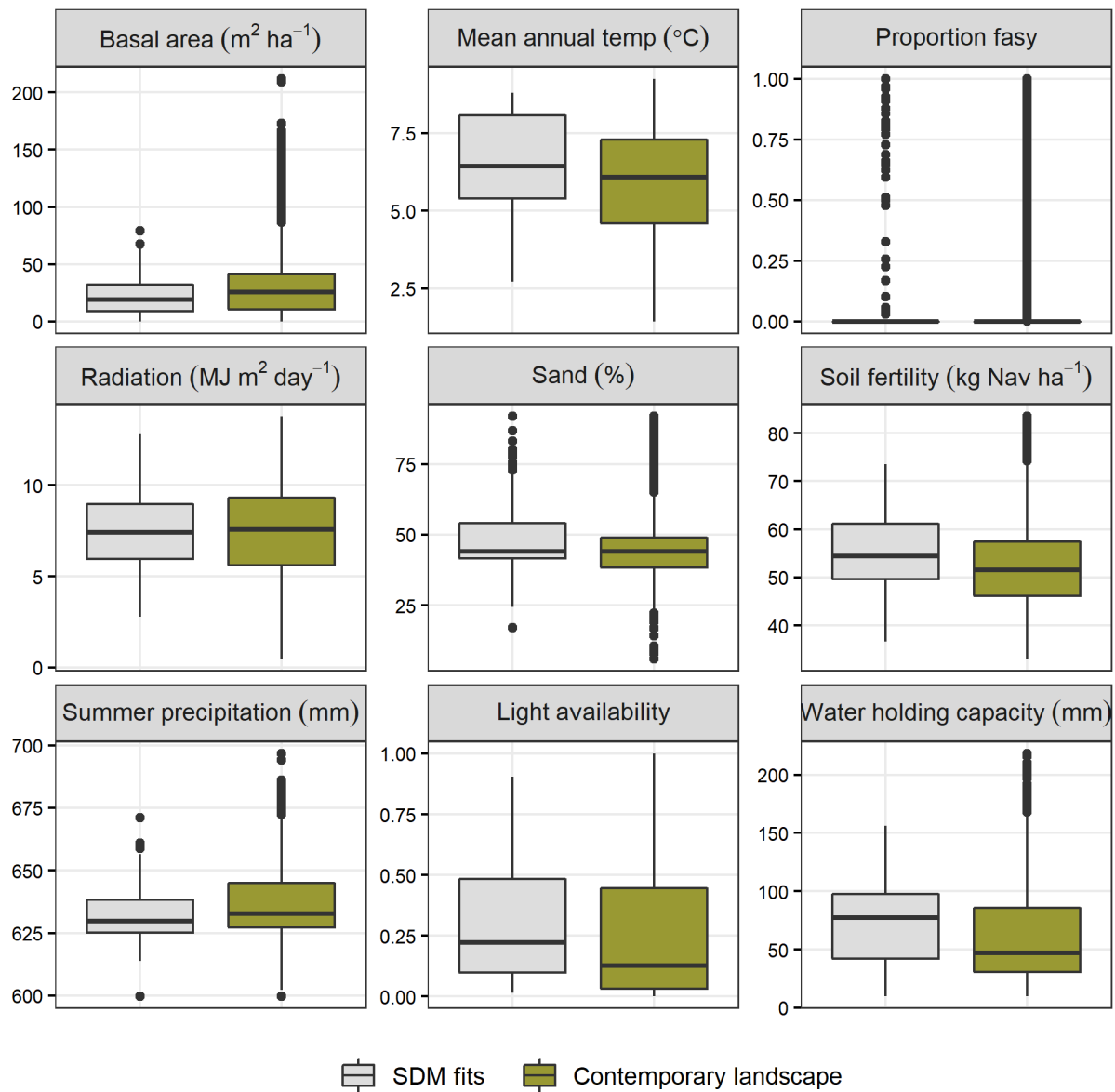


Figure S3. Boxplots showing the distributions of predictors used in fitting species distribution models (SDM fits, $n = 150$) compared to the distributions of predictors used in predicting understory communities across the contemporary Berchtesgaden landscape at 10 m spatial resolution (Contemporary landscape, $n = 864,466$). NA values for Proportion fasy are excluded. Light availability shows comparison between Total Site Factor (SDM fits) and modeled light availability in iLand (Contemporary landscape). Fasy: *Fagus sylvatica* (European beech); Nav: Plant-available nitrogen.

2. Supplementary tables and figures

Table S2. Understory species modeled with individual species distribution models.

Species name	Prevalence	Life form	PFT	AUC
<i>Achillea atrata</i>	0.05	herb	Light-Cold	0.82
<i>Achillea millefolium</i>	0.03	herb	Light-TempIndiff	0.86
<i>Acinos alpinus</i>	0.11	herb	Light-Cold	0.83
<i>Aconitum lycoctonum</i>	0.28	herb	Shade-Warm	0.69
<i>Actaea spicata</i>	0.20	herb	Shade-Warm	0.84
<i>Adenostyles alliariae</i>	0.34	herb	Light-Cold	0.90
<i>Adenostyles alpina</i>	0.47	herb	Light-Cold	0.61
<i>Aegopodium podagraria</i>	0.12	herb	Shade-Warm	0.77
<i>Agrostis alpina</i>	0.03	graminoid	Light-Cold	0.99
<i>Agrostis capillaris</i>	0.06	graminoid	Light-TempIndiff	0.92
<i>Ajuga pyramidalis</i>	0.05	herb	Light-TempIndiff	0.93
<i>Ajuga reptans</i>	0.45	herb	Light-TempIndiff	0.73
<i>Alchemilla vulgaris agg.</i>	0.20	herb	Light-Warm	0.92
<i>Amelanchier ovalis</i>	0.03	shrub	Light-TempIndiff	0.61
<i>Anemone nemorosa</i>	0.08	herb	Shade-TempIndiff	0.61
<i>Angelica sylvestris</i>	0.15	herb	Light-TempIndiff	0.61
<i>Anthoxanthum odoratum</i>	0.08	graminoid	Shade-TempIndiff	0.77
<i>Aposeris foetida</i>	0.59	herb	Shade-Warm	0.79
<i>Aquilegia atrata</i>	0.09	herb	Light-Warm	0.64
<i>Aruncus dioicus</i>	0.05	herb	Shade-Warm	0.70
<i>Asplenium ruta-muraria</i>	0.07	fern	Light-TempIndiff	0.75
<i>Asplenium scolopendrium</i>	0.05	fern	Shade-Warm	0.94
<i>Asplenium trichomanes</i>	0.15	fern	Shade-TempIndiff	0.75
<i>Asplenium viride</i>	0.42	fern	Shade-Warm	0.74
<i>Aster bellidiastrum</i>	0.45	herb	Light-Cold	0.84
<i>Athyrium distentifolium</i>	0.09	fern	Shade-Cold	0.80
<i>Athyrium filix-femina</i>	0.62	fern	Shade-TempIndiff	0.75
<i>Atropa bella-donna</i>	0.07	herb	Light-TempIndiff	0.76
<i>Bellis perennis</i>	0.08	herb	Light-TempIndiff	0.79
<i>Berberis vulgaris</i>	0.04	shrub	Light-TempIndiff	0.67
<i>Betonica alopecuros</i>	0.07	herb	Light-Cold	0.57
<i>Biscutella laevigata</i>	0.08	herb	Light-TempIndiff	0.85
<i>Blechnum spicant</i>	0.05	fern	Shade-TempIndiff	0.63
<i>Brachypodium sylvaticum</i>	0.35	graminoid	Shade-Warm	0.84
<i>Buphtalmum salicifolium</i>	0.09	herb	Light-TempIndiff	0.68
<i>Calamagrostis varia</i>	0.79	graminoid	Light-Cold	0.58
<i>Calamagrostis villosa</i>	0.07	graminoid	Light-Warm	0.86
<i>Calluna vulgaris</i>	0.03	shrub	Light-TempIndiff	0.78
<i>Campanula cochleariifolia</i>	0.16	herb	Light-Cold	0.74
<i>Campanula rotundifolia</i>	0.05	herb	Light-Warm	0.83

Species name	Prevalence	Life form	PFT	AUC
<i>Campanula scheuchzeri</i>	0.34	herb	Light-Cold	0.85
<i>Campanula trachelium</i>	0.11	herb	Shade-TempIndiff	0.81
<i>Cardamine enneaphyllos</i>	0.62	herb	Shade-Warm	0.56
<i>Carduus defloratus</i>	0.29	herb	Light-TempIndiff	0.72
<i>Carex alba</i>	0.43	graminoid	Shade-Warm	0.92
<i>Carex digitata</i>	0.27	graminoid	Shade-TempIndiff	0.69
<i>Carex ferruginea</i>	0.29	graminoid	Light-Cold	0.86
<i>Carex firma</i>	0.03	graminoid	Light-Cold	0.97
<i>Carex flacca</i>	0.36	graminoid	Light-TempIndiff	0.76
<i>Carex ornithopoda</i>	0.31	graminoid	Light-TempIndiff	0.66
<i>Carex pallescens</i>	0.05	graminoid	Light-Warm	0.78
<i>Carex sempervirens</i>	0.09	graminoid	Light-TempIndiff	0.70
<i>Carex sylvatica</i>	0.25	graminoid	Shade-Warm	0.78
<i>Carlina acaulis</i>	0.06	herb	Light-Warm	0.75
<i>Cephalanthera longifolia</i>	0.12	herb	Shade-Warm	0.73
<i>Cerastium fontanum</i>	0.04	herb	Light-Cold	0.91
<i>Chaerophyllum hirsutum</i>	0.49	herb	Light-Cold	0.75
<i>Chlorocrepis staticifolia</i>	0.03	herb	Light-Warm	0.84
<i>Chrysosplenium alternifolium</i>	0.04	herb	Shade-Warm	0.72
<i>Cicerbita alpina</i>	0.08	herb	Light-Cold	0.83
<i>Circaea alpina</i>	0.04	herb	Shade-Warm	0.61
<i>Circaea lutetiana</i>	0.03	herb	Shade-Warm	0.96
<i>Cirsium oleraceum</i>	0.07	herb	Light-TempIndiff	0.90
<i>Cirsium palustre</i>	0.05	herb	Light-Warm	0.49
<i>Clematis alpina</i>	0.24	shrub	Shade-Cold	0.78
<i>Clematis vitalba</i>	0.09	shrub	Light-Warm	0.88
<i>Clinopodium vulgare</i>	0.25	herb	Light-TempIndiff	0.71
<i>Coeloglossum viride</i>	0.07	herb	Light-TempIndiff	0.72
<i>Crepis aurea</i>	0.11	herb	Light-Cold	0.95
<i>Crepis paludosa</i>	0.09	herb	Light-TempIndiff	0.84
<i>Cyanus montanus</i>	0.21	herb	Light-Warm	0.57
<i>Cypripedium calceolus</i>	0.03	herb	Shade-Warm	0.87
<i>Cystopteris alpina</i>	0.04	fern	Light-Cold	0.83
<i>Cystopteris fragilis</i>	0.25	fern	Shade-TempIndiff	0.62
<i>Dactylis glomerata</i>	0.13	graminoid	Light-TempIndiff	0.80
<i>Dactylorhiza maculata</i>	0.31	herb	Light-TempIndiff	0.55
<i>Daphne mezereum</i>	0.59	shrub	Shade-TempIndiff	0.75
<i>Deschampsia cespitosa</i>	0.15	graminoid	Light-TempIndiff	0.85
<i>Doronicum austriacum</i>	0.06	herb	Shade-Cold	0.71
<i>Dryas octopetala</i>	0.07	herb	Light-Cold	0.87
<i>Dryopteris affinis</i>	0.13	fern	Shade-Warm	0.93
<i>Dryopteris carthusiana</i>	0.28	fern	Shade-TempIndiff	0.73

Species name	Prevalence	Life form	PFT	AUC
<i>Dryopteris dilatata</i>	0.42	fern	Shade-TempIndiff	0.69
<i>Dryopteris expansa</i>	0.03	fern	Shade-Cold	0.62
<i>Dryopteris filix-mas</i>	0.60	fern	Shade-TempIndiff	0.67
<i>Epilobium montanum</i>	0.22	herb	Shade-TempIndiff	0.76
<i>Epipactis atrorubens</i>	0.10	herb	Light-TempIndiff	0.63
<i>Epipactis helleborine</i>	0.09	herb	Shade-Warm	0.83
<i>Erica carnea</i>	0.17	herb	Light-TempIndiff	0.75
<i>Eupatorium cannabinum</i>	0.25	herb	Light-Warm	0.84
<i>Euphorbia amygdaloides</i>	0.11	herb	Shade-Warm	0.72
<i>Euphorbia cyparissias</i>	0.14	herb	Light-TempIndiff	0.70
<i>Festuca gigantea</i>	0.06	graminoid	Shade-Warm	0.86
<i>Festuca rubra</i>	0.07	graminoid	Shade-TempIndiff	0.77
<i>Fragaria vesca</i>	0.75	herb	Light-TempIndiff	0.82
<i>Frangula alnus</i>	0.08	shrub	Light-Warm	0.87
<i>Galeobdolon flavidum</i>	0.28	herb	Shade-Cold	0.81
<i>Galeobdolon montanum</i>	0.38	herb	Shade-Warm	0.86
<i>Galium album</i>	0.08	herb	Light-TempIndiff	0.67
<i>Galium anisophyllum</i>	0.38	herb	Light-Cold	0.81
<i>Galium mollugo</i>	0.14	herb	Light-Warm	0.86
<i>Galium odoratum</i>	0.05	herb	Shade-Warm	0.49
<i>Galium rotundifolium</i>	0.09	herb	Shade-Warm	0.71
<i>Gentiana asclepiadea</i>	0.30	herb	Light-TempIndiff	0.70
<i>Geranium robertianum</i>	0.24	herb	Shade-TempIndiff	0.77
<i>Geranium sylvaticum</i>	0.36	herb	Light-Warm	0.96
<i>Geum rivale</i>	0.13	herb	Light-TempIndiff	0.88
<i>Geum urbanum</i>	0.03	herb	Shade-Warm	0.92
<i>Globularia nudicaulis</i>	0.03	herb	Light-Cold	0.83
<i>Gymnadenia conopsea</i>	0.05	herb	Light-TempIndiff	0.71
<i>Gymnadenia odoratissima</i>	0.05	herb	Light-TempIndiff	0.60
<i>Gymnocarpium dryopteris</i>	0.27	fern	Shade-Warm	0.68
<i>Gymnocarpium robertianum</i>	0.56	fern	Light-Warm	0.56
<i>Helianthemum nummularium</i> subsp. <i>grandiflorum</i>	0.04	herb	Light-Cold	0.94
<i>Helleborus niger</i>	0.26	herb	Shade-Warm	0.83
<i>Hepatica nobilis</i>	0.11	herb	Shade-Warm	0.92
<i>Heracleum austriacum</i>	0.13	herb	Light-Cold	0.89
<i>Heracleum sphondylium</i>	0.07	herb	Light-Warm	0.60
<i>Hieracium bifidum</i> agg.	0.03	herb	Light-TempIndiff	0.38
<i>Hieracium murorum</i>	0.63	herb	Shade-TempIndiff	0.69
<i>Homogyne alpina</i>	0.57	herb	Light-Warm	0.84
<i>Hordelymus europaeus</i>	0.03	graminoid	Shade-Warm	0.63
<i>Huperzia selago</i>	0.21	fern	Shade-Cold	0.70

Species name	Prevalence	Life form	PFT	AUC
<i>Hypericum maculatum</i>	0.41	herb	Light-TempIndiff	0.78
<i>Hypericum montanum</i>	0.04	herb	Shade-Warm	0.96
<i>Impatiens noli-tangere</i>	0.04	herb	Shade-Warm	0.98
<i>Impatiens parviflora</i>	0.04	herb	Shade-Warm	0.88
<i>Juncus monanthos</i>	0.07	graminoid	Light-Cold	0.86
<i>Knautia dipsacifolia</i>	0.53	herb	Shade-Warm	0.59
<i>Laserpitium latifolium</i>	0.04	herb	Light-Warm	0.50
<i>Leontodon hispidus</i>	0.17	herb	Light-TempIndiff	0.85
<i>Ligusticum mutellina</i>	0.04	herb	Light-Cold	0.96
<i>Lilium martagon</i>	0.17	herb	Shade-TempIndiff	0.58
<i>Linum catharticum</i>	0.03	herb	Light-TempIndiff	0.66
<i>Listera ovata</i>	0.40	herb	Light-TempIndiff	0.71
<i>Lonicera alpigena</i>	0.14	shrub	Shade-Warm	0.42
<i>Lonicera nigra</i>	0.21	shrub	Shade-Warm	0.79
<i>Lonicera xylosteum</i>	0.19	shrub	Shade-Warm	0.73
<i>Lotus corniculatus</i>	0.23	herb	Light-TempIndiff	0.69
<i>Luzula glabrata</i>	0.05	graminoid	Light-Cold	0.95
<i>Luzula luzulina</i>	0.11	graminoid	Shade-Cold	0.84
<i>Luzula pilosa</i>	0.17	graminoid	Shade-TempIndiff	0.80
<i>Luzula sieberi</i>	0.21	graminoid	Shade-Cold	0.83
<i>Luzula sylvatica</i>	0.19	graminoid	Shade-Warm	0.94
<i>Lycopodium annotinum</i>	0.45	fern	Shade-Warm	0.69
<i>Lysimachia nemorum</i>	0.49	herb	Shade-Warm	0.74
<i>Maianthemum bifolium</i>	0.50	herb	Shade-TempIndiff	0.66
<i>Melampyrum sylvaticum</i>	0.32	herb	Shade-Warm	0.78
<i>Melica nutans</i>	0.60	graminoid	Shade-TempIndiff	0.67
<i>Mercurialis perennis</i>	0.61	herb	Shade-TempIndiff	0.84
<i>Moehringia muscosa</i>	0.51	herb	Shade-Cold	0.62
<i>Molinia caerulea</i>	0.08	graminoid	Light-TempIndiff	0.90
<i>Mycelis muralis</i>	0.38	herb	Shade-Warm	0.80
<i>Myosotis alpestris</i>	0.10	herb	Light-Cold	0.92
<i>Myosotis decumbens</i>	0.03	herb	Light-Cold	0.98
<i>Neottia nidus-avis</i>	0.11	herb	Shade-Warm	0.68
<i>Origanum vulgare</i>	0.11	herb	Light-TempIndiff	0.62
<i>Oxalis acetosella</i>	0.85	herb	Shade-TempIndiff	0.76
<i>Paris quadrifolia</i>	0.72	herb	Shade-TempIndiff	0.74
<i>Persicaria vivipara</i>	0.12	herb	Light-Cold	0.92
<i>Petasites albus</i>	0.25	herb	Shade-Warm	0.57
<i>Petasites paradoxus</i>	0.11	herb	Light-Cold	0.75
<i>Peucedanum ostruthium</i>	0.13	herb	Light-Cold	0.92
<i>Phegopteris connectilis</i>	0.18	fern	Shade-Warm	0.60
<i>Phleum rhaeticum</i>	0.06	graminoid	Light-Cold	0.89

Species name	Prevalence	Life form	PFT	AUC
<i>Phyteuma orbiculare</i>	0.21	herb	Light-Warm	0.79
<i>Phyteuma spicatum</i>	0.27	herb	Shade-TempIndiff	0.57
<i>Pimpinella major</i>	0.23	herb	Light-Warm	0.56
<i>Platanthera bifolia</i>	0.07	herb	Light-TempIndiff	0.66
<i>Poa alpina</i>	0.15	graminoid	Light-Cold	0.93
<i>Poa nemoralis</i>	0.10	graminoid	Shade-TempIndiff	0.75
<i>Polygala alpestris</i>	0.03	herb	Light-Cold	0.71
<i>Polygala amara</i>	0.05	herb	Light-Cold	0.84
<i>Polygala chamaebuxus</i>	0.28	herb	Light-Warm	0.76
<i>Polygala vulgaris</i>	0.04	herb	Light-TempIndiff	0.50
<i>Polygonatum multiflorum</i>	0.05	herb	Shade-TempIndiff	0.89
<i>Polygonatum verticillatum</i>	0.51	herb	Shade-Warm	0.70
<i>Polypodium vulgare</i>	0.15	fern	Shade-Warm	0.77
<i>Polystichum aculeatum</i>	0.29	fern	Shade-Warm	0.77
<i>Polystichum lonchitis</i>	0.41	fern	Light-Warm	0.74
<i>Potentilla aurea</i>	0.07	herb	Light-Cold	0.82
<i>Potentilla erecta</i>	0.39	herb	Light-TempIndiff	0.67
<i>Prenanthes purpurea</i>	0.43	herb	Shade-Warm	0.75
<i>Primula auricula</i>	0.03	herb	Light-Cold	0.59
<i>Primula elatior</i>	0.09	herb	Light-TempIndiff	0.76
<i>Prunella vulgaris</i>	0.08	herb	Light-TempIndiff	0.75
<i>Ranunculus acris</i>	0.10	herb	Light-TempIndiff	0.66
<i>Ranunculus alpestris</i>	0.09	herb	Light-Cold	0.80
<i>Ranunculus lanuginosus</i>	0.10	herb	Shade-Warm	0.79
<i>Ranunculus montanus</i>	0.31	herb	Light-Cold	0.83
<i>Ranunculus nemorosus</i>	0.40	herb	Light-TempIndiff	0.70
<i>Rhamnus cathartica</i>	0.03	shrub	Light-Warm	0.53
<i>Rhinanthus glacialis</i>	0.04	herb	Light-Cold	0.71
<i>Rhododendron hirsutum</i>	0.19	shrub	Light-Cold	0.90
<i>Rhodothamnus chamaecistus</i>	0.08	shrub	Light-Cold	0.82
<i>Ribes alpinum</i>	0.03	shrub	Shade-Warm	0.36
<i>Rosa pendulina</i>	0.26	shrub	Light-Warm	0.66
<i>Rubus fruticosus agg.</i>	0.20	shrub	Light-Warm	0.96
<i>Rubus idaeus</i>	0.41	shrub	Light-TempIndiff	0.67
<i>Rubus saxatilis</i>	0.26	shrub	Light-TempIndiff	0.59
<i>Rumex alpestris</i>	0.08	herb	Light-Cold	0.81
<i>Rumex scutatus</i>	0.03	herb	Light-TempIndiff	0.87
<i>Salix appendiculata</i>	0.31	shrub	Light-Cold	0.73
<i>Salix waldsteiniana</i>	0.04	shrub	Light-Cold	0.93
<i>Salvia glutinosa</i>	0.37	herb	Shade-Warm	0.84
<i>Sambucus nigra</i>	0.04	shrub	Light-Warm	0.44
<i>Sambucus racemosa</i>	0.14	shrub	Light-Warm	0.72

Species name	Prevalence	Life form	PFT	AUC
<i>Sanicula europaea</i>	0.37	herb	Shade-Warm	0.83
<i>Saxifraga rotundifolia</i>	0.29	herb	Shade-Cold	0.89
<i>Scabiosa lucida</i>	0.05	herb	Light-Cold	0.69
<i>Scrophularia nodosa</i>	0.07	herb	Shade-Warm	0.73
<i>Selaginella selaginoides</i>	0.12	fern	Light-Cold	0.76
<i>Senecio abrotanifolius</i>	0.05	herb	Light-Cold	0.88
<i>Senecio hercynicus</i>	0.12	herb	Light-Warm	0.98
<i>Senecio ovatus</i>	0.48	herb	Light-TempIndiff	0.79
<i>Sesleria caerulea</i>	0.48	graminoid	Light-Warm	0.70
<i>Silene dioica</i>	0.15	herb	Shade-TempIndiff	0.68
<i>Silene vulgaris subsp. vulgaris</i>	0.15	herb	Light-TempIndiff	0.86
<i>Soldanella alpina</i>	0.23	herb	Light-Cold	0.80
<i>Solidago virgaurea</i>	0.75	herb	Shade-TempIndiff	0.61
<i>Sorbus chamaemespilus</i>	0.12	shrub	Light-Cold	0.88
<i>Stachys sylvatica</i>	0.06	herb	Shade-TempIndiff	0.64
<i>Stellaria nemorum</i>	0.05	herb	Shade-TempIndiff	0.65
<i>Streptopus amplexifolius</i>	0.07	herb	Shade-Cold	0.91
<i>Taraxacum officinale agg.</i>	0.07	herb	Light-TempIndiff	0.67
<i>Thalictrum aquilegiifolium</i>	0.09	herb	Shade-TempIndiff	0.59
<i>Thelypteris limbosperma</i>	0.17	fern	Shade-Warm	0.63
<i>Thesium alpinum</i>	0.09	herb	Light-Cold	0.87
<i>Thymus praecox subsp. polytrichus</i>	0.09	herb	Light-Cold	0.94
<i>Tofieldia calyculata</i>	0.14	herb	Light-TempIndiff	0.84
<i>Trifolium pratense</i>	0.13	herb	Light-TempIndiff	0.75
<i>Trollius europaeus</i>	0.23	herb	Light-Cold	0.82
<i>Tussilago farfara</i>	0.11	herb	Light-TempIndiff	0.72
<i>Urtica dioica</i>	0.21	herb	Shade-TempIndiff	0.68
<i>Vaccinium myrtillus</i>	0.71	shrub	Shade-TempIndiff	0.66
<i>Vaccinium uliginosum</i>	0.03	shrub	Light-TempIndiff	0.74
<i>Vaccinium vitis-idaea</i>	0.31	shrub	Shade-TempIndiff	0.80
<i>Valeriana montana</i>	0.13	herb	Light-Cold	0.50
<i>Valeriana saxatilis</i>	0.07	herb	Light-Cold	0.86
<i>Valeriana tripteris</i>	0.63	herb	Light-Cold	0.77
<i>Veratrum album</i>	0.23	herb	Light-Warm	0.86
<i>Veronica aphylla</i>	0.04	herb	Light-Cold	0.90
<i>Veronica chamaedrys</i>	0.31	herb	Light-TempIndiff	0.76
<i>Veronica officinalis</i>	0.14	herb	Light-TempIndiff	0.68
<i>Veronica urticifolia</i>	0.38	herb	Shade-Warm	0.64
<i>Vincetoxicum hirundinaria</i>	0.08	herb	Light-Warm	0.85
<i>Viola biflora</i>	0.56	herb	Shade-Cold	0.80
<i>Viola reichenbachiana</i>	0.40	herb	Shade-TempIndiff	0.82

Notes: **PFT (Plant Functional Type)** is based on species temperature and light preference derived from Ellenberg indicator values (EIVs). Shade: Shade-tolerant or indifferent to light, light EIV = 1-5 or x; Light: Light-preferring, light EIV = 6-9; Warm: Warm-preferring, associated with submontane-montane habitats, temperature EIV = 4-7; Cold: Cold-preferring, associated with subalpine-alpine habitats, temperature EIV = 1-3; TempIndiff: Indifferent to temperature, temperature EIV = x. **Prevalence** is the number of plots in which this species was observed out of 150 field plots. **AUC (Area Under the receiver operating characteristic Curve)** is the individual model fit for predictions of 30% holdout test data for $n = 20$ replicates of repeated subsampling.

Table S3. Combinations of forest and climate drivers used to determine the relative importance of drivers of understory community change in 2050 and 2100.

Climate levels	Forest levels	GCM (RCP)	Observations (<i>n</i>)
Contemporary	Contemporary	NA	1000
Contemporary	Baseline disturbance future	ICHEC-EC-EARTH (4.5)	1000
Contemporary	Baseline disturbance future	ICHEC-EC-EARTH (8.5)	1000
Contemporary	Baseline disturbance future	MPI-ESM-LR (4.5)	1000
Contemporary	Baseline disturbance future	MPI-ESM-LR (8.5)	1000
Contemporary	High disturbance future	ICHEC-EC-EARTH (4.5)	1000
Contemporary	High disturbance future	ICHEC-EC-EARTH (8.5)	1000
Contemporary	High disturbance future	MPI-ESM-LR (4.5)	1000
Contemporary	High disturbance future	MPI-ESM-LR (8.5)	1000
Future	Contemporary	ICHEC-EC-EARTH (4.5)	1000
Future	Contemporary	ICHEC-EC-EARTH (8.5)	1000
Future	Contemporary	MPI-ESM-LR (4.5)	1000
Future	Contemporary	MPI-ESM-LR (8.5)	1000
Future	Baseline disturbance future	ICHEC-EC-EARTH (4.5)	1000
Future	Baseline disturbance future	ICHEC-EC-EARTH (8.5)	1000
Future	Baseline disturbance future	MPI-ESM-LR (4.5)	1000
Future	Baseline disturbance future	MPI-ESM-LR (8.5)	1000
Future	High disturbance future	ICHEC-EC-EARTH (4.5)	1000
Future	High disturbance future	ICHEC-EC-EARTH (8.5)	1000
Future	High disturbance future	MPI-ESM-LR (4.5)	1000
Future	High disturbance future	MPI-ESM-LR (8.5)	1000

Notes: GCM: General Circulation Model; RCP: Representative Concentration Pathway; NA: Not applicable, based on historical climate rather than a GCM. Observations are for 1 simulation replicate.

Table S4. Linear mixed effects model fits for all 10 replicates, including marginal fits for full models, forest drivers only, and climate drivers only, which were used to determine relative importance of forest versus climate change. Most important driver is also noted.

Understory community response	Year	Model number	R ² _{fixed(full)}	R ² _{total(full)}	R ² _{fixed(forest)}	R ² _{fixed(climate)}	Most important driver
Species richness	2050	1	0.02	0.57	0.00	0.02	Climate
		2	0.02	0.57	0.00	0.02	Climate
		3	0.02	0.56	0.01	0.02	Climate
		4	0.02	0.56	0.00	0.02	Climate
		5	0.02	0.56	0.00	0.02	Climate
		6	0.02	0.56	0.00	0.02	Climate
		7	0.02	0.56	0.01	0.02	Climate
		8	0.02	0.57	0.00	0.02	Climate
		9	0.02	0.56	0.00	0.02	Climate
		10	0.02	0.56	0.00	0.02	Climate
Temperature EIV	2050	1	0.05	0.82	0.00	0.05	Climate
		2	0.05	0.82	0.00	0.05	Climate
		3	0.05	0.81	0.00	0.05	Climate
		4	0.05	0.81	0.00	0.05	Climate
		5	0.05	0.81	0.00	0.05	Climate
		6	0.05	0.81	0.00	0.05	Climate
		7	0.05	0.81	0.00	0.05	Climate
		8	0.05	0.81	0.00	0.05	Climate
		9	0.05	0.81	0.00	0.05	Climate
		10	0.05	0.82	0.00	0.05	Climate
Understory cover	2050	1	0.01	0.57	0.01	0.01	Climate
		2	0.01	0.56	0.00	0.01	Climate
		3	0.03	0.48	0.03	0.01	Forest
		4	0.01	0.54	0.01	0.01	Forest
		5	0.01	0.54	0.01	0.01	Forest
		6	0.01	0.56	0.00	0.01	Climate
		7	0.03	0.48	0.02	0.01	Forest
		8	0.01	0.56	0.01	0.01	Forest
		9	0.01	0.56	0.00	0.01	Climate
		10	0.01	0.56	0.01	0.01	Climate
Species richness	2100	1	0.04	0.44	0.00	0.04	Climate
		2	0.04	0.44	0.00	0.04	Climate
		3	0.04	0.45	0.00	0.04	Climate
		4	0.04	0.44	0.00	0.04	Climate
		5	0.04	0.46	0.00	0.04	Climate
		6	0.04	0.45	0.00	0.04	Climate
		7	0.04	0.46	0.00	0.04	Climate
		8	0.04	0.45	0.00	0.04	Climate
		9	0.04	0.46	0.00	0.04	Climate
		10	0.05	0.45	0.00	0.05	Climate

Understory community response	Year	Model number	R²_{fixed(full)}	R²_{total(full)}	R²_{fixed(climate)}	R²_{fixed(forest)}	Most important driver
Temperature EIV	2100	1	0.12	0.67	0.01	0.12	Climate
		2	0.12	0.67	0.01	0.12	Climate
		3	0.12	0.67	0.01	0.11	Climate
		4	0.12	0.67	0.01	0.12	Climate
		5	0.12	0.66	0.01	0.12	Climate
		6	0.12	0.67	0.01	0.11	Climate
		7	0.11	0.66	0.01	0.11	Climate
		8	0.12	0.66	0.01	0.12	Climate
		9	0.12	0.66	0.01	0.12	Climate
		10	0.12	0.66	0.01	0.12	Climate
Understory cover	2100	1	0.02	0.38	0.00	0.01	Climate
		2	0.02	0.39	0.00	0.01	Climate
		3	0.02	0.41	0.01	0.01	Climate
		4	0.02	0.36	0.00	0.01	Climate
		5	0.01	0.36	0.00	0.01	Climate
		6	0.02	0.41	0.01	0.01	Forest
		7	0.02	0.39	0.01	0.01	Forest
		8	0.02	0.35	0.01	0.01	Forest
		9	0.02	0.39	0.01	0.01	Forest
		10	0.01	0.36	0.00	0.01	Forest

Note: **R²_{fixed(full)}:** Marginal R², variance explained by fixed effects in full model. **R²_{total(full)}:** Conditional R², variance explained by full model, including random effect of observation number. **R²_{fixed(forest)}:** Marginal R², variance explained by fixed effects in model with forest change as only predictor. **R²_{fixed(climate)}:** Marginal R², variance explained by fixed effects in model with climate change as only predictor. **EIV:** Ellenberg Indicator Value.

Table S5. Alternate version of Table 1, derived from stacked individual random forest species distribution models for species with AUC > 0.7 ($n = 174$ species). Average linear mixed effects model fits ($n = 10$ models for each response x year) and relative importance of forest versus climate drivers of understory community change.

Understory community response	Year	R ² _{fixed} mean (se)	R ² _{total} mean (se)	Forest relative importance mean (se)	Climate relative importance mean (se)
Species richness	2050	0.03 (0.00)	0.65 (0.00)	0.12 (0.02)	0.88 (0.02)
Temperature EIV	2050	0.05 (0.00)	0.78 (0.00)	0.07 (0.00)	0.93 (0.00)
Species richness	2100	0.05 (0.00)	0.50 (0.00)	0.03 (0.00)	0.97 (0.00)
Temperature EIV	2100	0.12 (0.00)	0.64 (0.00)	0.06 (0.00)	0.94 (0.00)

Note: R²_{fixed}: Marginal R², variance explained by fixed effects. R²_{total}: Conditional R², variance explained by full model, including random effect of sample cell number. se: Standard error among $n = 10$ models fit to each replicate. EIV: Ellenberg Indicator Value.

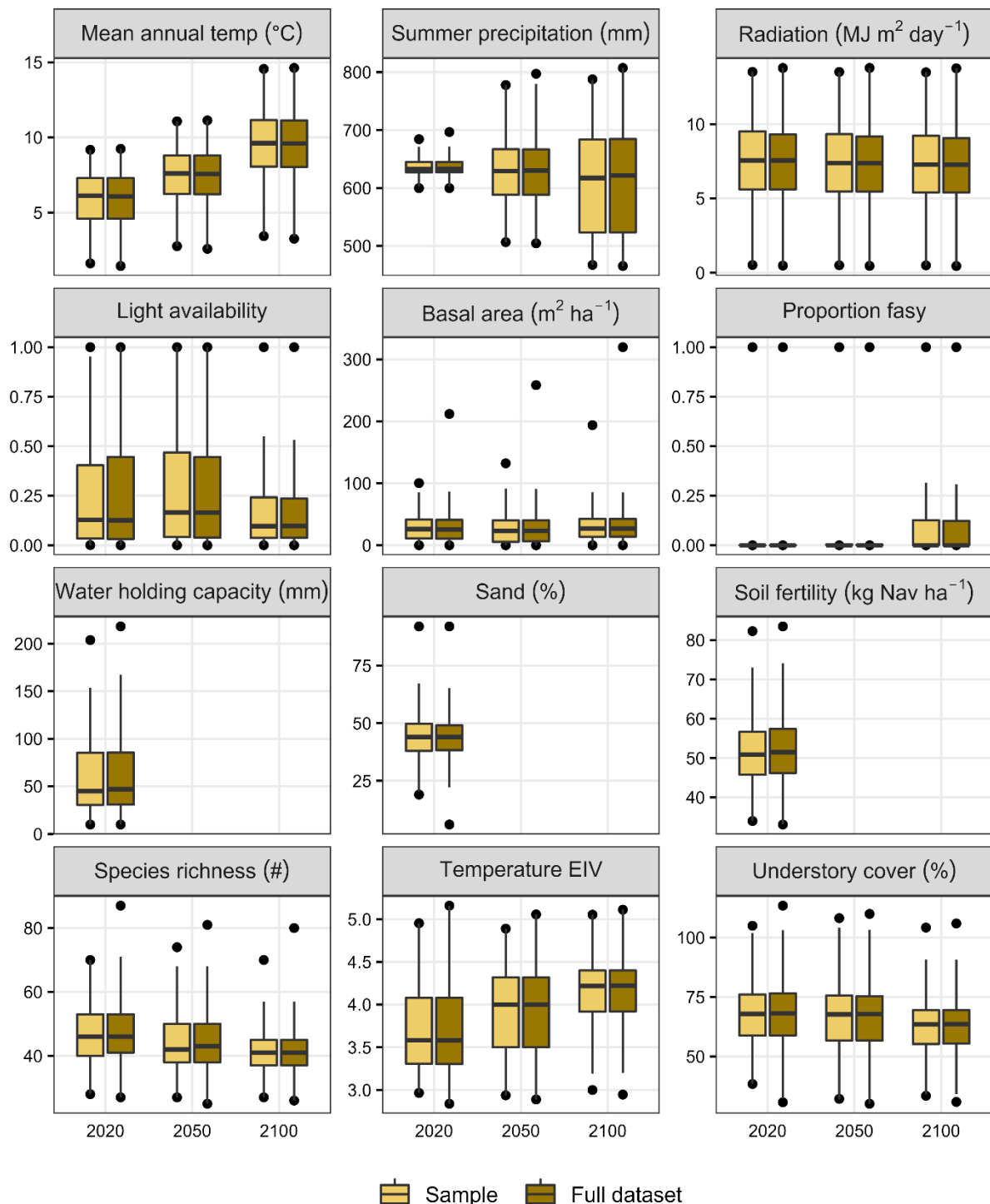


Figure S4. Boxplots showing the distributions of predictors and responses in simple random samples ($n = 1,000$ in 2020 and 80,000 each in 2050 and 2100) compared to the full landscape ($n = 864,466$ in 2020 and 69,157,280 each in 2050 and 2100). Points are minimum and maximum values, and other outliers are not shown. EIV: Ellenberg Indicator Value.

Light-preferring, cold-preferring species (n = 56)

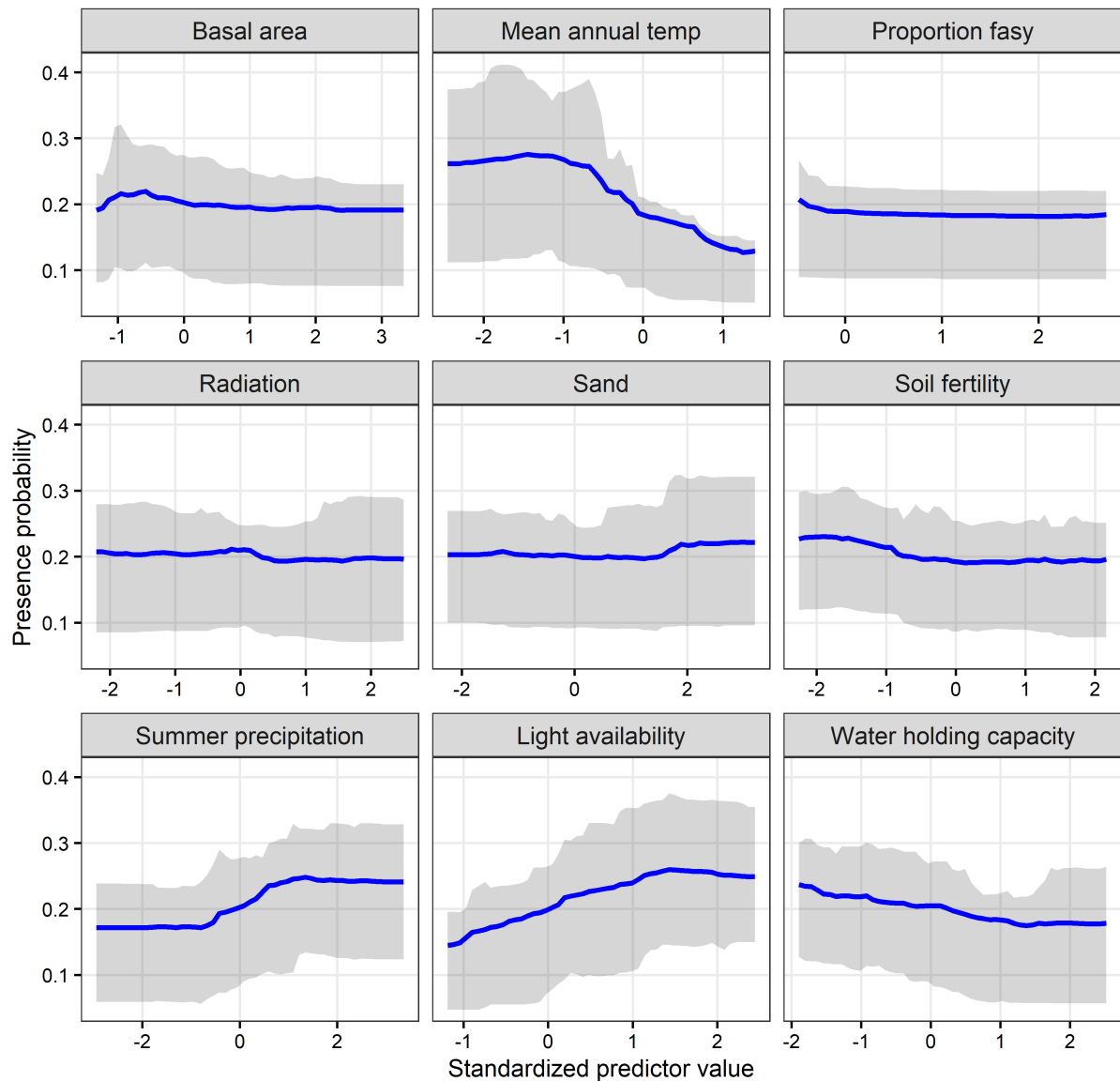


Figure S5. Partial dependence plots for average responses of light-preferring, cold-preferring species ($n = 56$) to predictors across individual species distribution models (final models fit to full dataset). Blue lines are means and shading shows 25th to 75th percentile values.

Light-preferring, warm-preferring species (31)

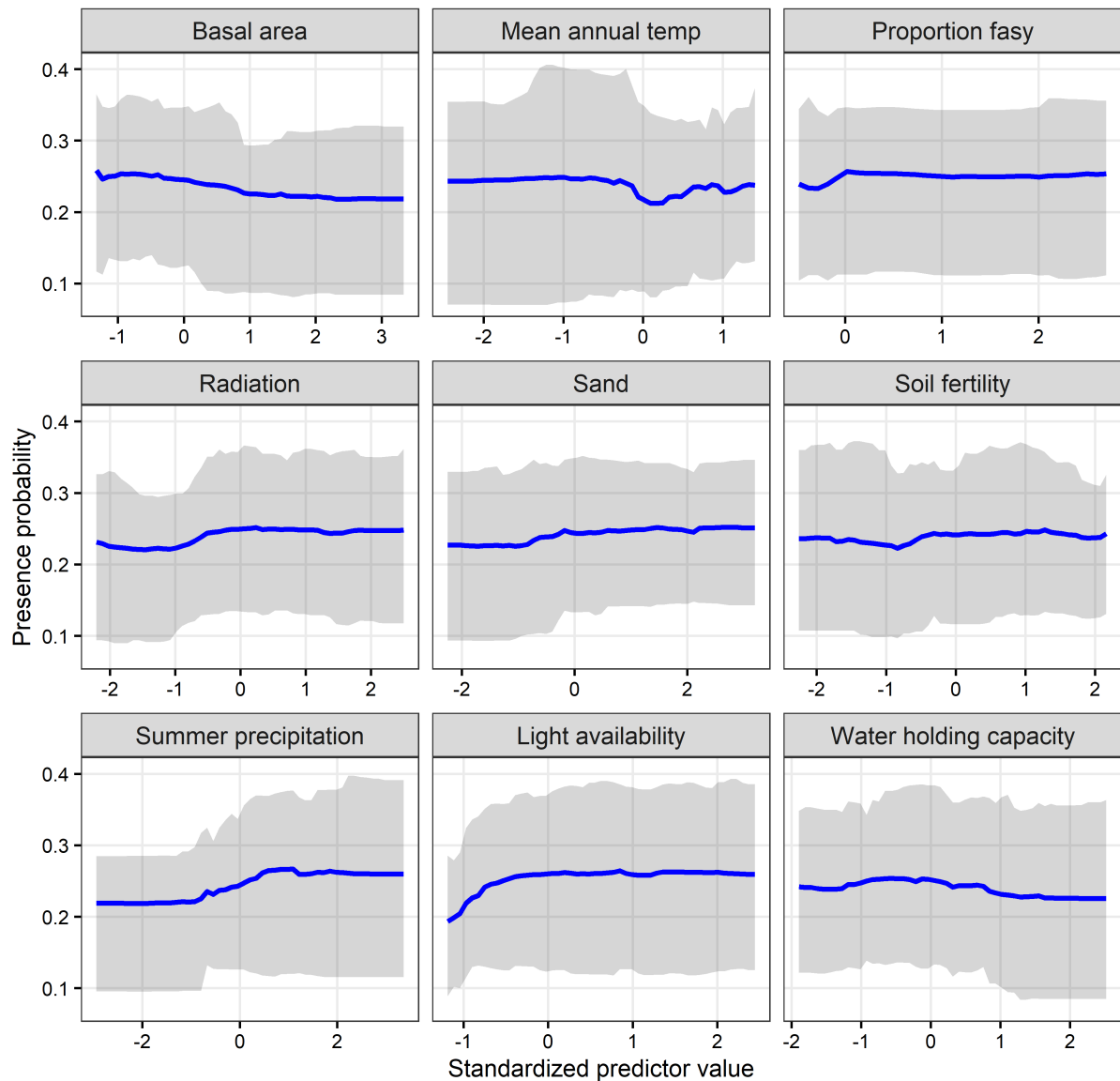


Figure S6. Partial dependence plots for average responses of light-preferring, warm-preferring species ($n = 31$) to predictors across individual species distribution models (final models fit to full dataset). Blue lines are means and shading shows 25th to 75th percentile values.

Light-preferring, temperature-indifferent species (60)

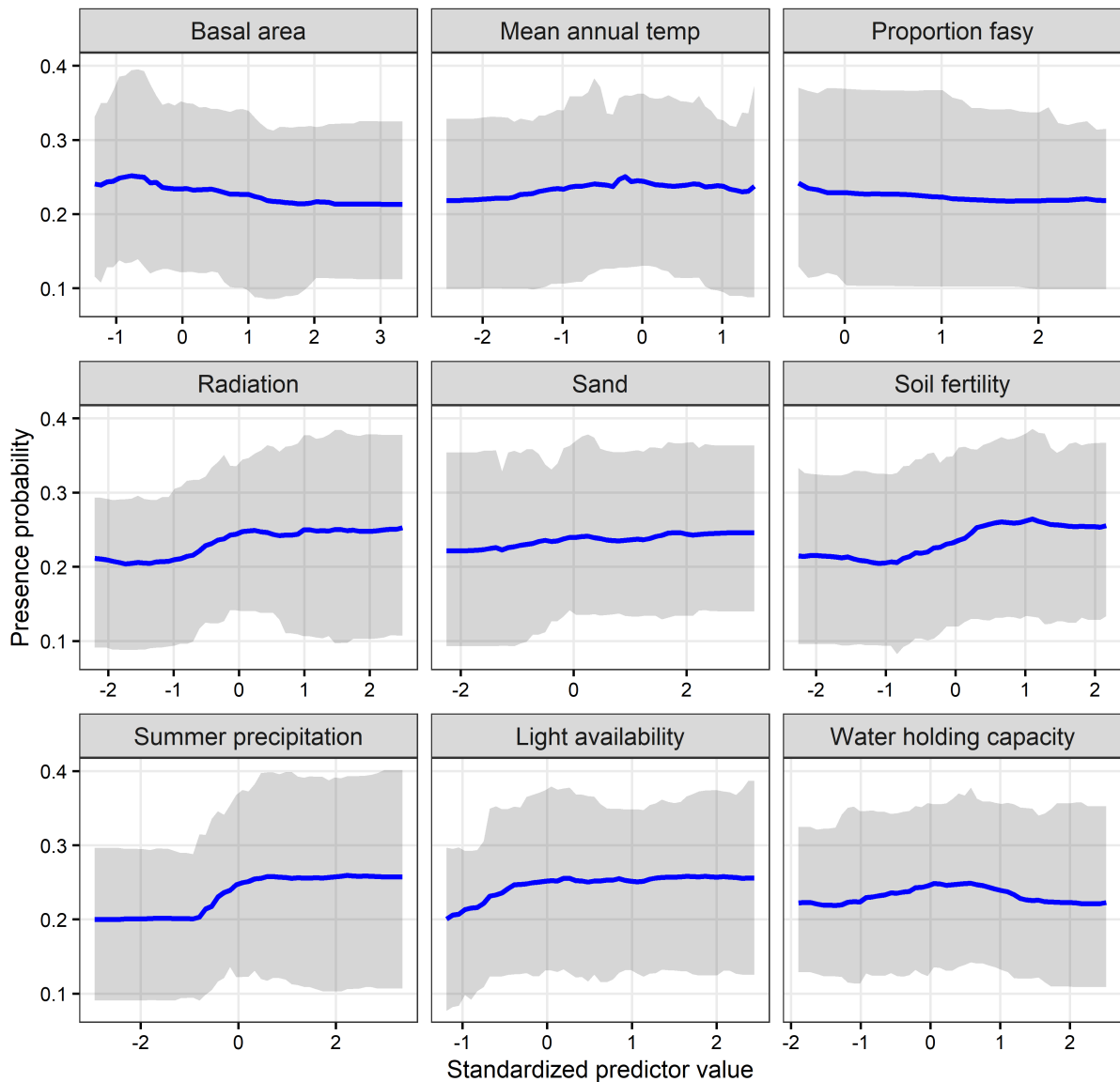


Figure S7. Partial dependence plots for average responses of light-preferring, temperature-indifferent species ($n = 60$) to predictors across individual species distribution models (final models fit to full dataset). Blue lines are means and shading shows 25th to 75th percentile values.

Shade-tolerant, cold-preferring species (12)

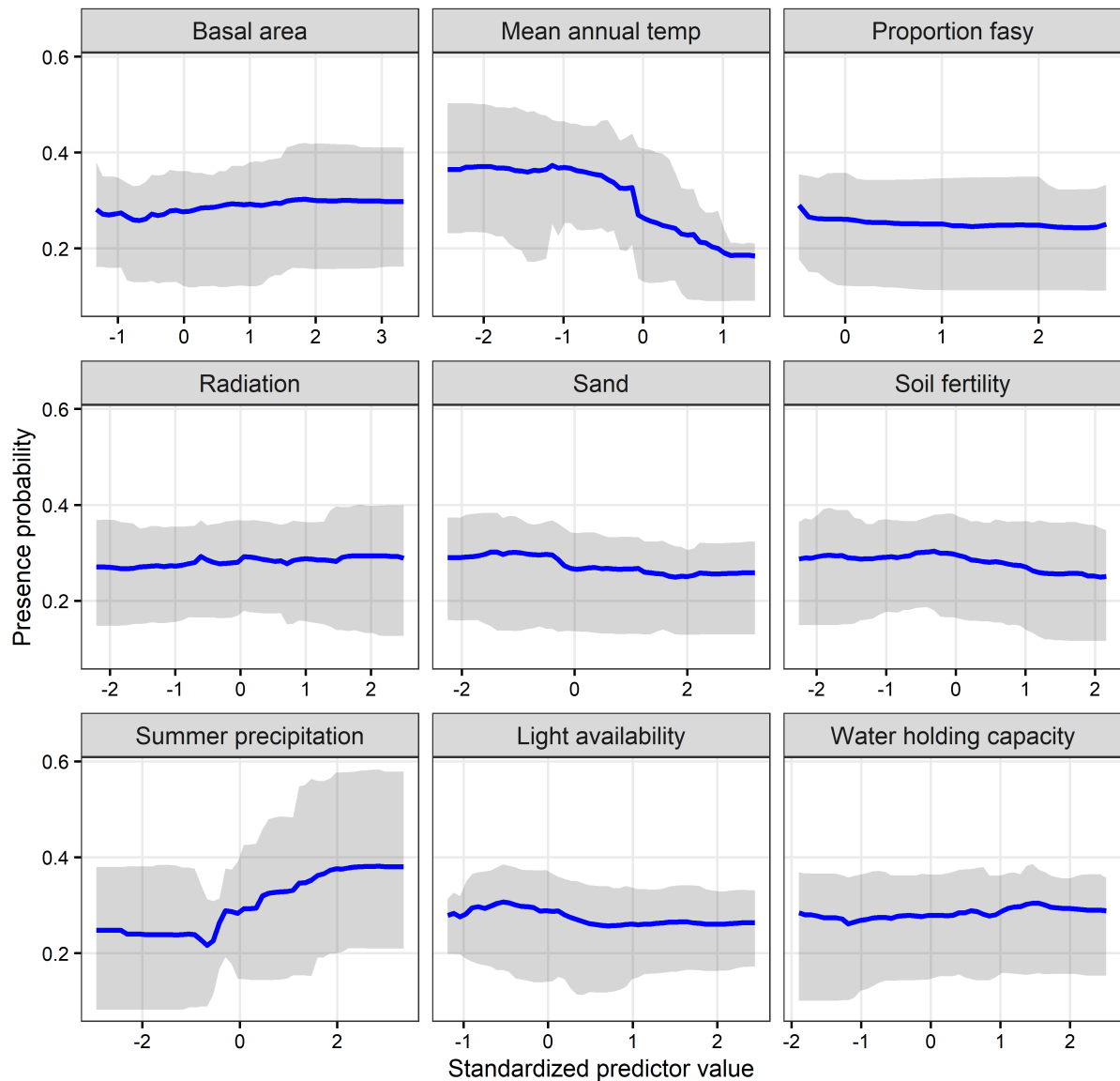


Figure S8. Partial dependence plots for average responses of shade-tolerant, cold-preferring species ($n = 12$) to predictors across individual species distribution models (final models fit to full dataset). Blue lines are means and shading shows 25th to 75th percentile values.

Shade-tolerant, warm-preferring species (54)

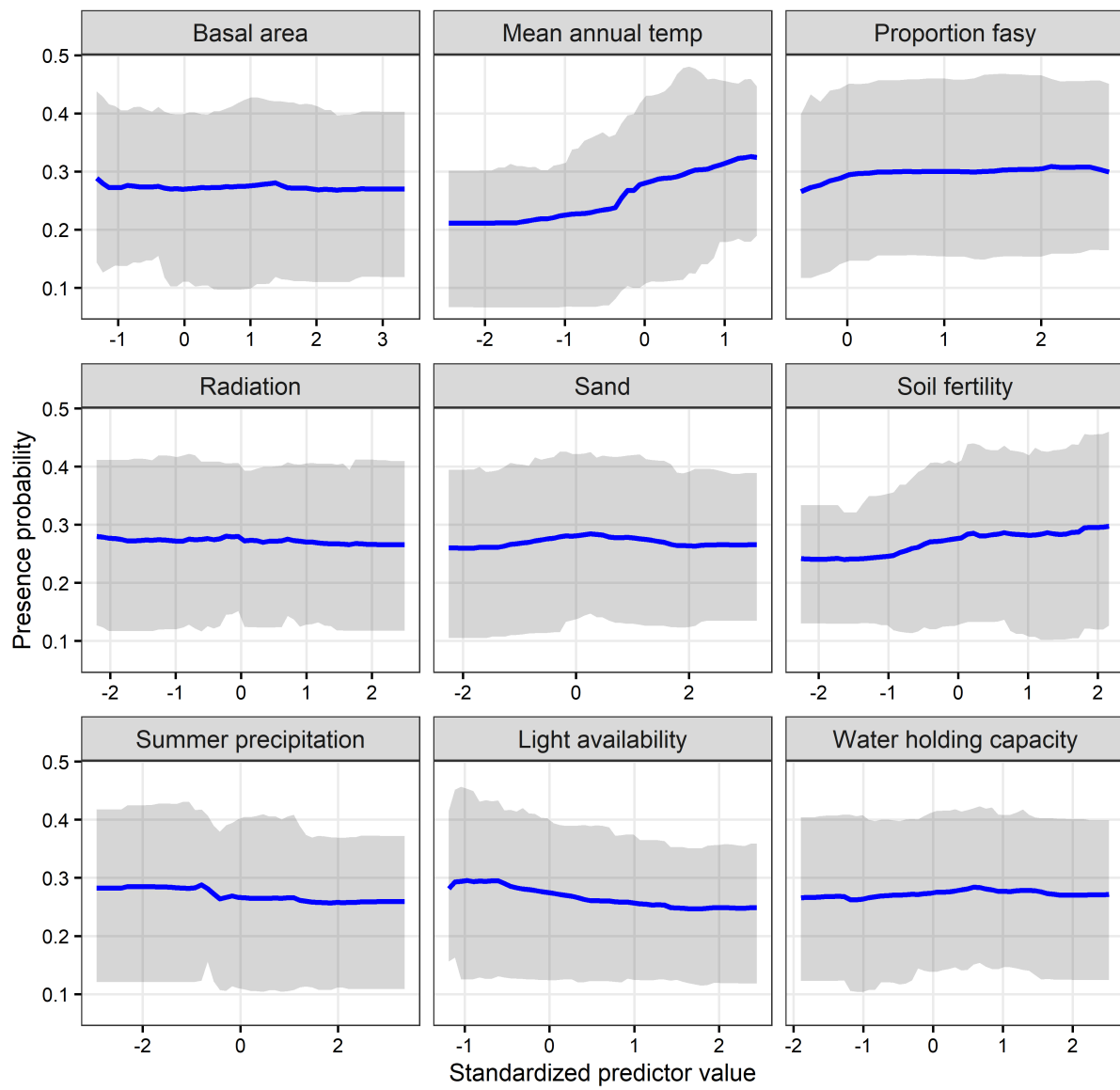


Figure S9. Partial dependence plots for average responses of shade-tolerant, warm-preferring species ($n = 54$) to predictors across individual species distribution models (final models fit to full dataset). Blue lines are means and shading shows 25th to 75th percentile values.

Shade-tolerant, temperature-indifferent species (35)

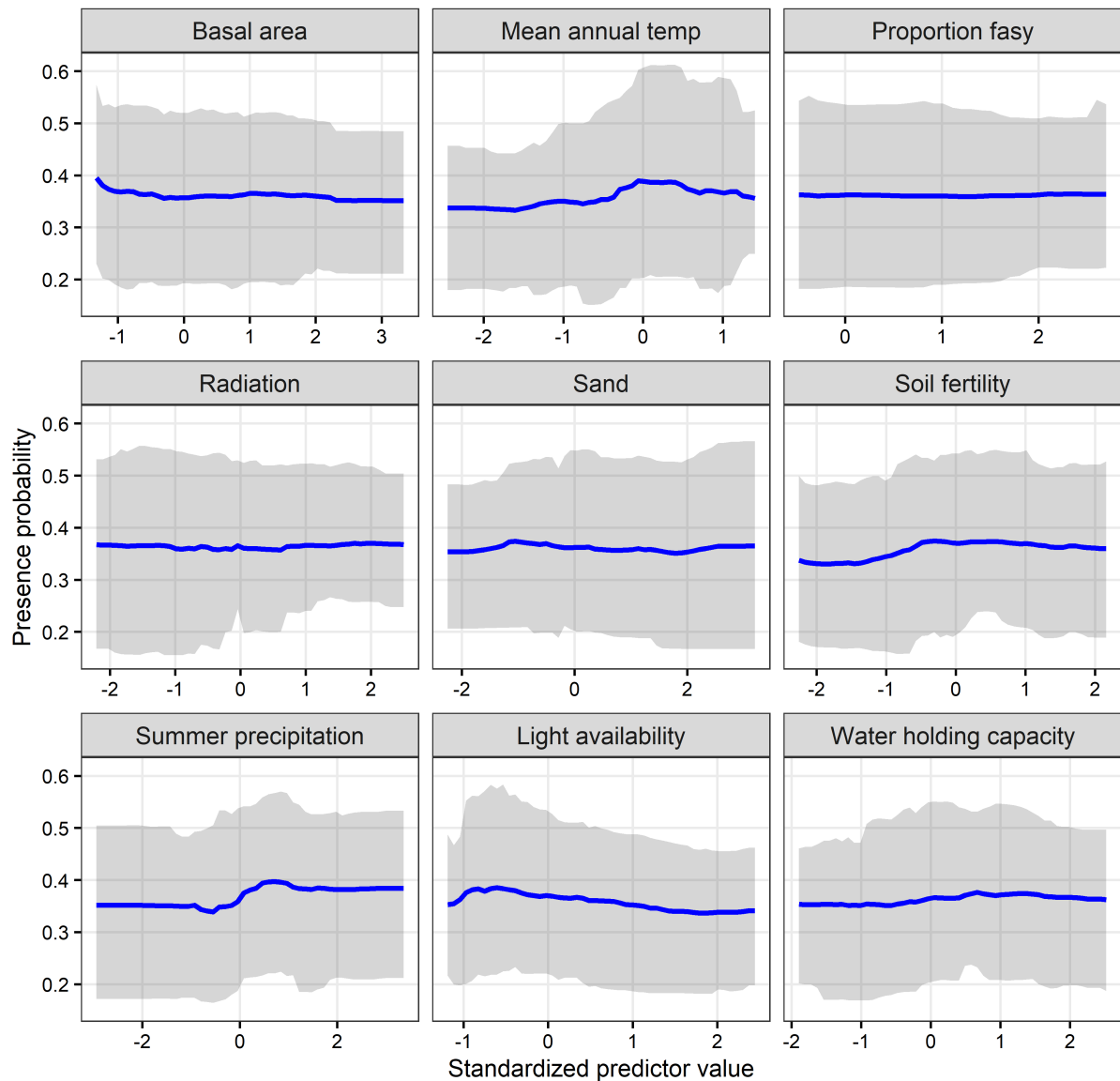


Figure S10. Partial dependence plots for average responses of shade-tolerant, temperature-indifferent species ($n = 35$) to predictors across individual species distribution models (final models fit to full dataset). Blue lines are means and shading shows 25th to 75th percentile values.

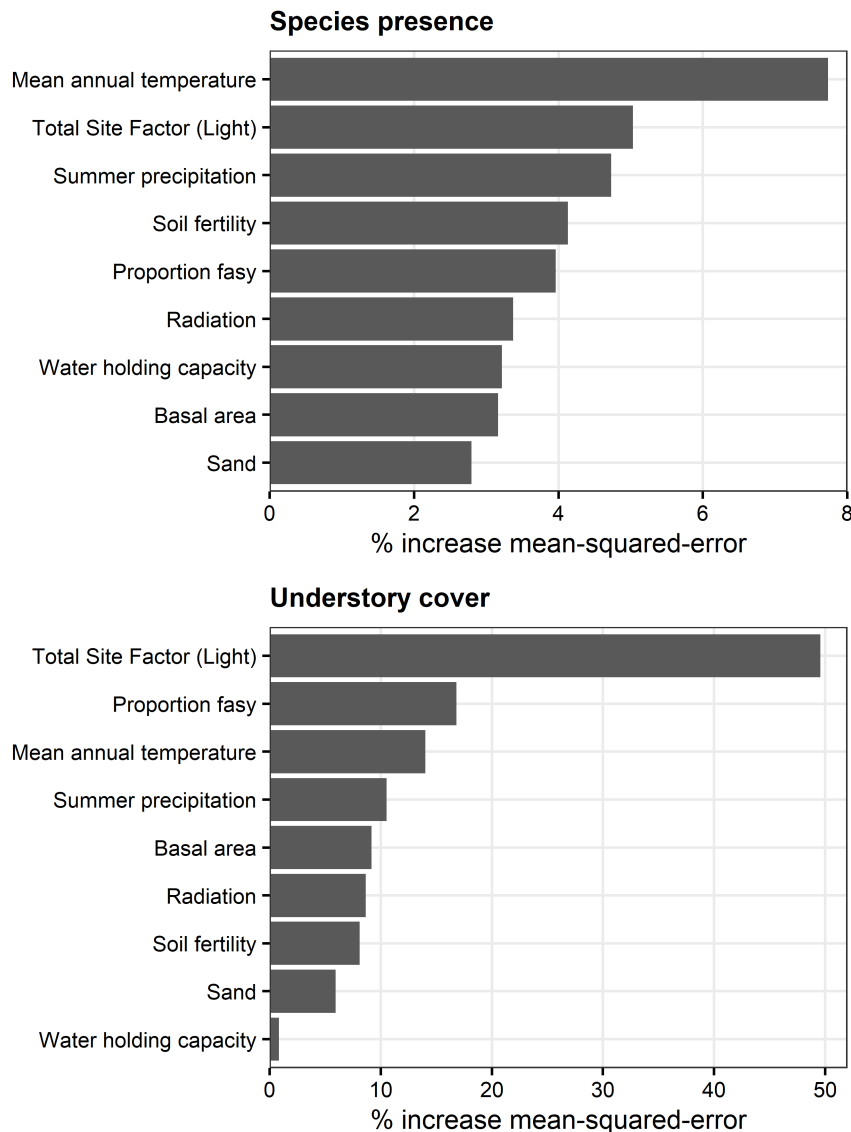


Figure S11. Predictor variable importance ranking for species presence (average of positive values across all individual species distribution models) and understory cover.

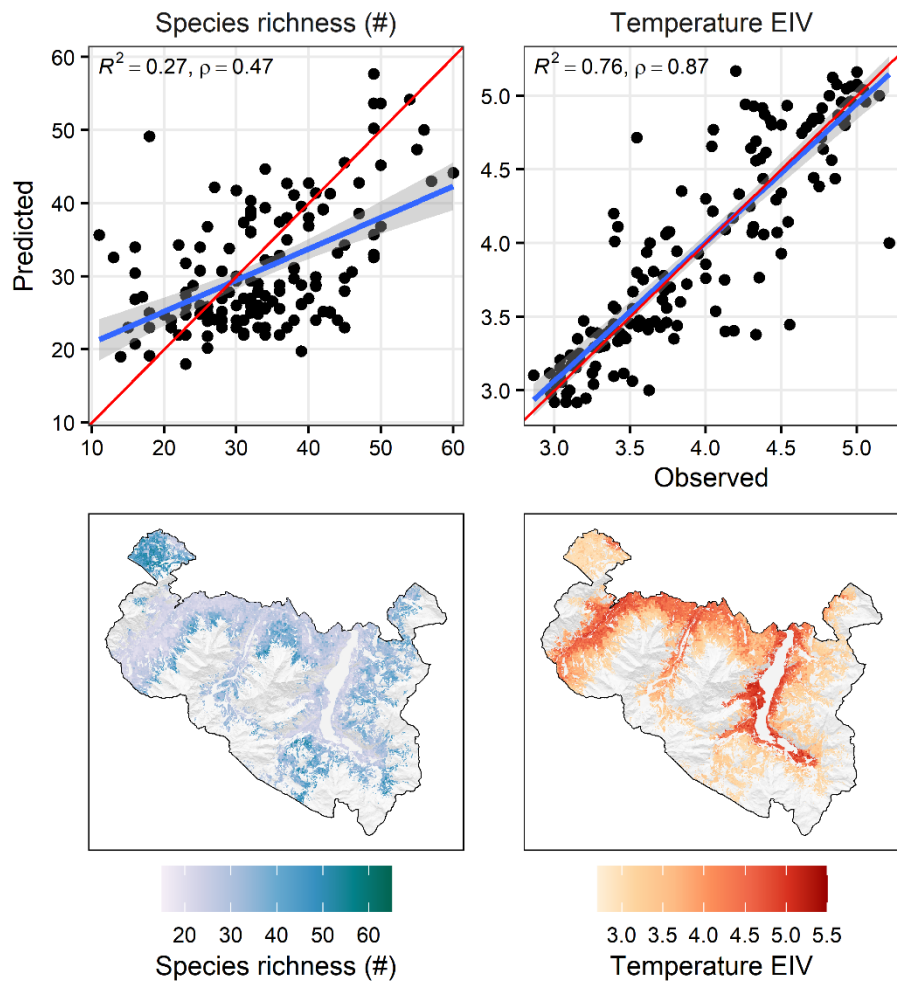


Figure S12. Alternate version of Figure 2, derived from stacked individual random forest species distribution models for species with $AUC > 0.7$ ($n = 174$ species). (Top row) Evaluation of model fit against holdout test data for species richness and mean temperature Ellenberg indicator value (EIV). Points are predicted versus observed values, red lines are 1:1 lines, and blue lines are linear regression fits with shaded confidence intervals; model goodness-of-fit (R^2) and Spearman's rank correction are shown. (Bottom row) Contemporary understory plant community predictions in Berchtesgaden National Park for species richness and mean temperature EIV based on species with $AUC > 0.7$.

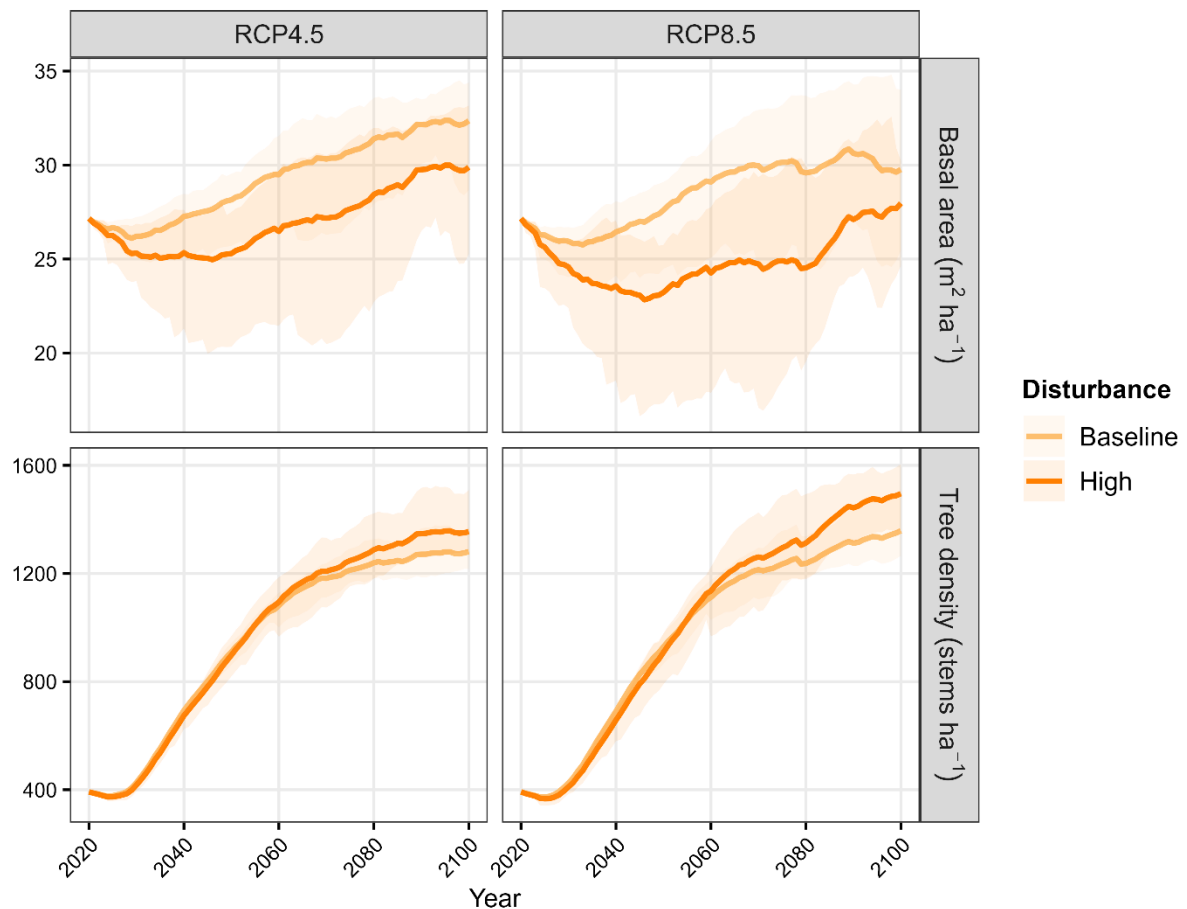


Figure S13. Simulated change in forest structure (landscape average basal area and stand density) over the 21st century under two representative concentration pathways (RCP4.5 = warmer climate, RCP8.5 = hotter climate) and two disturbance scenarios (baseline = historical wind speed, high = 15% increase in wind speed). Solid line is mean, shading is minimum to maximum across two general circulation models, $n = 10$ replicates of each.

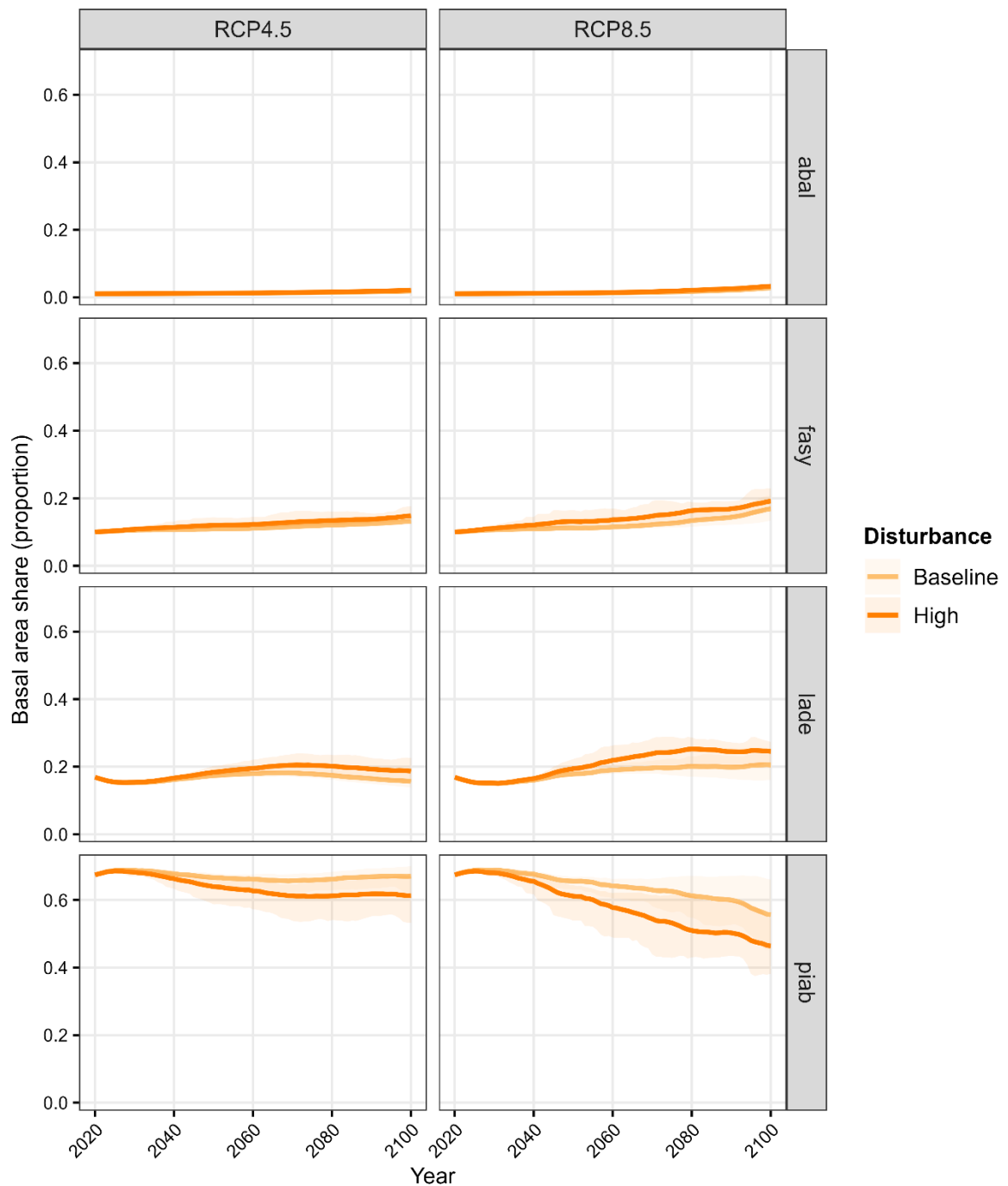


Figure S14. Simulated change in forest composition for four tree species (landscape average basal area share) over the 21st century under two representative concentration pathways (RCP4.5 = warmer climate, RCP8.5 = hotter climate) and two disturbance scenarios (baseline = historical wind speed, high = 15% increase in wind speed). Solid line is mean, shading is minimum to maximum across two general circulation models, $n = 10$ replicates of each. Additional species were present in the landscape and made minor contributions to average basal area. Abal: *Abies alba* (Silver fir); fasy: *Fagus sylvatica* (European beech); lade: *Larix decidua* (European larch); piab: *Picea abies* (Norway spruce).

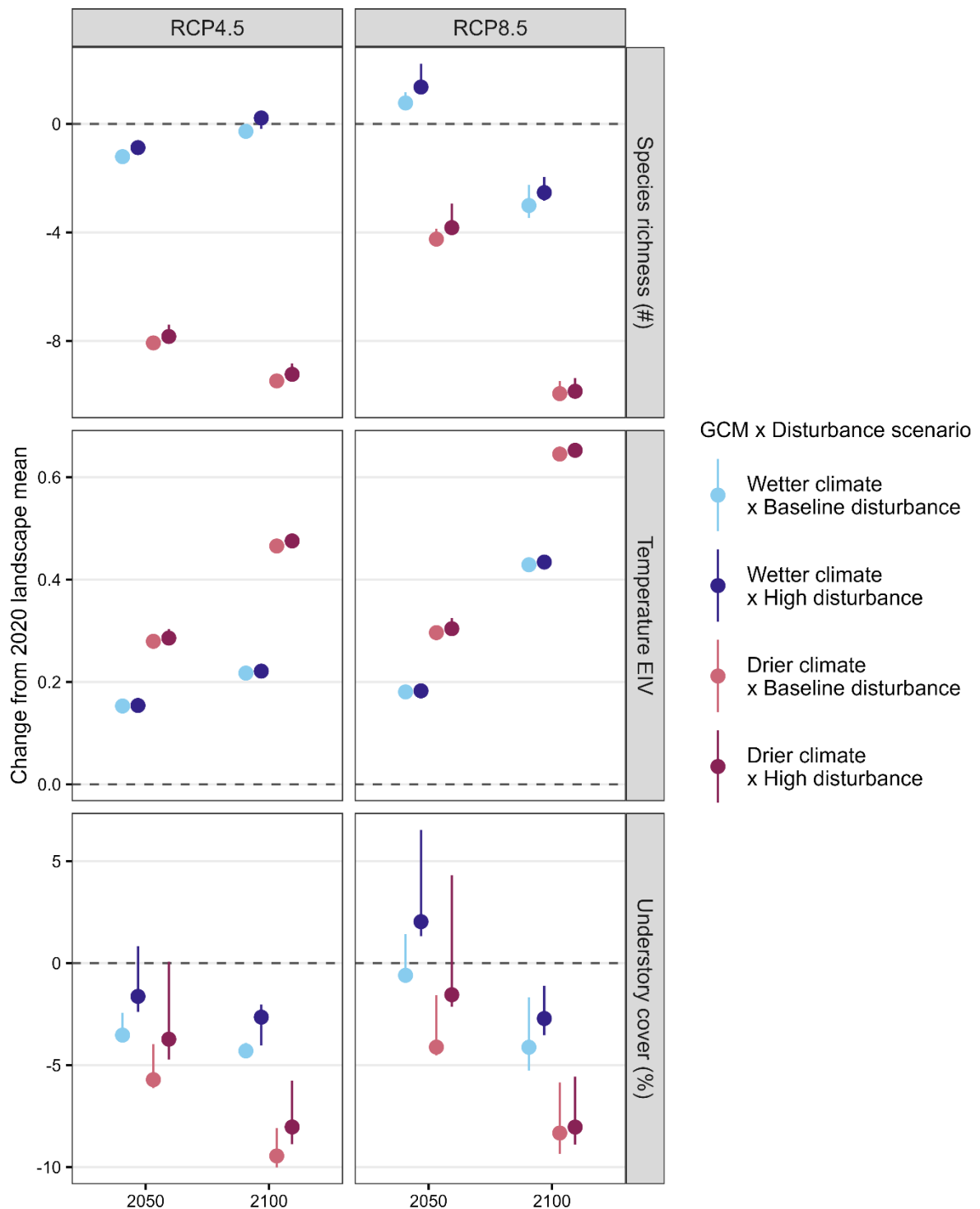


Figure S15. Change in landscape mean species richness, temperature Ellenberg indicator value (EIV), and total understory cover in 2050 and 2100 relative to contemporary plant communities in 2020, by representative concentration pathway (RCP4.5 = warmer climate, RCP8.5 = hotter climate), general circulation model (GCM; wetter or drier), and disturbance scenario (baseline or high). Dashed lines at 0 show relative position of 2020 values, points are median change, and point ranges are 5th to 95th percentile change across scenarios ($n = 10$ replicates per scenario).

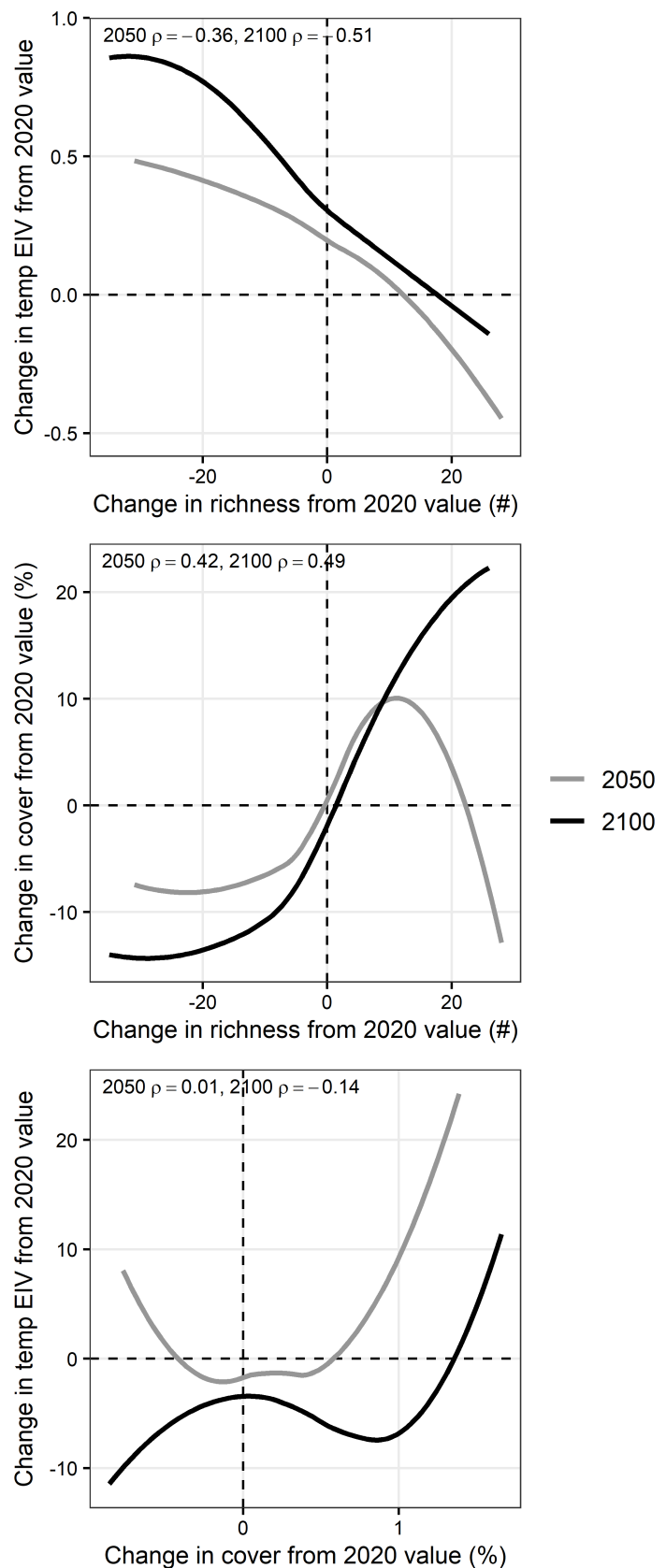


Figure S16. Pairwise relationships among changes from 2020 values in species richness, mean temperature Ellenberg Indicator Value (EIV), and understory cover. Spearman's rho is reported for all cells and replicates ($n = 69,157,280$). Line is a loess smooth regression (smoothing span = 0.75) fit to a random sample of 1,000 cells per replicate. Dashed lines at 0 show relative position of 2020 values.

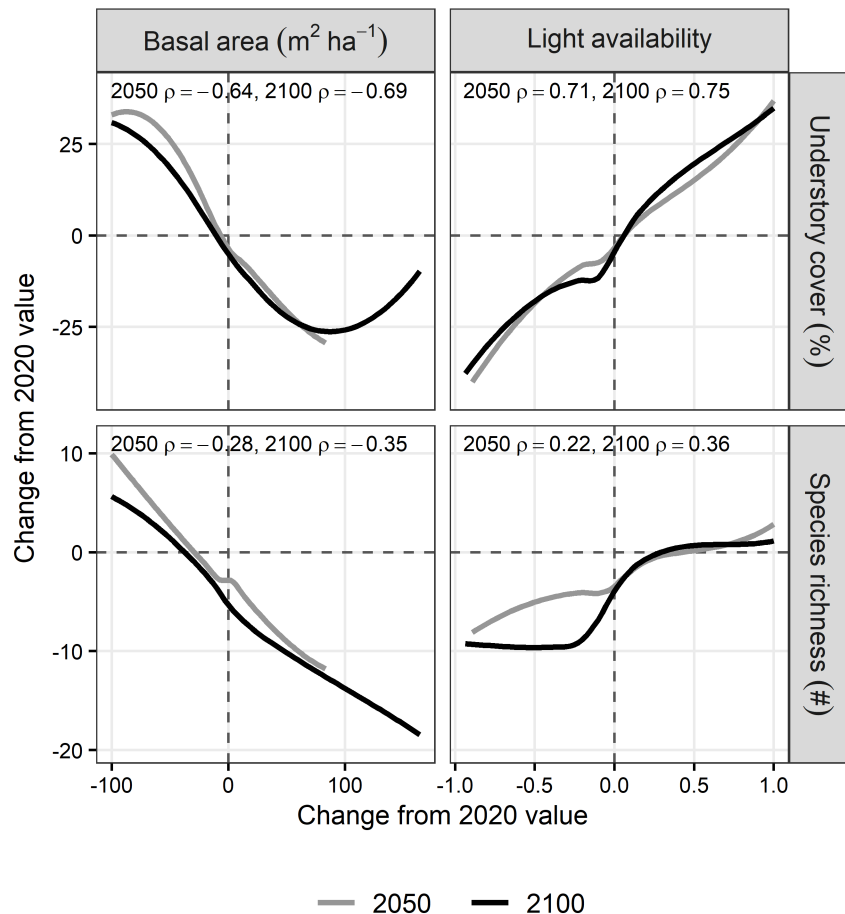


Figure S17. Change from 2020 values in species richness and understory cover versus change from 2020 values in basal area and light availability. Spearman's rho is reported for all cells and replicates ($n = 69,157,280$). Line is a loess smooth regression (smoothing span = 0.75) fit to a random sample of 1,000 cells per replicate. Dashed lines at 0 show relative position of 2020 values.

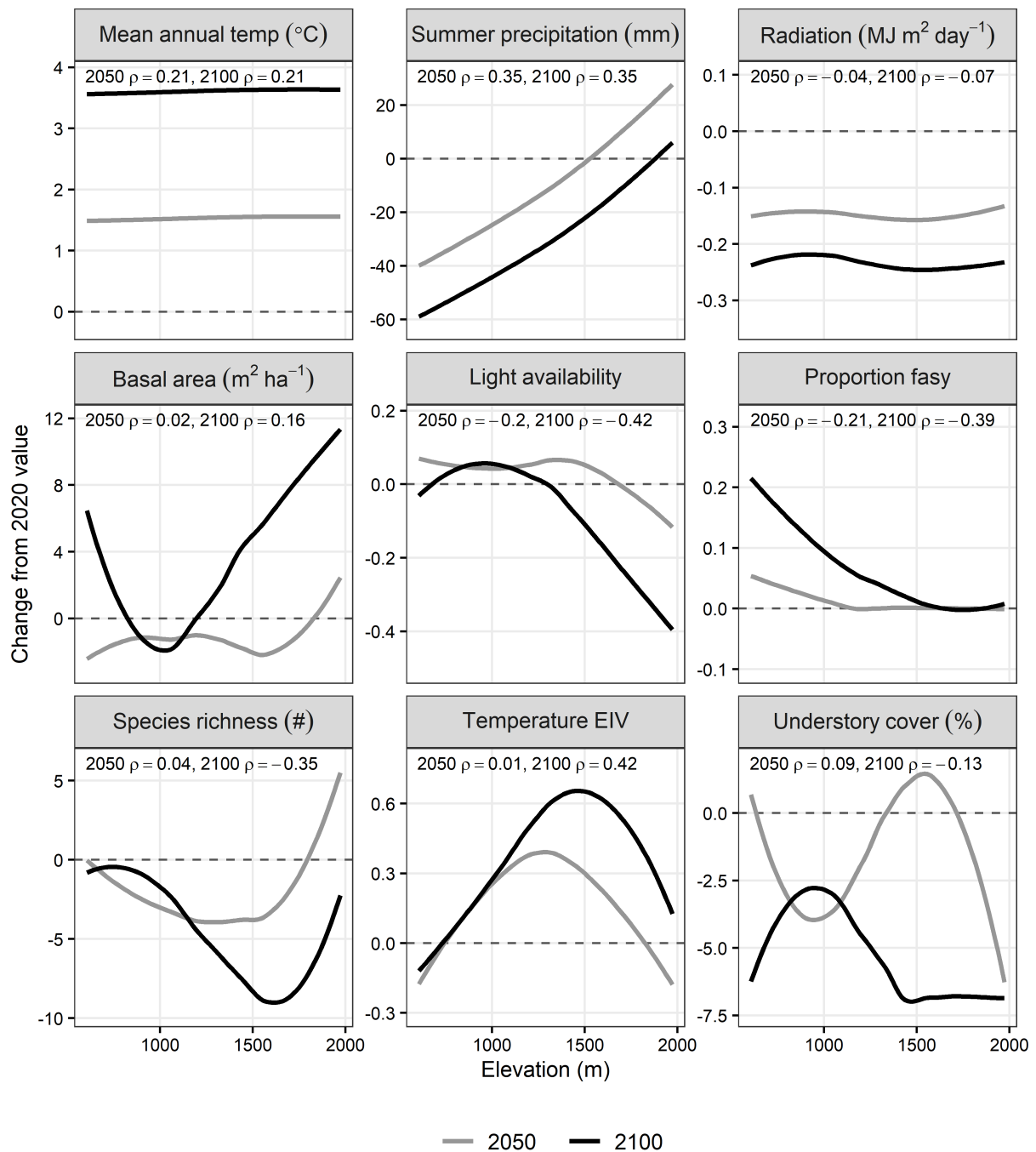


Figure S18. Change from 2020 values in drivers and responses along an elevational gradient. Spearman's rho is reported for all cells and replicates ($n = 69,157,280$). Line is a loess smooth regression (smoothing span = 0.75) fit to a random sample of 1,000 cells per replicate. Dashed lines at 0 show relative position of 2020 values.

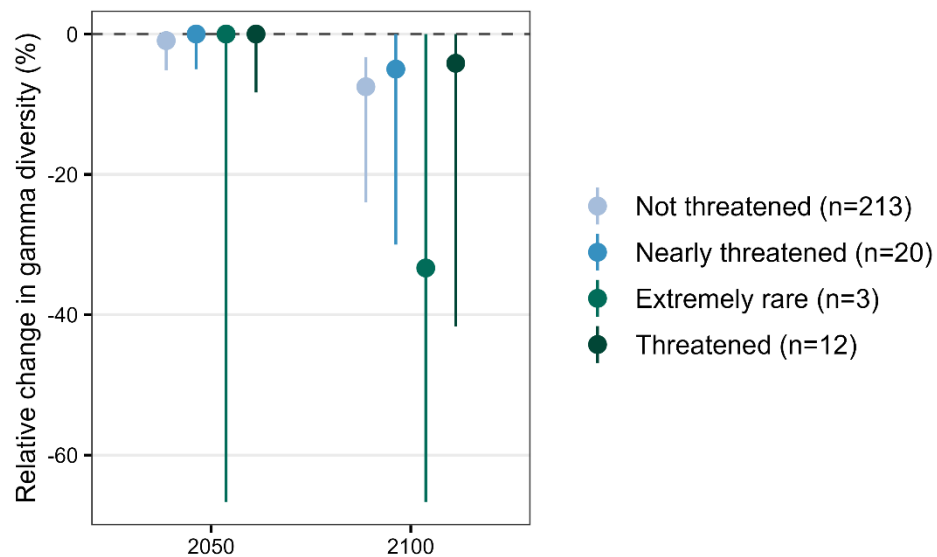


Figure S19. Relative change in gamma diversity (i.e., percent change in number of species present in at least one cell in the landscape) in 2050 and 2100 by German Red List classification. Dashed lines at 0 show relative position of 2020 values, points are median change, and point ranges are 5th to 95th percentile change across scenarios.

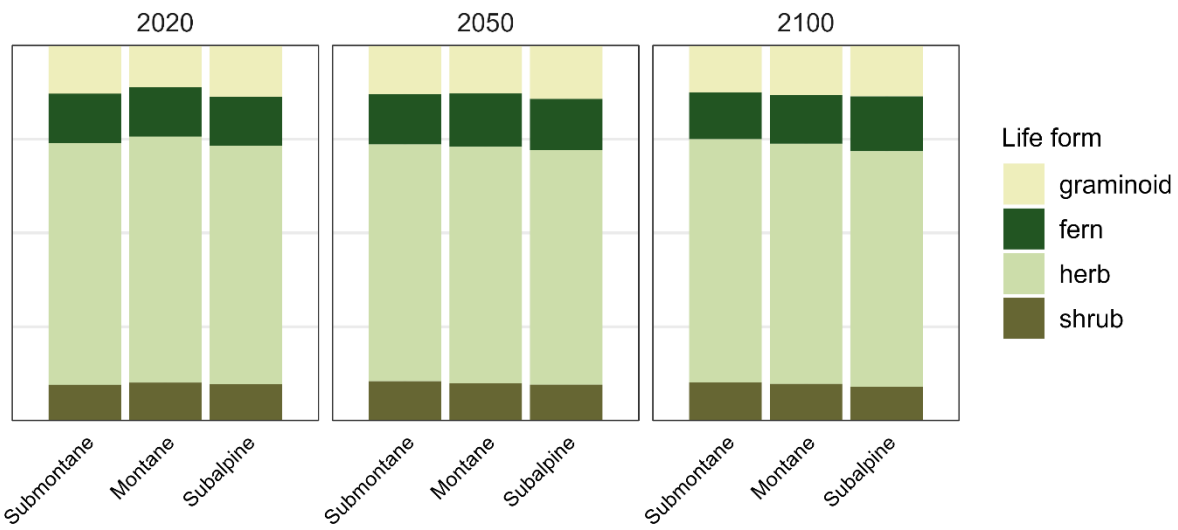


Figure S20. Relative dominance of life forms in contemporary and future understory plant communities, grouped by time period and elevation zone (submontane, montane, or subalpine). Dominance is calculated from species presence at 10 m resolution.

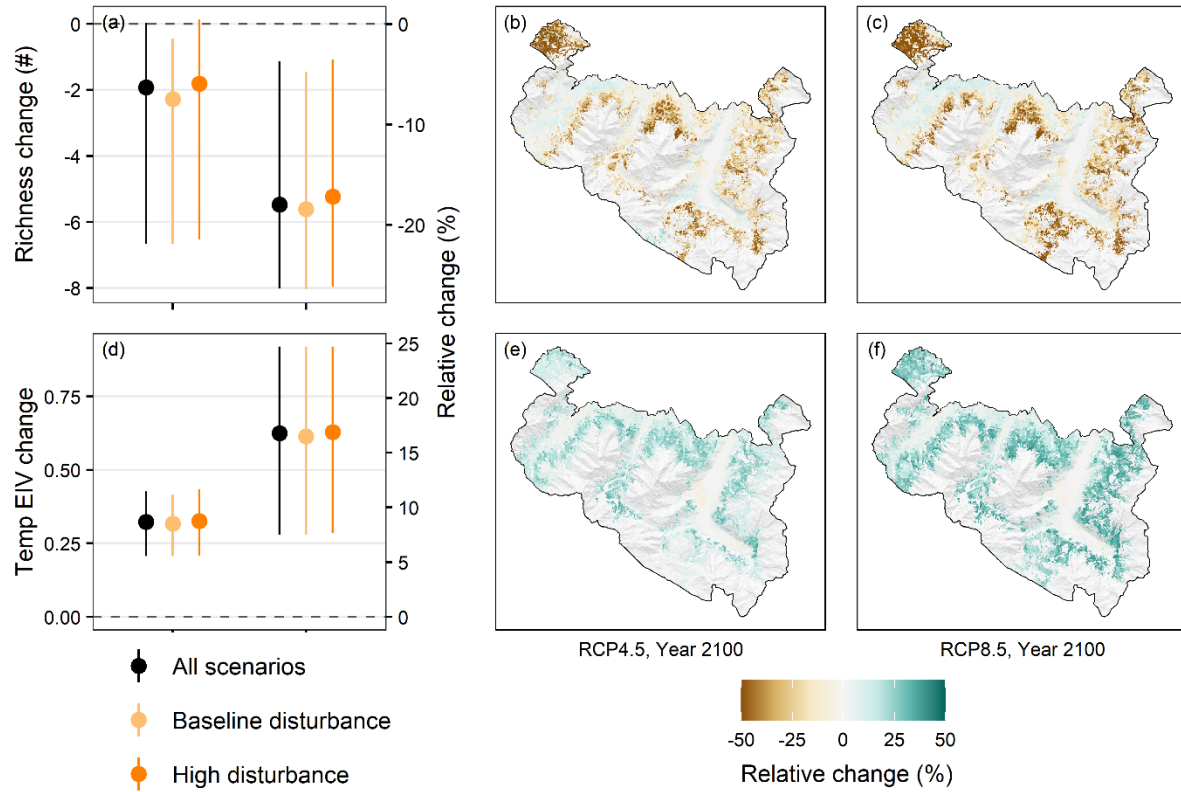


Figure S21. Alternate version of Figure 3, derived from stacked individual random forest species distribution models for species with $AUC > 0.7$ ($n = 174$ species). Change in (a-c) species richness and (d-f) mean temperature Ellenberg indicator value (EIV) relative to contemporary plant communities in 2020. Left column (a, d) shows near-term (2050) and long-term (2100) change in landscape mean values for all scenarios and for different disturbance scenarios. Dashed lines at 0 show relative position of 2020 values, points are median change, and point ranges are 5th to 95th percentile change across scenarios. Right two columns (b-c, e-f) show change at 10 m spatial resolution in 2100 relative to the 2020 landscape mean value under warmer (RCP4.5) or hotter (RCP8.5) climate scenarios. Values $<-50\%$ and $>50\%$ are truncated to this minimum and maximum.

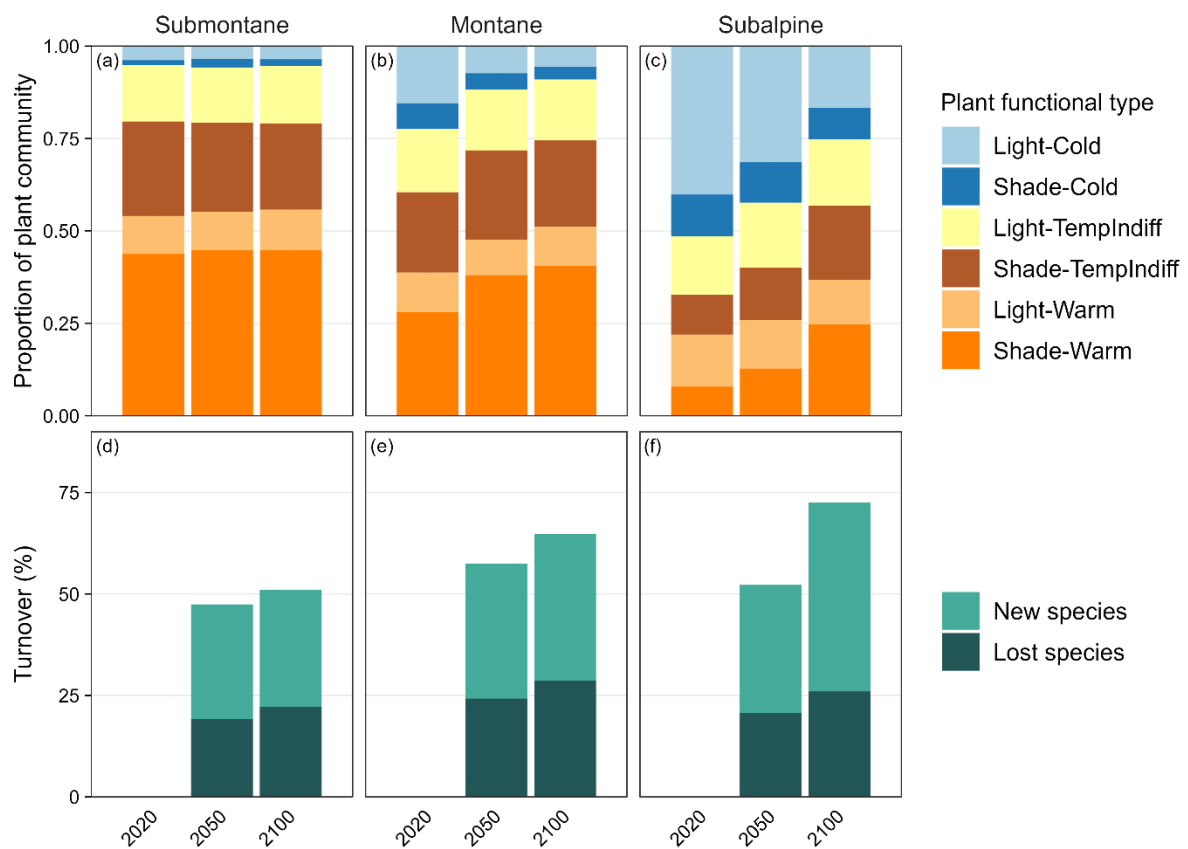


Figure S22. Alternate version of Figure 4, derived from stacked individual random forest species distribution models for species with $AUC > 0.7$ ($n = 174$ species). (a-c) Change in relative dominance of Plant Functional Types (PFTs) in (a) submontane, (b) montane, and (c) subalpine elevation zones between contemporary and future time periods. Dominance is calculated from species presence at 10 m resolution. (d-f) Turnover in species communities at 10 m resolution relative to contemporary 2020 understory plant communities, grouped by elevation zone (d, submontane; e, montane; f, subalpine). Turnover is the sum of new plus lost species divided by the total species pool x 100%. TempIndiff: Indifferent to temperature.

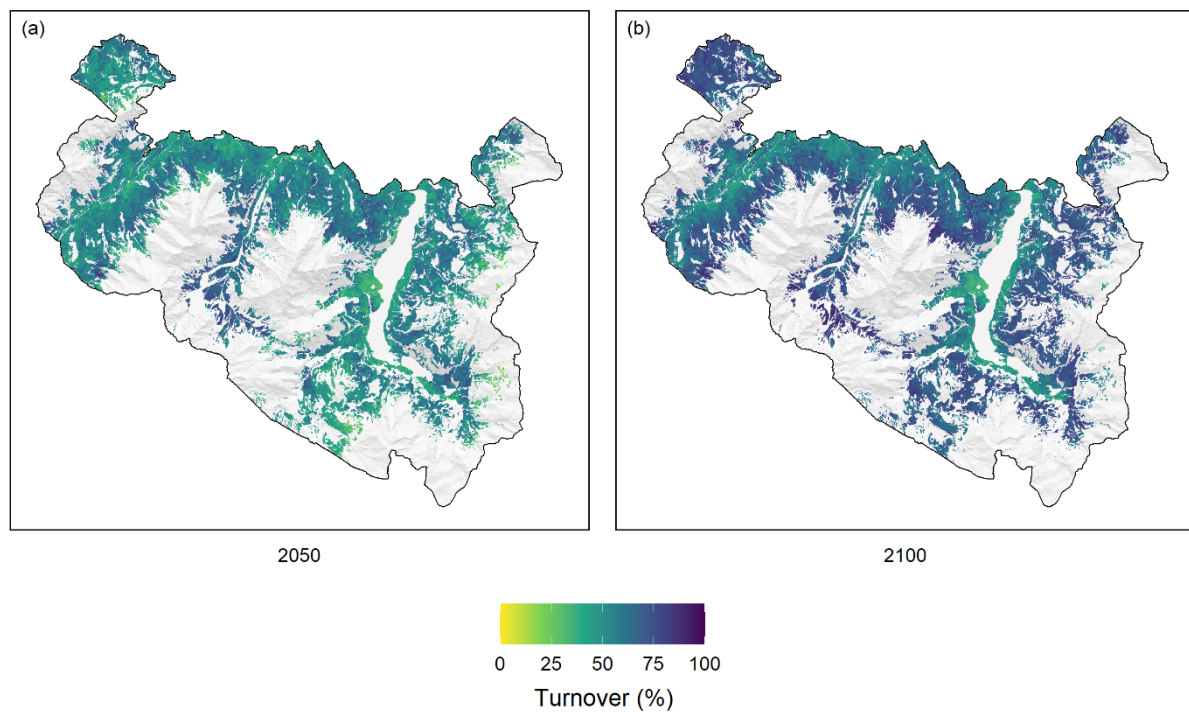


Figure S23. Alternate version of Figure 5, derived from stacked individual random forest species distribution models for species with $AUC > 0.7$ ($n = 174$ species). Turnover in species communities at 10 m resolution under (a) near-term change (2050) and (b) long-term change (2100) relative to contemporary 2020 understory plant communities. Turnover is the sum of new plus lost species divided by the total species pool $\times 100\%$.

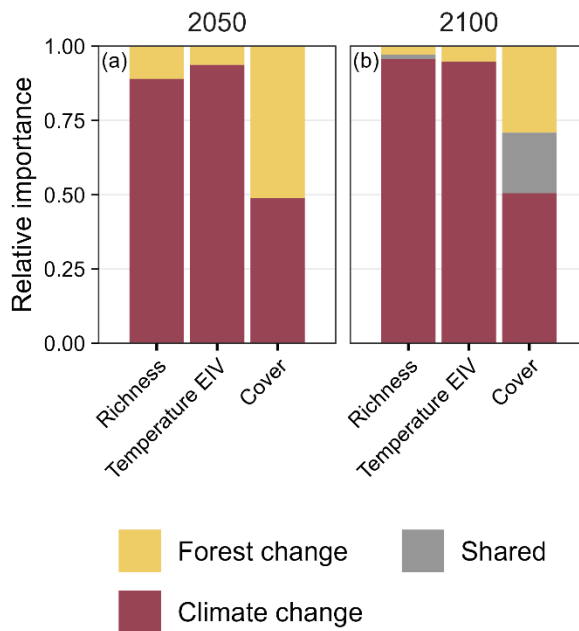


Figure S24. Relative importance of climate versus forest change in driving understory community richness, temperature Ellenberg Indicator Value (EIV), and percent cover responses under near-term (2050) and long-term (2100). Height of bars is mean importance value across linear mixed effects models fit to each of $n = 10$ replicate simulations.